UNITED STATES DEPARTMENT OF THE INTERIOR

GEOLOGICAL SURVEY

SUMMARY GEOLOGIC REPORT FOR THE ST. GEORGE OUTER CONTINENTAL SHELF (OCS) PLANNING AREA BERING SEA, ALASKA

by

Alan K. Cooper[1]; Michael S. Marlow[1]; and Tracy L. Vallier[1]

Open-File Report 84-418

1.
U.S. Geological Survey, MS 999
345 Middlefield Road
Menlo Park, California 94025

1984

Table of Contents

SUMMARY

In this report, the shelf (St. George basin) and deep-water (Umnak Plateau region) areas of the St. George basin OCS planning area are described separately, (Fig. 1) as was done with the previous resource reports of Marlow and others (1979c) and Cooper and others (1980). At the time of the writing of this report, information for two cost wells in St. George basin are in final preparation for public release, however this information is not included herein.

ST. GEORGE BASIN

St. George basin is a long (300 km), narrow (30-50 km) graben whose long axis strikes northwestward, parallel to the continental margin of the southern Bering Sea. Located near the Pribilof Islands, and beneath the virtually featureless Bering Sea shelf, the basin is filled with more than 10 km of sedimentary deposits. These sedimentary rocks are ruptured by normal faults associated with the sides of the graben; these ruptures commonly correlate with offsets in the basement surface. Offset along these faults increases with depth implying that they are growth-type structures.

Dredging from the continental margin near St. George basin suggests that the southwestern flank of the basin is underlain by Jurassic rocks equivalent to the Naknek Formation on the Alaska Peninsula. Dredging and seismic reflection data also show that at least the upper part of the basin fill is late Cenozoic in age. Regional plate tectonic reconstructions suggest that collapse of the continental margin and initial formation of St. George basin probably began in earliest Tertiary time (Marlow and Cooper, 1984).

Cretaceous mudstone dredged from the nearby continental slope in Pribilof Canyon contains as much as 1 percent organic carbon (Marlow and others, 1976, p. 179). Other rocks dredged from the Beringian continental slope include lithified volcanic sandstone of Late Jurassic age, mudstone of Late Cretaceous age, and less consolidated deposits of early Tertiary age. Geochemical analyses of these rocks were published in Marlow and others, (1979b). Pyrolytic analyses of these rocks show that they are not good source beds for petroleum. However, the outcrops sampled by rock dredging are generally more resistant sandy units that may not be representative of finer-grained sedimentary sections in St. George basin or the other outer shelf basins.

Other Tertiary mudstone also crops out on the continental slope; some of these rocks contain more than 0.25 percent organic carbon (Marlow and others, 1979b, p. 178). However, many of these rocks crop out too far down on the continental slope to be representative of the lower sediment sections in the outer shelf basins. Because the stratigraphically lower basin beds wedge out against the flanks of the shelf basins, correlative outcrops are virtually unknown along the nearby continental slope.

The porosities of Eocene to Pliocene-Pleistocene rocks dredged from 15 sites along the Bering Sea continental margin range from 14-70 percent and average 44 percent (Marlow and others, 1979b; Jones and others, 1981). The Cenozoic samples are generally porous - probably because of abundant diatom frustules in many of the samples. However, the permeability of these rocks is variable, probably because of submarine weathering and subsequent cementation effects. These Cenozoic outcrops can be traced as seismic reflectors to two subshelf basins, St. George and Navarin basins, where, if the beds remain diatomaceous, good potential reservoir beds may occur.

Within St. George basin, structural traps include broad anticlinal closures and tight folds associated with normal faults. Closure and fault offset increase with depth; hence, growth-type structural traps formed

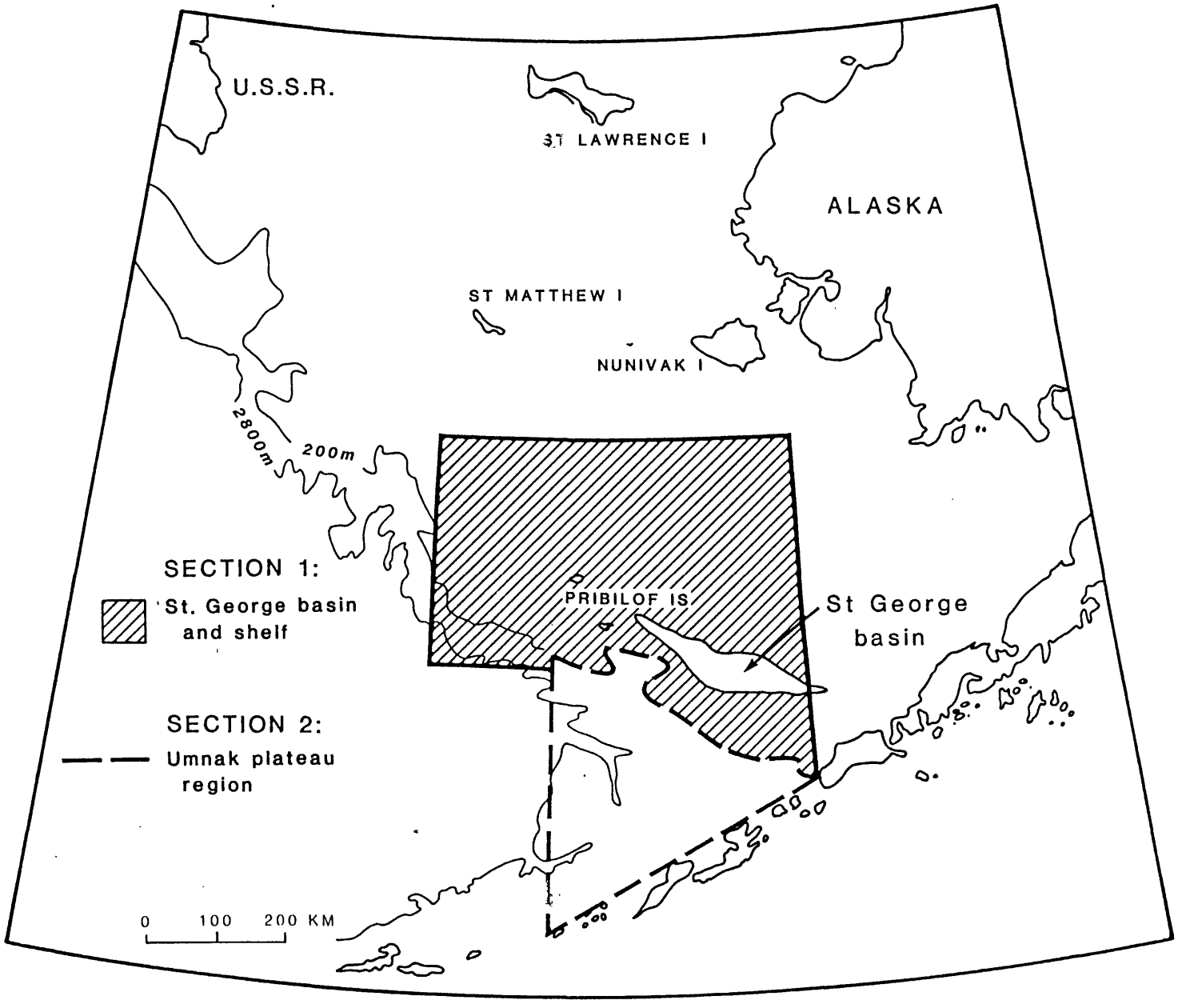

Figure 1. Index map of St. George basin OCS planning area.

continuously with basin filling.

Potential stratigraphic traps are recognizable in the thinning and wedging of the older stratigraphic sequence toward the flanks of St. George basin. These beds dip toward the axis of the basin, hence up-dip migrating fluids could be trapped against the much denser and less permeable rocks of the Mesozoic basement. The basin's lower stratigraphic sequence is discordantly overlapped by the younger acoustically reflective sequence. Hydrocarbons migrating up-dip along the lower beds might, therefore, be trapped beneath the overlapping sedimentary sequences.

Many faults, high seismicity, and evidence of recent movement along some of the faults all show that faulting is a major environmental concern for the outer continental shelf region of the southern Bering Sea, especially in St. George basin. Most of the faults are potentially active and their movement is probably influenced by the local geology, including basement structures and sediment loading. Unstable sediment masses pose potential threats for resource development near Pribilof Canyon. Volcanic activity along the Aleutian arc south of St. George basin may also pose an environmental hazard to petroleum development in the area. Another environmental hazard is shallow gas pockets, which may pose problems during drilling such as blowouts and liquefaction of bottom sediment.

Prospective hydrocarbon areas of the shelf are shown in Figure 2 (from Marlow and others, 1979c).

UMNAK PLATEAU REGION

The triangular Umnak Plateau region lies at the junction of the Bering shelf and the Aleutian Ridge. The region includes those sections of the St. George basin OCS planning area that lie in water depths greater than 200 meters (the shelf break) as well as those sections on the summit of the Aleutian Ridge.

The structural framework and geologic history of the Umnak Plateau region are dominated by the two major rock belts that border the region, a eugeosynclinal assemblage of Mesozoic age rocks underlying the Bering shelf and an island-arc suite of Cenozoic rocks that form the Aleutian Ridge. The deep igneous crustal rocks that underlie the Umnak Plateau region may be typical of either the rocks that form these two bordering belts or the oceanic crustal rocks that floor the adjacent abyssal Aleutian Basin.

During Mesozoic time, the Umnak Plateau region was an oceanic area, similar to that found presently in the North Pacific, that bordered an active continental margin. The major constructional phase of the Aleutian Ridge occurred in early Tertiary time and isolated a segment of oceanic crust within the Umnak Plateau region. Since early Tertiary time, the igneous and volcanic basement rocks beneath the summit basins of the Aleutian Ridge, and the structural depressions beneath the plateau and continental slope have been covered by a 1 to 9 km thick suite of marine volcanic-rich clastic, and diatomaceous sedimentary rocks. These thick sedimentary deposits were diapirically intruded and cut by large submarine canyons during late Cenozoic time.

Regional geologic and geophysical mapping indicates that the four requisites for hydrocarbon accumulations may be present in the Umnak Plateau region; source beds, reservoir beds, traps, and an adequate thermal and sedimentation history. However, the presence of hydrocarbons other than methane gas has not been proven in either of the two 900 meter deep DSDP holes drilled in the region.

Average organic carbon values for Oligocene to Holocene diatomaceous

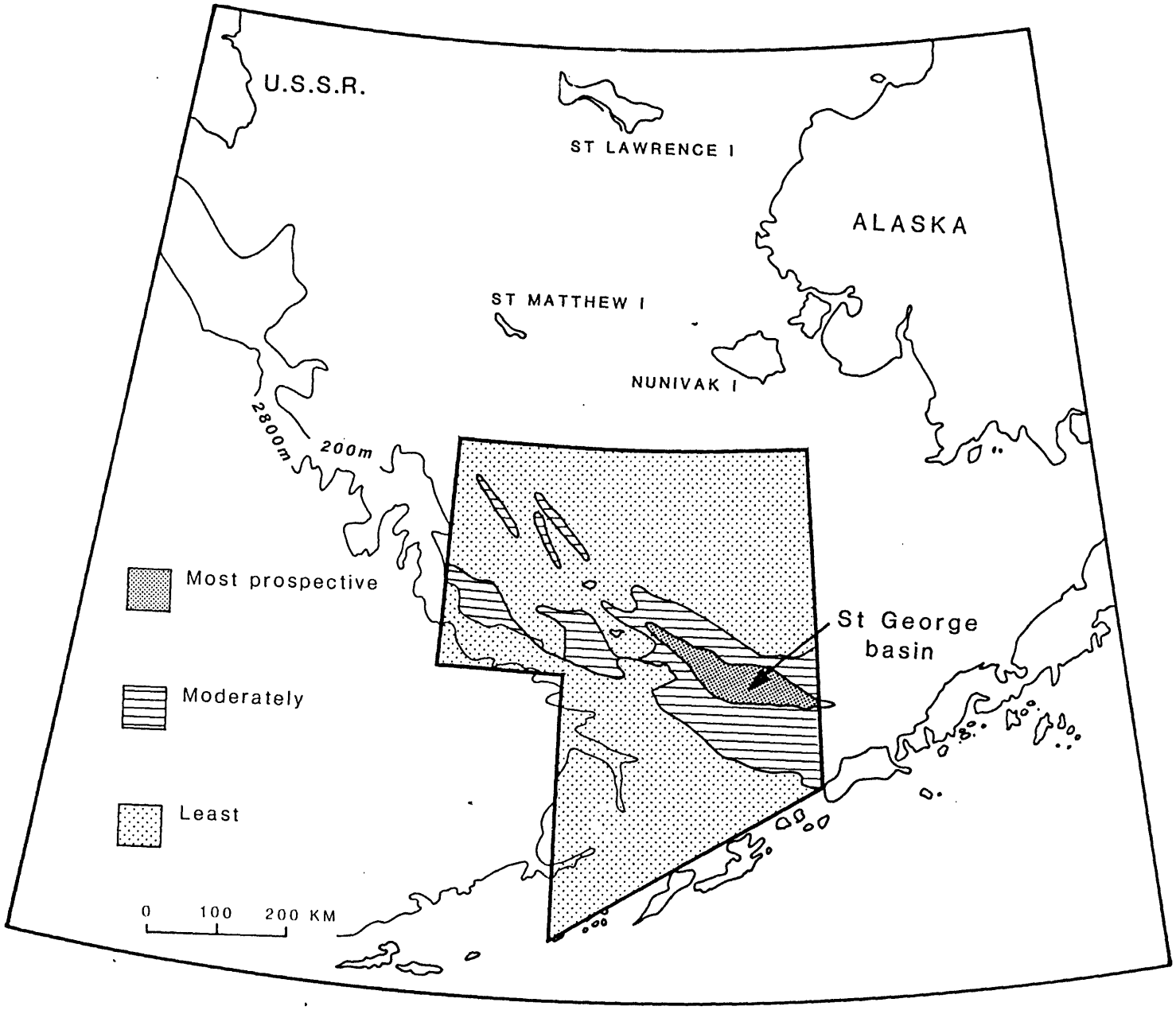

Figure 2. Ranking of areas in the St. George basin planning area as to potential for containing hydrocarbon deposits.

sedimentary rocks from the Aleutian Ridge and Umnak Plateau range from 0.50 to 0.66%. These rocks comprise nearly the entire 1 to 9 km thick sedimentary section above acoustic basement. Porosities of these rocks range from 14 to nearly 80%, like those measured along the continental slope. Permeability values in Oligocene sandstone (0.09 to 38 mdarcy) and middle Miocene to Holocene sandstone and mudstone (1.23 to 45 mdarcy) are variable.

Potential traps are associated with diapirs (shale?), thinning and onlap of older sedimentary horizons against basement, as well as growth structures within structural depressions beneath the continental slope and the summit of the Aleutian Ridge.

Temperature gradients (50-80 degrees °C/km), when projected downward into the 1 to 9 km thick sedimentary section, reach the onset temperature (75°) for hydrocarbon generation at 0.6 to 2.0 km sub-bottom. Consequently, most of the Umnak Plateau region has thermal potential for hydrocarbon generation.

Based on present information, the Umnak Plateau region must be considered a potentially important future hydrocarbon province. Further geologic and geophysical investigations are required to specify the location, amount, and types of hydrocarbons, if any, that may be present. Figure 3 shows those areas that have the greatest potential for economic development in the future as production technology advances into the deep water areas.

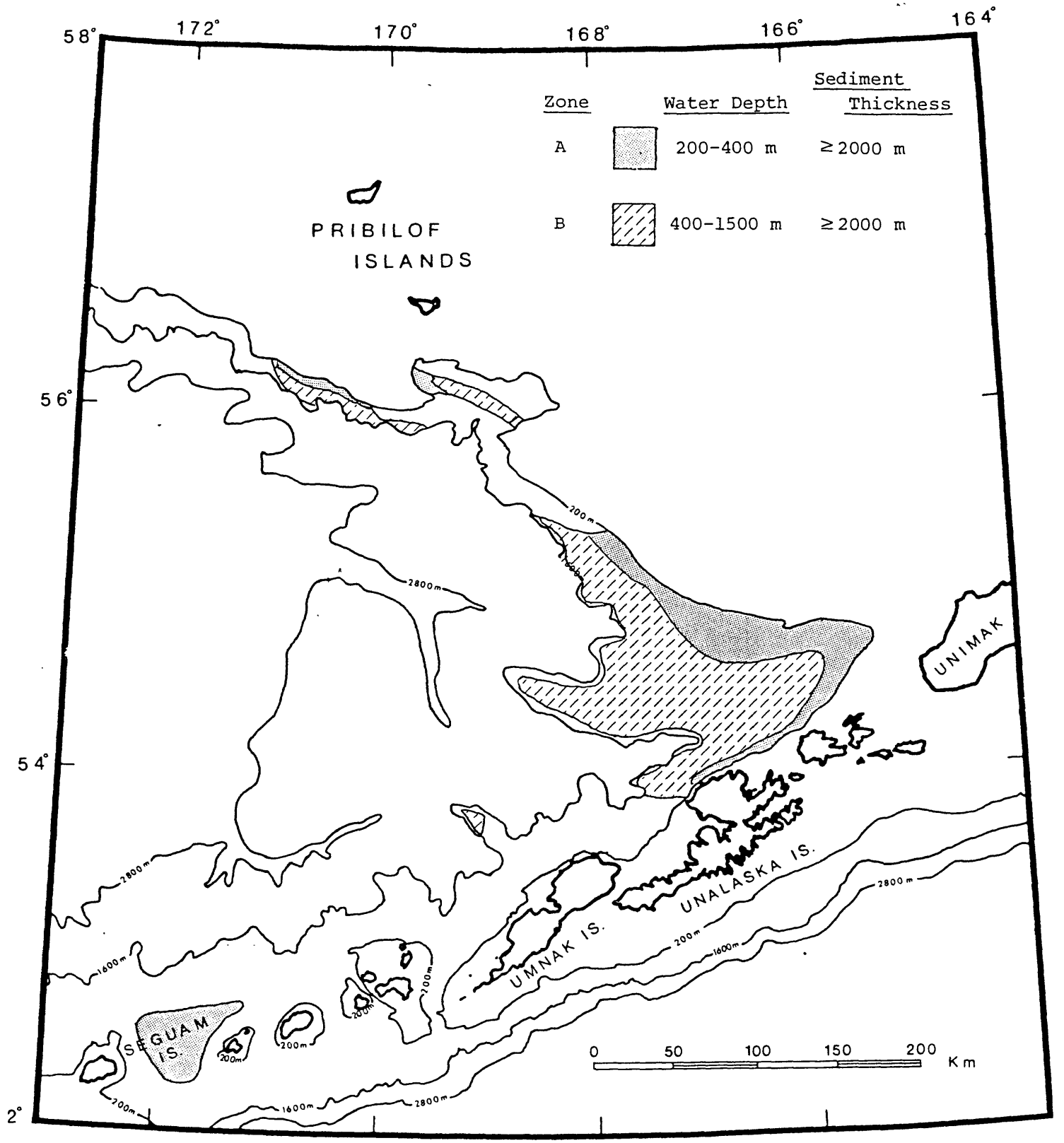

Figure 3. Prospective hydrocarbon areas of the Umnak Plateau region. The map shows areas that have the best prospects for hydrocarbon generation (sediment thickness greater than 2000 m or 6560 ft). Zone A shows areas where offshore production is currently feasible (water depths less than 400 m or 1300 ft). Zone B covers those areas where exploratory drilling is also presently feasible.

SECTION 1: ST. GEORGE BASIN AND SHELF

CHAPTER 1-1

GEOLOGICAL FRAMEWORK

Seismic Reflection Data

Marlow and others first delineated the elongate, sediment-filled St. George basin, that underlies the flat, shallow Bering Sea shelf and that trends northwest from near the southern Alaska Peninsula toward the Pribilof Islands (see Figs. 4 and 5; also see Figs. 2 and 7 in Marlow and others, 1976b). In that study, structure contours on acoustic basement derived from 3,000 km of single-channel seismic reflection data show this basin to be 300 km long, 50 km wide, and filled with more than 6.5 km of Cenozoic sedimentary rocks (Marlow and others, 1976b). Multi-channel seismic reflection data recently acquired and in part described below, show that this graben is much deeper and that it represents a mammoth extensional rift in the crustal rocks of the southern Bering Sea Shelf.

Profile 8B

A 24-channel seismic reflection profile across St. George basin, diagrammatically interpreted in Figure 4, shows several subshelf structures beneath the southern Bering Sea shelf and St. George basin.

The flat acoustic basement underlying the southwest end of profiles 8B (Fig. 4; between shotpoints 3200 and 2700) is Pribilof ridge, which is overlain by an undisturbed, layered sequence 1.3-1.4 km thick (1.3-1.4 sec). Within the acoustic basement, several gently dipping reflectors suggest that the basement includes folded sedimentary beds. Farther north, between shotpoints 2700 and 2200, the basement, descends in a series of down-to-basin steps, plunging to a maximum subbottom depth of about 5.4 seconds (over 10 km) beneath the axis of St. George basin. The overlying reflectors are broken by at least three major normal faults that dip toward the basin axis and appear to be related to offsets in the acoustic basement. Within the basin fill, the offset along the faults increases with depth, implying that these are growth structures. Strata are synclinally deformed about the basin's structural axis. The free-air gravity anomaly reaches a minimum of -1 mgal over the basin axis (a decrease of 55 mgal from the 54 mgal high over the basement high near shotpoint 1860).

From shotpoints 2200 to about 1860, the acoustic basement rises rapidly to a minimum depth of 0.55 second (0.5 km; Figs. 4 and 5). Again the overlying reflectors are broken by normal faults that dip down to the basin axis.

A gentle concavity in the basement extends from shotpoints 1860 to 1080; the maximum thickness of overlying strata is about 1.7 seconds (1.8 km) near shotpoint 1330. A corresponding relative gravity low of 41 mgal is centered over the swale. Intrabasement reflectors dip at a gentle angle to the surface of the acoustic basement (between shotpoints 1200 and 1400). Reflectors in the lower part of the overlying sedimentary section wedge out against the acoustic basement (between shotpoints 1500 and 1720).

Structure Contours

To convert two-way traveltime on the seismic reflection records to depths in meters or kilometers, we use a generalized velocity function: $D = 1.266t + 1.033t^2 - 0.117t^3$

where:

D = Depth of thickness in km

t = One-way traveltime.

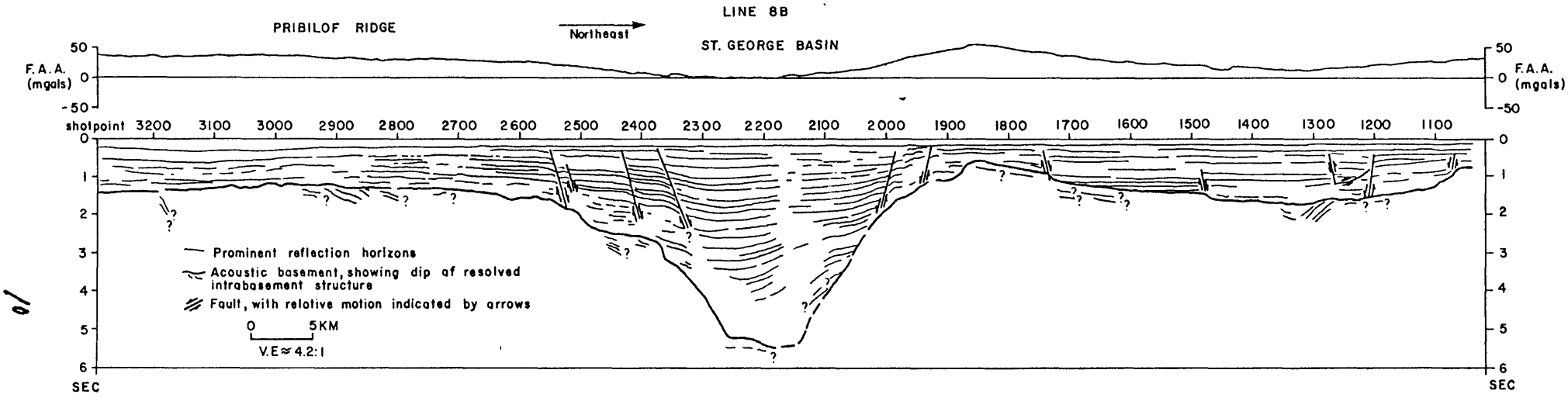

Figure 4. Interpretative drawing of a seismic-reflection profile published by Marlow and others (1977). Note that the vertical exaggeration applies only to the water layer (assumed velocity of sound in sea water of 1.5 km/sec) and will decrease with depth in the section. For location of profile see Figure 5.

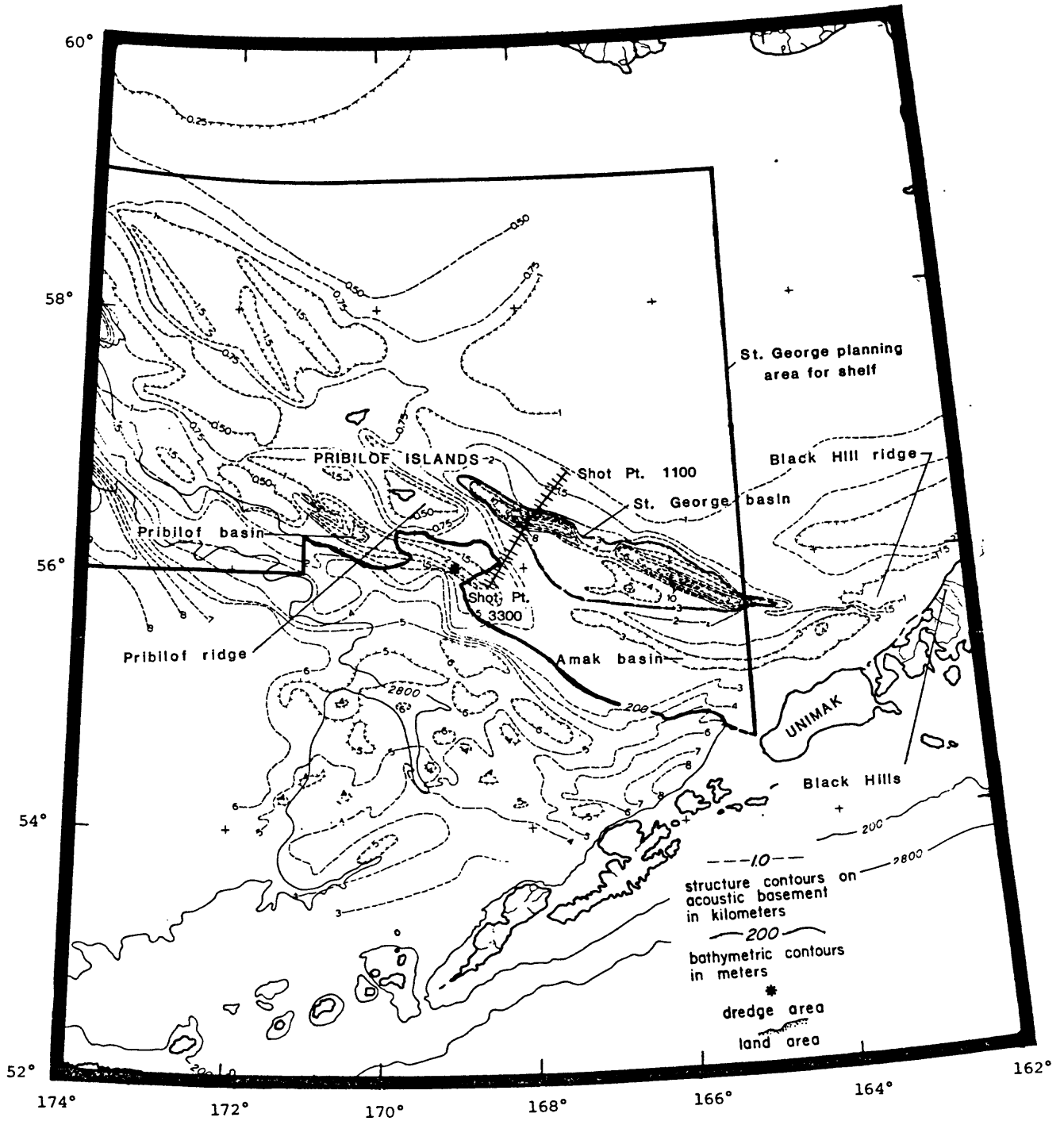

Figure 5. Sructure-contours of acoustic basement beneath the southern Bering Sea shelf. Derived in part from Scholl and others (1968), Scholl and Hopkins (1969), Marlow and others (1976a,b, 1977). Heavy solid line shows location of seismic-reflection profile interpreted in Figure 9.

This function was derived by fitting a polynomial curve to velocity data from 150 sonobuoy stations in the Bering Sea. The velocity function used here supersedes the curve published by Marlow and others (1976b).

Our new multichannel data show that St. George basin is filled near each end with more than 10 km of section. We do not know whether the section thickens toward the center of the basin. Two smaller basins, Amak and Pribilof basins, south of and parallel to St. George basin contain 3 to 4 km of layered fill (Fig. 5).

Northwest of St. George basin, the shelf is underlain by a complex of smaller basins and ridges, also parallel to the margin (Fig. 5; Marlow and others, 1976b). Most of these basins, like St. George basin, are structural grabens or half-grabens bordered by normal faults. The largest structural high or ridge in the western basement complex, the Pribilof ridge, is subaerially exposed in the Pribilof Islands (Fig. 5). To the southeast, the ridge flanks the southern side of St. George basin and extends toward the Black Hills ridge and the Alaska Peninsula (Fig. 5; also see Figs. 2 and 7 in Marlow and others, 1976b).

South of St. George basin, the acoustic basement deepens monoclinally toward the Aleutian Island arc, reaching depths greater than 8 km below sea level, within 20 km of Aleutian Ridge (Fig. 5; also Figs. 2 and 7 in Marlow and others, 1976b). Unfortunately, we do not have enough seismic reflection data to determine the structural relation between the basement complex of the Bering Sea margin and the presumably younger Aleutian Island arc (Scholl and others, 1975).

Geopotential Data

Gravity Data

A free air gravity anomaly map of the St. George basin area is shown in Figure 6. A regional map of the Bering Sea region that includes this area has been published by Watts (1975). The irregular gravity low extending from the tip of the Alaska Peninsula northwestward toward the Pribilof Islands outlines St. George basin (Fig. 6). The southeastern end of the low, adjacent to the peninsula, is the signature of a separate basin, Amak basin (Fig. 5, Marlow and others, 1976b). Immediately north of the Amak basin gravity low, a linear, 50-70 mgal gravity high extends about 70 km west of the Black Hills region of the Alaska Peninsula (Fig. 6). This high anomaly appears to turn and trend northwest along the southern flank of the gravity low associated with St. George basin, suggesting that the Jurassic rocks of the Black Hills area extend along the southern flank of St. George basin. Furthermore, the structural and gravity data (Figs. 5 and 6) imply that Pribilof ridge extends from the Pribilof Islands along the south flank of St. George basin.

Magnetic Data

Figure 7 is a reproduction of a portion of a total-field magnetic anomaly map of the Bering shelf published by Bailey and others (1976). The St. George, Amak, and Bristol Bay basin complex is characterized by low-frequency, low-amplitude anomalies. This band of anomalies extends north-westward from the Alaska Peninsula to the Pribilof Islands area.

North of the low-amplitude, low frequency anomaly belt, an accurate zone of high-amplitude, high-frequency anomalies is traceable from east to west (Fig. 7). This belt of high anomalies is part of a larger, arcuate zone of similar anomalies that swings across the central and inner Bering Sea shelf

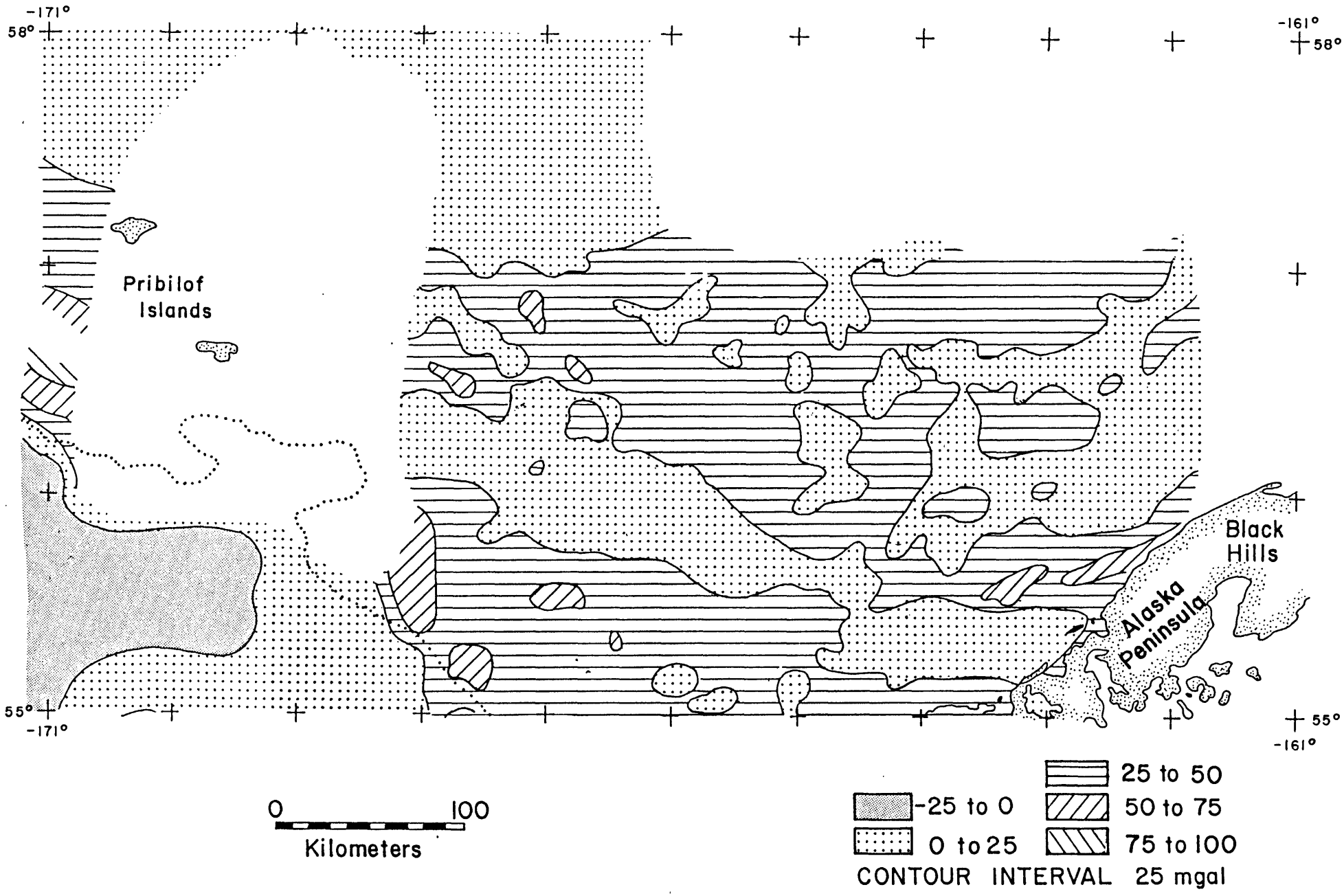

Figure 6. Map of free air gravity anomalies derived from Pratt and others (1972) and Watts (1975). Land areas shown by stipple pattern. Two hundred meter bathymetric contour shown by dotted line.

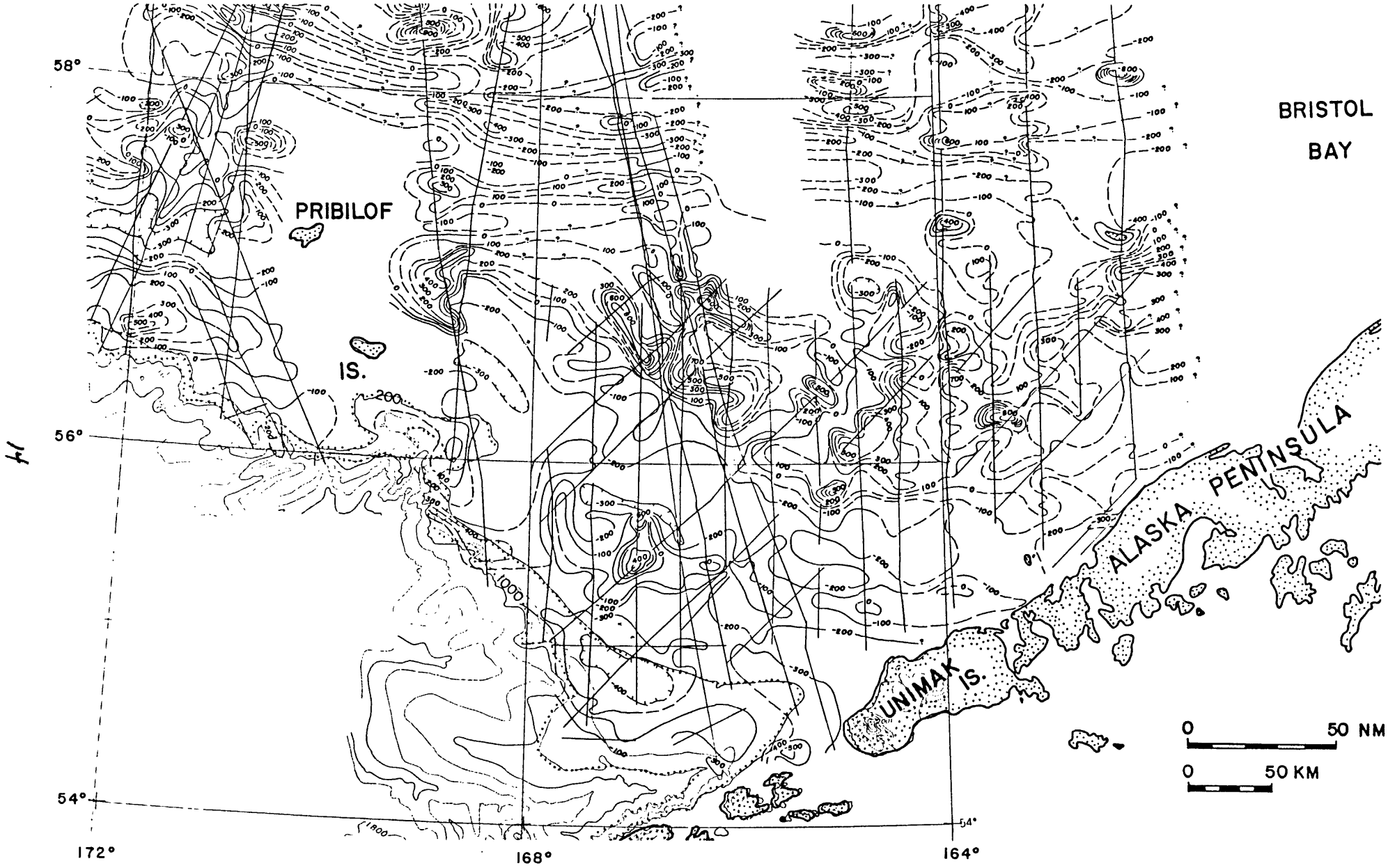

Figure 7. Map of total-field magnetic anomalies derived from Bailey and others (1976). Contour interval is 100 gammas. Individual profiles have been upward-continued to an elevation of one kilometer. Bathymetry in meters shown by dotted lines.

(Marlow and others, 1976b).

Geologic History

Mesozoic Structural Trends

Gravity, magnetic, seismic reflection, and dredge data suggest that the Upper Jurassic shallow-marine rocks exposed in the Black Hills on the Alaska Peninsula extend west to northwest along the south flank of St. George basin and connect with Pribilof ridge (Fig. 5). In addition, Upper Cretaceous (Campanian) rocks were dredged from the southern flank of this ridge in nearby Pribilof Canyon (Fig. 5; Hopkins and others, 1969). Seismic reflection data suggest that the Cretaceous dredge samples may have been recovered from a relatively isolated intra-basement basin perched on the southwest flank of Pribilof ridge. Other dredge samples from the margin west of Pribilof ridge show that the Mesozoic basement complex is unconformably overlain by shallow-water, diatomaceous mudstone of early Tertiary age (Marlow and others, 1979a,b). This belt of upper Jurassic rocks apparently occupied the former site of the Mesozoic margin of the Bering Sea and was a resistant high that began to collapse in early Tertiary time.

We speculated earlier that a Jurassic, Cretaceous, and earliest Tertiary magmatic arc extended parallel to and inside (landward to the east towards Alaska) of the outer belt of shallow-water deposits (Marlow and others, 1976b). This igneous belt is characterized by high-amplitude, high-frequency magnetic anomalies (Fig. 7). The magmatic arc is exposed as calc-alkalic volcanic and intrusive rocks of late Mesozoic and earliest Tertiary age on St. Matthew and St. Lawrence Islands on the Bering Shelf and as similar rocks in southern and western Alaska and eastern Siberia (Fig. 8; Patton and others 1974, 1976; Reed and Lanphere, 1973; Scholl and others, 1975; Marlow and others, 1976b).

Tertiary Deactivation and Crustal Collapse

In 1975 and 1976 we postulated that the arcuate geosynclinal and magmatic trends of the Bering Sea margin resulted from convergence and subduction of oceanic lithosphere (Kula (?) plate) beneath the Bering Sea continental margin, (Cooper and others, 1976a; Scholl and others, 1975; Marlow and others, 1976b). Thus, we predicted that either deep-water trench or slope deposits would have accumulated along the former base of a Mesozoic convergent margin. However, rocks dredged in 1978 suggest that the margin is composed, in part, of a resistant basement high that was emergent, from Late Jurassic to early Tertiary time (Marlow and others, 1979a,b). If former Mesozoic trench or slope deposits do exist, then they must be buried beneath the thick sediment accumulations now draping the base of the margin (Cooper and others, 1981). Alternately, the former Mesozoic margin may have been the site of predominantly strike-slip motion or oblique subduction until early Tertiary time. Thus, the former Mesozoic slope deposits may have been tectonically "rafted" to the northwest, perhaps into Siberia.

Plate motion along the Mesozoic Bering Sea margin apparently ceased with the formation of the Aleutian Island arc in late Mesozoic or earliest Tertiary time, when the subduction zone (transform fault?) shifted from the Bering Sea margin to a site near the present Aleutian Trench, thereby trapping a large section of oceanic plate (Kula?) within the abyssal Bering Sea. Cessation of plate motion apparently tectonically deactivated convergence or transform faulting along the Bering Sea margin. In early Tertiary time, the margin

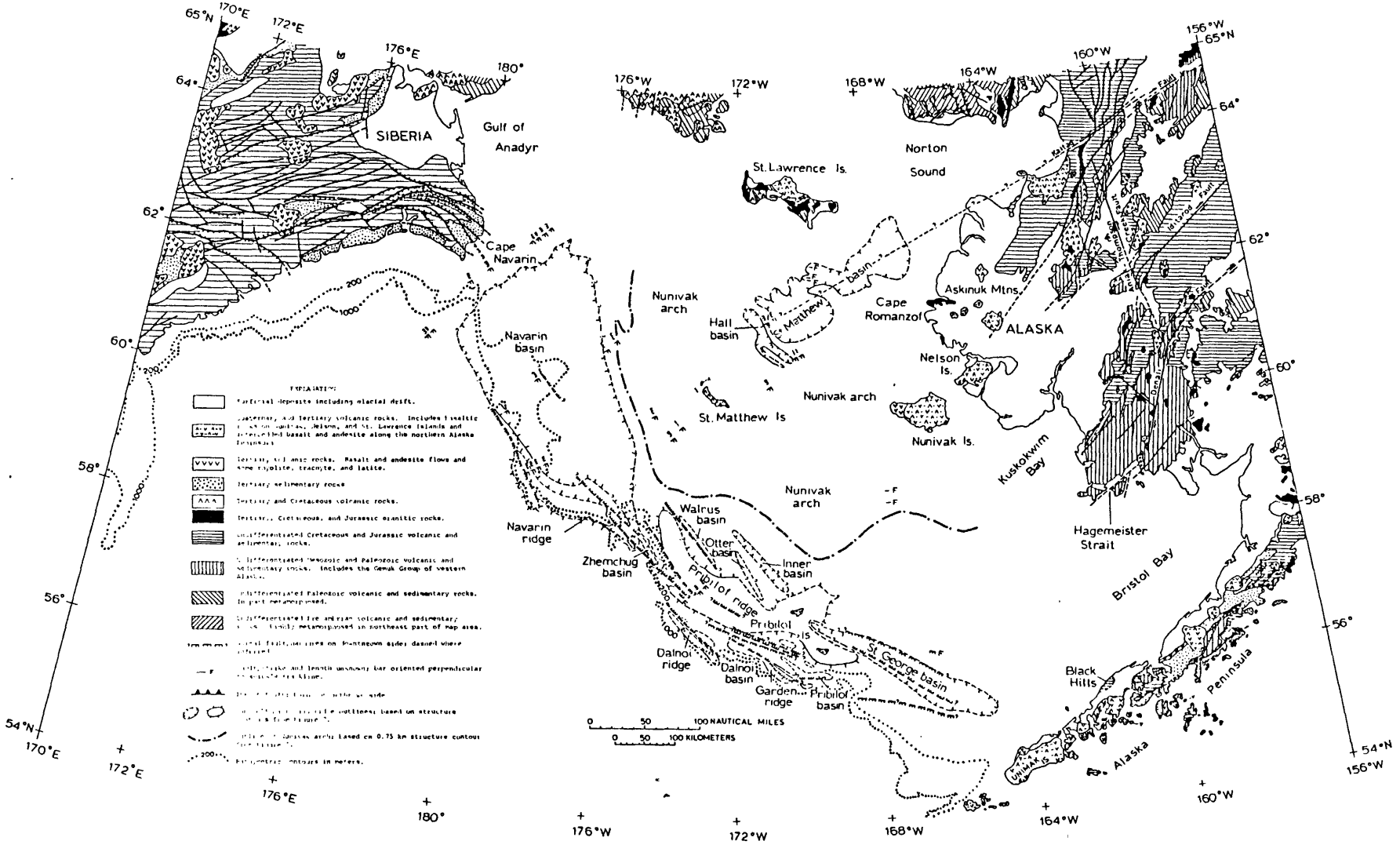

Figure 8. Generalized geologic map of western Alaska, the Alaska Peninsula, and eastern Siberia. Onshore geology is modified from Burk (1965), Bechman (1974), and Yanshin (1966). Offshore outlines of subshelf basins, ridges, and Nunivak arch from Marlow and others (1976a). The offshore extension of Kaltag Fault is diagramatic in that the expression of the fault beneath the shelf may include all of St. Matthew basin.

underwent extensional collapse and differential subsidence, which has continued during most of Cenozoic time.

Elongate basins of great size and depth, exemplified by St. George basin, formed near the modern outer Bering Sea shelf (Figs. 4 and 5; Marlow and others, 1976b). Extensional deformation of the folded rocks of the Mesozoic basement has continued to the present as evidenced by growth-type normal faults that flank the outer shelf basins and commonly rupture the entire Cenozoic basin fill. Collapse of the continental margin may have been aided by cooling and Cenozoic sediment-loading of the oceanic crust (Kula(?) plate) flooring the abyssal Bering Sea.

New Data

In 1982, the U.S. Geological Survey acquired a new geophysical profile across St. George basin (Fig. 9). The data include a 24-channel seismic reflection profile and five seismic refraction stations shown in Figure 9.

The seismic reflection data show that St. George basin around Line 2 is an asymmetric half-graben filled with about 3.5 seconds (5 km) of stratified section, which is down-faulted by normal faulting along the southwest side of the basin (Fig. 9). A sonobuoy refraction station near the basin axis shows the fill in the basin increases downward in velocity from 1.6 km/sec near the seafloor to over 4.0 km/sec at the base of the fill. This stratified section overlies a major unconformity cut into the bedrock of the shelf. Bedrock beneath the uncomformity has refractors with compressional velocities of 4.7 to over 7 km/sec and has scattered, dipping reflectors (Fig. 9).

The stratified section southwest of St. George basin dips and thickens to the southwest, reaching a thickness of about 4.5 seconds (5.4 km) at the end of the line. Compressional velocities within the bedrock near this end of the line are 4.8, 6.1, and 6.8 km/sec.

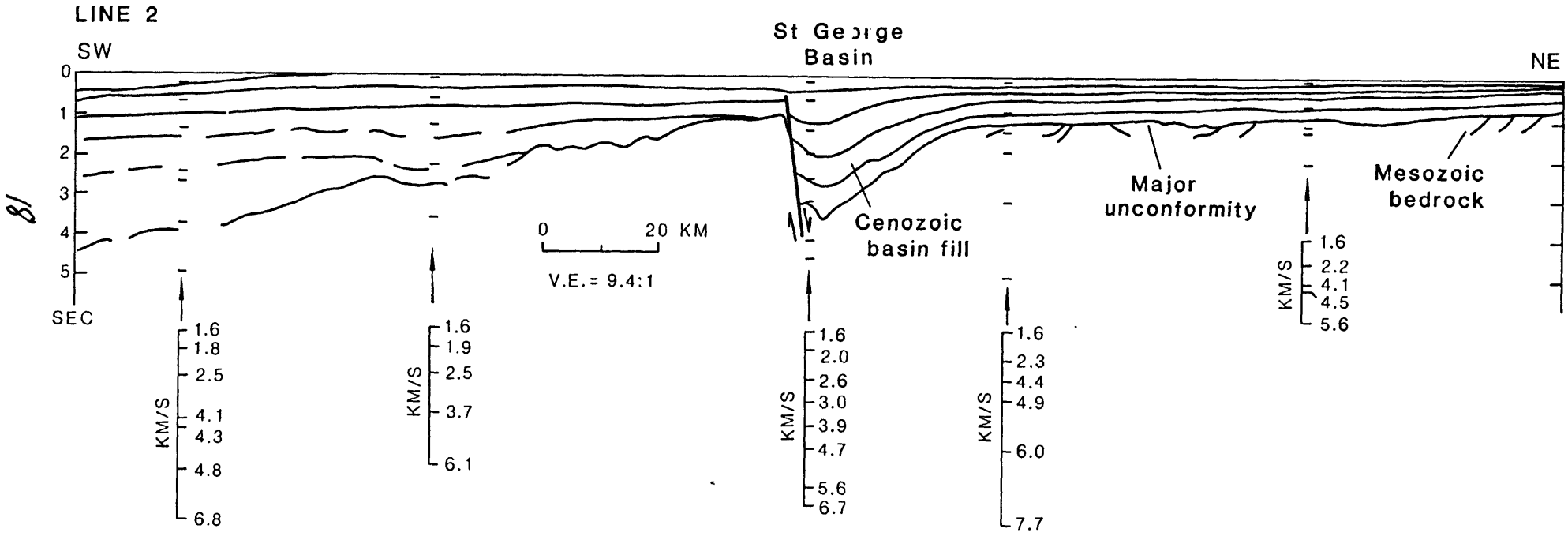

Figure 9. Interpretative drawing of seismic reflection Line 2. Tick marks and velocity values are sonobuoy refraction stations. Travel time is two-way time in seconds. See Figure 20 for location.

CHAPTER 1-2
PETROLEUM GEOLOGY
Alaska Peninsula

Drilling History

Since 1959, nine onshore wells have been drilled along the northern coastal lowland area of the Alaska Peninsula, and two offshore COST wells have been drilled in the St. George basin. For descriptive purposes, the wells on the Alaska Peninsula are divided here into a northern group of four wells that bottomed in volcanic or granitic rocks, and a southern group of five wells that bottomed in either Tertiary or Mesozoic sedimentary rocks.

The northern group includes the General Petroleum Great Basins No. 1 and 2, Great Basins Ewerath Ugashik No. 1, and the Gulf-Alaskco Port Heiden No. 1 (Fig. 10). The southern group included the Gulf Sandy River Federal No. 1, Pan American Hoodoo Lake No. 1 and 2, Pan American David River No. 1-a, and the Amoco Cathedral River No. 1 (Brockway and others, 1975).

In the northern group of wells, the thickness of the flat-lying Tertiary sequence varies from about 1220 m to 3350 m and consists of interbedded non-marine to shallow marine sandstone, siltstone, claystone and coal (Hatten, 1971). Granitic basement penetrated by the General Petroleum Great Basins No. 1 and 2 wells has been dated radiometrically as about 177 m.y. old (late Early Jurassic). Radiometric ages from the volcanic sequence underlying the flat-lying Tertiary sedimentary rocks in the Gulf Port Heiden and Great Basins Ugashik wells range from 33 to 42 m.y. old (Brockway and others, 1975; Oligocene to late Eocene, according to the time scale of Berggren, 1969). No significant shows of oil or gas have been reported from the northern group of wells. To the south the Gulf Sandy River well encountered gas associated with coal in the middle part of the Bear Lake Formation (Miocene) between 1970 and 1940 m. Oil and gas shows were also encountered in the basal sandstone beds of the Sandy River well. However, in this well the oil encountered within the basal portion of the Bear Lake Formation may have been derived from source rocks within the underlying Stepovak Formation (Oligocene).

In offshore areas where the flat-lying Cenozoic sequence overlies older, folded and truncated sedimentary rocks, such as the Mesozoic strata of the Black Hills, oil may have migrated upward into the more porous sandstone beds of the overlying Bear Lake Formation. The possibility of oil and gas migration from older sedimentary formations renders the offshore area between Port Moller, Amak Island and the Pribilof Islands more prospective than the area north of Port Heiden, where the basement consists of volcanic and granitic rocks. The offshore arcuate gravity and magnetic discontinuity described by Pratt and others (1972), which extends from the Pribilof Islands toward Port Moller (Fig. 6 and 7), may define two different basement rock types beneath the flat-lying Cenozoic sequence. The high-amplitude magnetic anomalies on the northeast side of the discontinuity may represent volcanic or granitic and metamorphic basement rock, and the low-amplitude anomalies on the southwest side may reflect a thick sequence of early Tertiary or late Mesozoic sedimentary rocks. The flat-lying sequence of Cenozoic sedimentary rocks is locally folded and uplifted along the foothill belt of the Alaska Peninsula. Further offshore the strata may be depositionally draped over fault blocks within the acoustic basement (Hatten, 1971). Data on the size and extent of such structures are not available. The rocks considered to have the greatest petroleum potential in the offshore area of St. George basin are flat-lying to

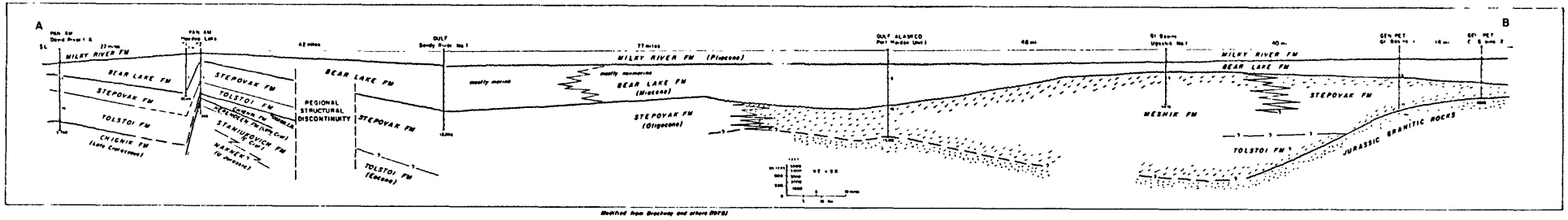

Figure 10. Generalized stratigraphic cross-section of Bristol Bay basin along the Alaska Peninsula. Modified from Brockway and others (1975).

gently folded Cenozoic sandstone, siltstone, and shale beds. These rock units probably range in age from Eocene to Holocene.

Source Beds

The best source rocks in the Tertiary sequence appear to be the black marine siltstone and shale beds in the Oligocene Stepovak Formation. On the Alaska Peninsula, the Stepovak Formation is locally at least 4500 m thick (Burk, 1965). Scattered shows of oil and gas in Stepovak rocks have been reported from three Alaska Peninsula wells, Gulf Sandy River, Pan American Hoodoo Lake No. 2, and Pan American David River 1-A (Fig. 10; Brockway and others, 1975). Potential source rocks may also occur in the Miocene Bear Lake Formation because locally the basal portion containing marine siltstone and shale may have been buried deep enough to generate hydrocarbons. Marine shale of Late Jurassic and Late Cretaceous age might also be considered as potential source rocks. These rocks are often in angular discordance with overlying Cenozoic sandstone reservoir beds.

Core chips and drill cuttings from eight of the nine wells drilled along the Bering Sea lowlands of the Alaska Peninsula were subjected to lithologic and paleontologic analyses by McLean (1977). Results suggest that at least locally, sedimentary rocks of Tertiary age (excluding Paleogene strata) contain oil and gas source and reservoir rocks capable of generating and accumulating liquid and gas hydrocarbons.

Paleogene strata on the Alaska Peninsula are rich in organic carbon but they are immature. However, strata in offshore basins to the north and south (St. George and Bristol Bay basins) may have been subjected to a more productive thermal environment. Total organic carbon content of fine-grained, Neogene strata appears to be significantly lower than in Paleogene rocks, possibly reflecting nonmarine or brackish water environments of deposition. Neogene sandstone beds locally yield high values of porosity and permeability to depths of about 2,439 m (8,000 feet; McLean, 1977). Below this depth, reservoir potential rapidly declines.

The General Petroleum, Great Basins No. 1 well drilled along the shore of Bristol Bay reached granitic rocks. Other wells drilled closer to the axis of the present volcanic arc indicate that both Tertiary and Mesozoic sedimentary rocks have been intruded by dikes and sills of andesite and basalt. Although the Alaska Peninsula has been the focus of igneous activity throughout much of Mesozoic and Tertiary time, thermal maturity indicators such as vitrinite reflectance and coal rank suggest, that on a regional scale, sedimentary rocks have not been subjected to abnormally high geothermal gradients.

Lyle and others (1979) studied 14 stratigraphic sections totaling 5,000 m along the Alaska Peninsula. They found that 63 percent of the total measured stratigraphic section contains potential Tertiary reservoir sandstone. However, the porosities and permeability for these sandstones were generally low in most areas because of pervasive pore-filling mineralization. The best preserved and most probable reservoir rocks are sandstone beds in the Bear Lake Formation of Miocene age. In studying potential Tertiary source rocks, Lyle and others (1979) found that the total organic carbon for their samples ranged from less than 0.2 to 8.0 percent, that the hydrocarbon C_{15+} extracts averaged 362 ppm, that the major or organic constituents are herbaceous-spore debris, and that most samples have a thermal alteration index of 2- to 2+. They concluded that dry gas is the most probable hydrocarbon to form in Tertiary source rocks on the Alaska Peninsula.

Reservoir Beds and Seals

The rocks that have the greatest reservoir potential for oil and gas in the offshore area of Bristol Bay and St. George basins are probably the sandstone units equivalent to the Bear Lake Formation of middle to late Miocene age (Lyle and others, 1979). Bear Lake sandstone beds are both marine and nonmarine and contain a combination of volcanic grains, dioritic grains and chert, and sedimentary lithic fragments. Most of the sandstones could be classified as lithic subgraywackes and others as lithic arenites (Burk, 1965). Shows of oil and gas have been reported from the basal Bear Lake Formation sandstones in the Gulf Sandy River and Pan American David River wells.

Sandstones in the older Tertiary formations, Tolstoi and Stepovak, have an abundance of volcanic detritus as well as matrix clay. These rocks are dense and highly indurated and thus are not considered good reservoir beds.

Traps and Timing

Most of the potential oil and gas traps in the offshore St. George basin area are probably anticlinal structures. Anticlines in the Cenozoic sequence are primarily formed by draping and differential compaction of strata over eroded and block-faulted highs that developed within the acoustic basement complex. The resultant structures are probably large in area but have a limited amount of closure. Structural traps in the offshore area probably formed during the early filling of St. George basin. Most structures appear to decrease in amplitude upward through the Cenozoic section, and the upper 100 to 200 m of strata are often flat-lying and undeformed.

Stratigraphic traps formed by buttress onlap during transgression around topographic highs, by local truncation of sandstone beds, and by lenticular sandstone bodies probably occur in the Cenozoic sequence, but their size and number are unknown.

Western Alaska

Drilling History

The petroleum potential of the Bethel and Nushagak basins is difficult to assess because the bulk of prospective rocks are concealed by a thick mantle of alluvial deposits and only one exploratory well has been drilled in the area. In the 1961, Pan American Oil Company drilled the Napatuk Creek No. 1 well to a depth of 4500 m (14,877 feet) about 56 km west of Bethel (Fig. 11). No hydrocarbon shows were reported in the well. The well penetrated about 300 m of Quaternary sediment that unconformably overlies a relatively flat-lying sequence of Upper Cretaceous graywacke and shale. Several mafic volcanic dikes of unknown age were encountered in the Cretaceous section. Rapid facies changes have been noted within the Kuskokwim Group and thus, adequate reservoir rocks may occur elsewhere within the Bethel basin (Hoare, 1961). Reconnaissance aeromagnetic data show that the maximum depth to magnetic basement in the vicinity of the Napatuk Creek No. 1 well is about 6100 m (20,000 feet); therefore about 1600 m (5,000 feet) of Cretaceous rocks remain undrilled below the bottom of the well.

No wells have been drilled in the Nushagak basin. Limited outcrop data from around the margin of the basin suggest that pre-Tertiary rocks have a limited petroleum potential because they are highly indurated and deformed. No data are available on the thickness of Cenozoic rocks underlying the Nushagak lowlands.

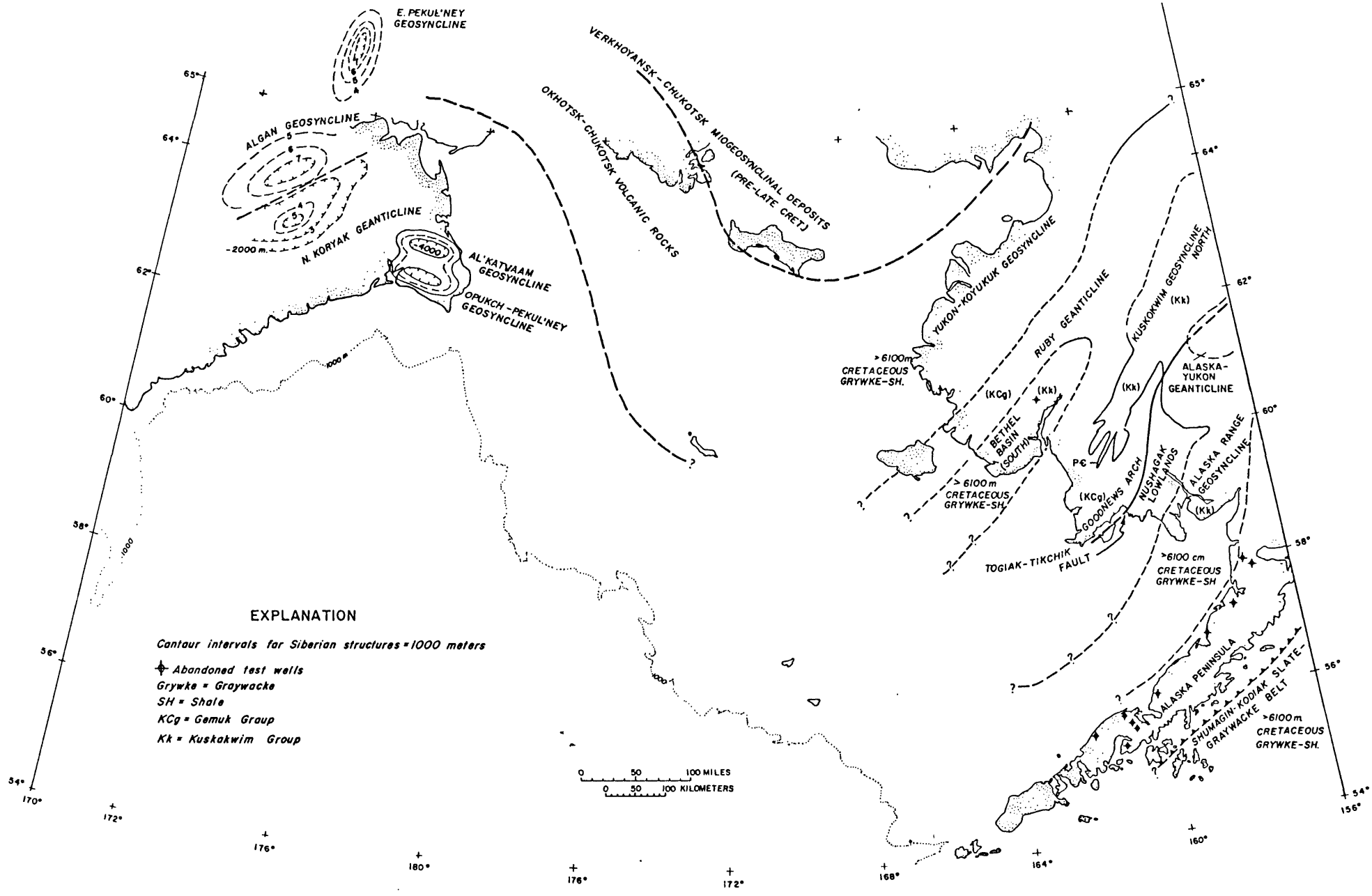

PRESENT DISTRIBUTION OF MIDDLE EARLY TO MIDDLE LATE CRETACEOUS BERING SEA SEDIMENTARY BASINS

Figure 11. Tectonic map showing distribution of middle Early to middle Late Cretaceous Alaska and Bering Sea geosynclines and geanticlines. Based on data from Agapitov and Ivanov (1969), Burk (1965), Hoare (1961), Pratt and others (1972), and Patton and others (1976).

St. George Basin

Source beds

Little is known about possible source beds in the St. George basin.

Rocks dredged from the Beringian continental slope include lithified volcanic sandstone of Late Jurassic age, mudstone of Late Cretaceous age, and less consolidated deposits of early Tertiary age. Cretaceous mudstone dredged from Pribilof Canyon contains as much as 1 percent organic carbon (Marlow and others, 1976b, p. 179). Geochemical analyses of some of these rocks are listed below:

Table 1. Geochemical analyses of rocks dredged from the Bering Sea Continental Margin. See Marlow and others (1976b) for locations.

Sample Number	Lithology	Age	Organic carbon (Wt%)	Pyrolytic hydrocarbon (Wt. %)	Vitrinite reflectance (Avg. %)
S6-77-BS					
DR1-20	Volcanic sandstone	L. Jurassic	0.79	0.24	0.38
DR1-26	Volcanic sandstone	L. Jurassic	0.26	0.01	1.14
TT-1-021					
001	Mudstone	L. Cretaceous	0.62	0.11	.40
L5-78-BS					
5-5	Sandstone	L. Jurassic	0.27	0.02	.63
2-3	Mudstone	Paleogene	0.33	0.02	.41
16-9	Mudstone	M. Eocene	0.83	0.04	.31

Pyrolytic analyses of these rocks show that none are good source beds for petroleum. However, outcrops sampled by rock dredging are generally sandy units, and may not have sampled fine-grained source beds that could be present either along the margin or within the subshelf basins.

Other Tertiary mudstones have been dredged from the continental slope; these rocks commonly contain more than 0.25 percent organic carbon (Marlow and others, 1976b, p. 178). However, many of these rocks crop out too far down on the continental slope to be representative of the sediment sections in the basins. Because the stratigraphically lower basin beds wedge out against the flanks of the basins, correlative outcrops are virtually unknown along the nearby continental slope.

Reservoir beds

The Cenozoic samples are generally porous - probably because of abundant diatom frustules. The porosities of Eocene to Pliocene-Pleistocene rocks dredged from 15 sites along the Bering Sea continental margin range from 14 to 70 percent (avg. 44 percent; Table 2). The permeability of these rocks is variable, probably because of submarine weathering and cementation effects.

These Cenozoic outcrops can be traced as seismic reflectors to the subshelf basins, where, if the beds remain diatomaceous, good potential reservoir beds may occur. The dredge samples may therefore be equivalent to the upper sedimentary section in St. George basin, implying that good reservoir beds may be present in the basin. Neogene reservoir rock beds of

shallow-water origin are also likely to be present in St. George basin because sedimentation has matched subsidence, which averaged 100 to 200 m/106 yr during Cenozoic time (Marlow and others, 1976b). The thick sections of the basins beneath the Bering Sea shelf accumulated near the mouths of major Alaska and Siberian rivers, including the Yukon and Kuskokwim. During Neogene time, the shelf was swept by numerous marine transgressions and regressions (Hopkins, 1967; Hopkins and Scholl, 1970). All these factors suggest the likely deposition of neritic and deltaic strata and hence good reservoir beds in the basin.

Table 2. Physical properties of rocks dredged from the Bering Sea continental margin. For location, see Marlow and others (1976b, 1979b).

Sample number	Lithology	Age	Permeability (md)	Porosity (%)
70-B93-3*	Calcareous wacke	Pliocene-Pleistocene	--	14.0
70-B101-1S2*	Diatomaceous mudstone	L. Miocene	--	59.0
70-B97-1S1*	Diatomaceous siltstone	M. or L. Miocene	--	57.0
L5-78-BS-28-1	Sandy mudstone	L. Miocene	1.35	54.5
L5-78-BS-9-2	Glauconitic mudstone	L. Middle Miocene	29.00	34.4
L5-78-BS-7-3	Mudstone	M. Miocene	1.67	57.4
L5-78-BS-2-5	Diatomaceous mudstone	E. Miocene	0.92	40.9
L5-78-BS-5-3	Diatomaceous mudstone	E. Miocene	1.49	22.0
L5-78-BS-6-7	Diatomaceous mudstone	L. Oligocene or E. Miocene	1.75	61.1
L5-78-BS-2-4	Sandy mudstone	L. Oligocene	5.46	68.3
L5-78-BS-2-11	Calcareous siltstone	L. Oligocene	1.25	45.1
L5-78-BS-5-10	Andesite tuff	L. Oligocene	19.00	50.7
70-B97-1S2	Pebbly conglomerate	M. Oligocene	--	29.0
L5-78-BS-4-3	Diatomaceous mudstone	E. Oligocene(?)	9.67	46.9
L5-78-BS-16-12	Mudstone	Eocene(?)	0.77	57.0
L5-78-BS-27-1	Sandy Siltstone	Eocene(?)	3.61	55.9
L5-78-BS-22-2*	Glauconitic sandstone	--	8.43	70.6
70-B92-3S1*#	Calcareous argillite	--	--	21.0
70-B92-3S2*#	Lithic wacke	--	--	21.0
690B92-3S5*#	Lithic wacke	--	--	17.0

Note: * These values from Marlow and others (1976b). No permeability values measured.

\# No age given because of a lack of diagnostic fossils.

CHAPTER 1-3
REGIONAL HAZARDS
Introduction

Major potential geologic hazards in the area of St. George basin include faulting and earthquakes, sea floor instability because of erosion and slumping, volcanic activity, and ice. This section on environmental hazards is derived mainly from Gardner and others (1979) and Marlow and others (1979b), although some parts are taken from Lisitsyn (1966), Askren (1972), Nelson and others (1974), Sharma (1974), and Marlow and others (1976a,b). Faulting and sea floor stability are probably the greatest potential hazards in the region, although other hazards may be important locally.

Seismicity and Faulting

Classification of Faults

Two aspects of faults provide a basis for their evaluation as potential hazards - their magnitude and their recency of movement. Magnitude can be estimated from the amount of offset and recency of movement can be determined by the age of the strata that are displaced. Faults that offset the sea floor must be considered as potentially active.

The following seismic reflection systems were used to delineate faults in this area: 1) 3.5 kHz; 2) 1.5 kHz; 3) single-channel seismic reflection (60 KJ to 160 KJ sparker, and up to 1326 in^3 air-gun sources); and 4) 24- channel system using a 1326 in^3 air gun array. The resolutions of the seismic systems, which determine the minimum offset we can detect with each system, are shown in Table 3. The resolutions were calculated using the velocity of sound in water and by following the procedures of Moore (1969).

Table 3. Ranges of resolution for seismic systems.

Peak Frequency	Range of Minimum Resolution (m)
40 Hz (multichannel)	9.4 to 28.1
100 Hz (single channel)	3.2 to 11.2
1.5 kHz	0.15 to 0.5
3.5 kHz	0.1 to 0.3

Faults are classified as surface, minor, and major faults. Surface faults are any faults detected that offset the surface of the sea floor. In St. George basin, these faults offset are resolved on 1.5 kHz and/or 3.5 kHz records, but not on single or multichannel seismic reflection profiles. These faults typically displace reflectors less than 0.006 sec (5 m). Most minor faults are close to but do not break the sea floor; in places sediment drapes over these features. Major faults are defined as those resolved on multichannel and single-channel seismic reflection profiles. These faults generally are growth structures and many displace the acoustic basement. A subcategory of major faults are boundary faults; these are major faults that mark the boundaries of St. George basin.

Fault Distribution

Distribution of faults is shown in Figure 12. The strike of most faults is unknown because of the relatively wide spacing of tracklines. Faults found on northeast-southwest tracklines, perpendicular to the long axis of St. George basin, greatly outnumber those observed on northwest-southeast

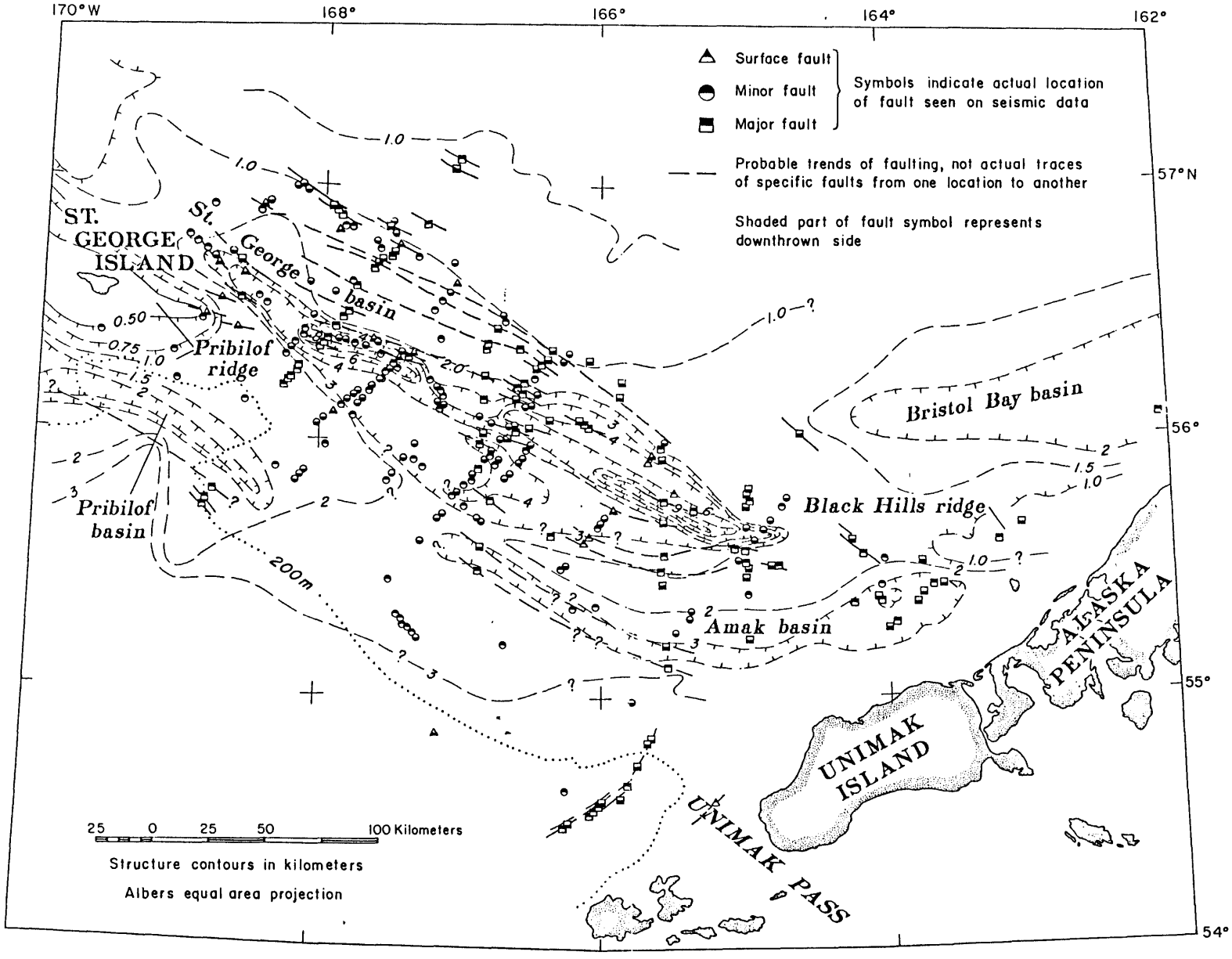

Figure 12. Distribution of faults in the southern Bering Sea. Lines through fault symbols are inferred trend of the fault, not any known strike. Structure-contours of acoustic basement from Figure 4.

tracklines which indicates that the majority of the faults have a northwest-southeast trend and parallel the trend of the basin. Faults bounding St. George basin can be confidently traced between tracklines. We believe that most faults beneath the shelf and those in St. George basin in particular, trend northwest-southeast parallel to the basin and to the margin.

Boundary faults clearly delineate St. George basin, and the north side of Pribilof ridge. These faults are normal faults, occur in groups, and exhibit increased offset with depth, which indicates growth-type structures. These faults in many places cut nearly all of the sedimentary sections, and often offset acoustic basement, but rarely offset the sea floor.

Major faults (other than boundary faults) principally occur within St. George basin, although a few occur within Amak basin (Fig. 12). This class of fault decreased in abundance toward the Pribilof Islands. Major faults show displacements that generally are much less than the larger boundary faults but offsets greater than 0.08 sec (60m) occur in the central region of St. George basin. Major faults are not always offset in the same sense as adjacent boundary faults.

Surface faults tend to be more abundant along the southern side of St. George basin and along Pribilof ridge than in the center of the basin (Fig. 13). Most surface faults can be traced from high-resolution to low-resolution records, which suggest that most surface faults are expressions of major faults and of boundary faults.

Minor faults (Fig. 14) occur throughout the southern outer shelf, although, like other classes of faults, they are also concentrated in the middle region of St. George basin, away from the Pribilof ridge. Minor faults are more frequent south of the ridge than to the north (Fig. 14). Most minor faults offset reflectors less than 0.006 sec (5 m) and almost all these faults cut the top 0.005 sec (approximately 4 m) of the sedimentary section. Diatoms recovered in sediment from gravity cores up to 2 m long are younger than 260,000 years (all within the Denticula seminae Zone; John Barron, pers. commun., 1976, 1977). If we assume that a 2 m core just penetrated the entire Denticula seminae Zone, then the minimum accumulation rate is 0.8 cm/10^3. If we assume that this minimum accumulation rate is typical for the top 4 m of sediment (the thickness recently affected by minor faults), then the maximum age of the sediment, calculated using 0.8 cm/10^3 yr., is 520,000 MYBP. Thus, minor faulting may be no older than Pleistocene in age. Accumulation rates may be much greater, for example 10 cm/10^3 yr. as suggested by C^{14} dates from areas farther north (Askren, 1972), in which case the minor faults could cut sediment as young as 40,000 YBP.

Earthquakes

The southern Bering Sea margin is within 500 km of the Aleutian Trench, the present site of subduction between the Pacific and North American plates. Several intermediate-to-deep-focus (71 to 300 km deep) and many shallow-focus (less than 71 km deep) earthquakes were recorded beneath the southern Bering Sea margin from 1962 to 1969 as shown in Figure 15. The St. George basin and surrounding areas have been subject to earthquakes with intensities as high as VIII (modified Mercalli scale), which corresponds to a magnitude 5.7 earthquake (Meyers and others, 1976). Recurrence rates of earthquakes for the area bounded by latitudes 50° and 60° N and longitudes of 160° to 175° W have been as high as 6.4 earthquakes per year from 1963 to 1974 for magnitudes of 4.0 to 8.4, and 0.013 earthquakes per year of magnitude 8.5 to 8.9 (1 every 130 years) from 1899 to 1974 (Meyers and others, 1976).

The correlation of earthquakes to shallow faulting is not well understood

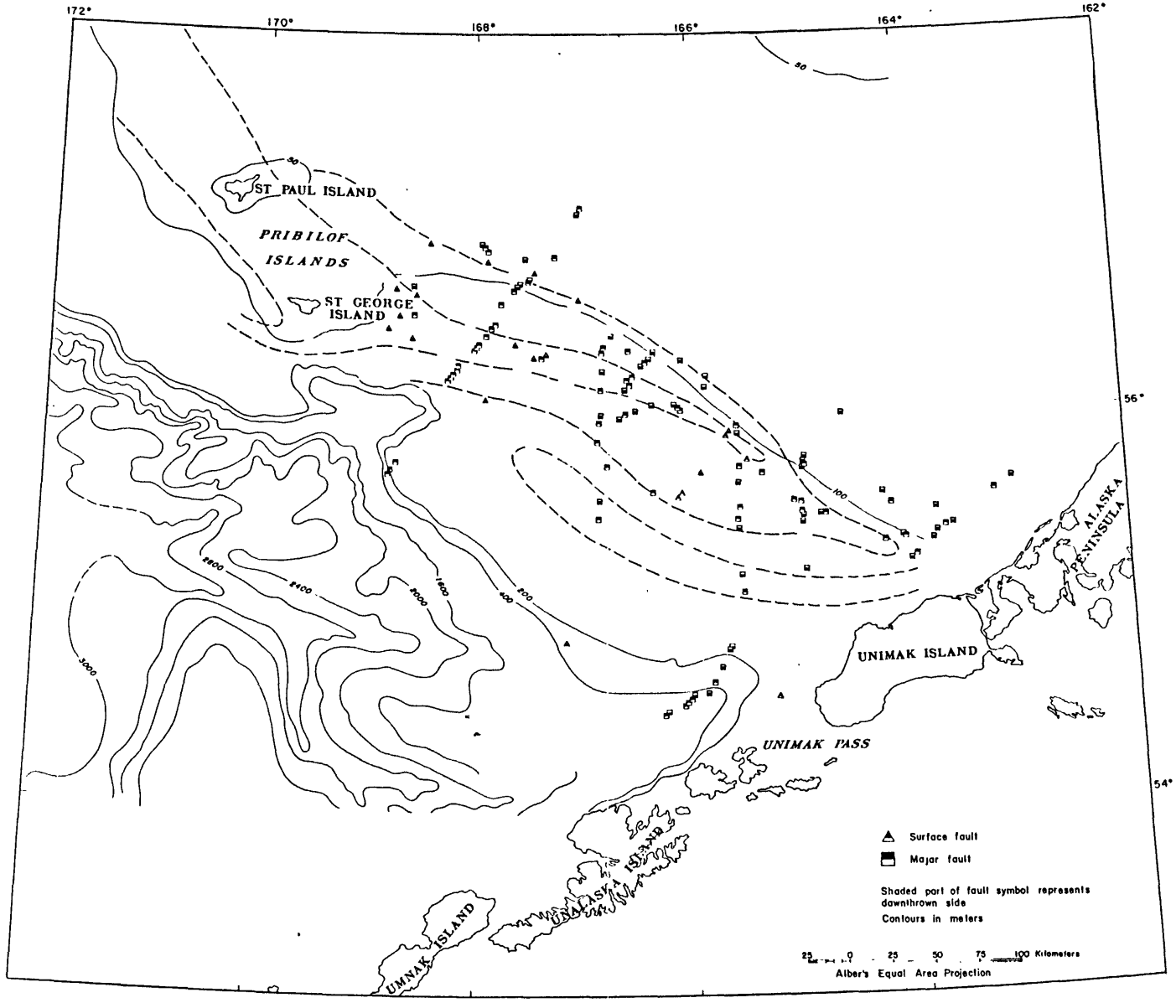

Figure 13. Distribution of surface and major faults.

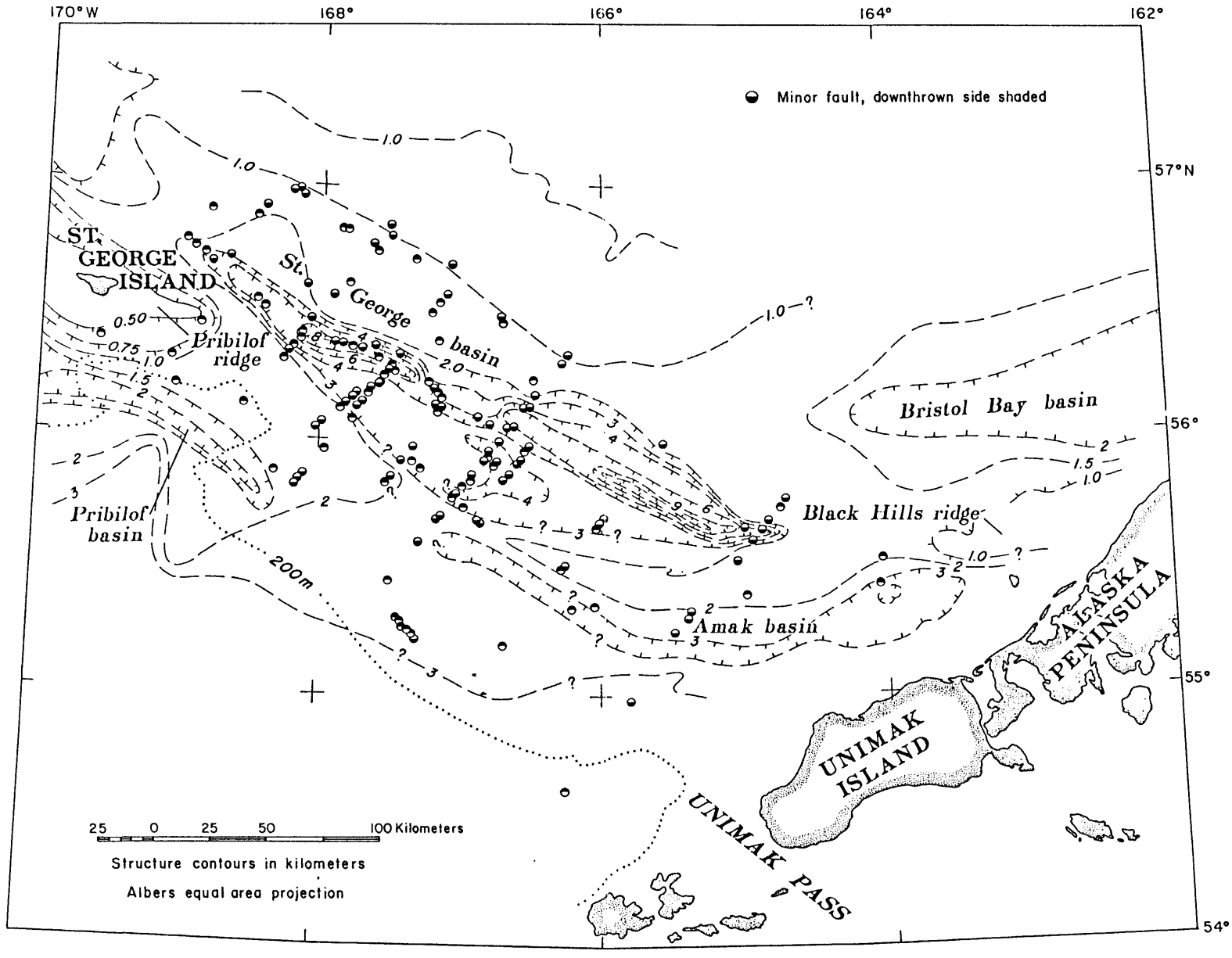

Figure 14. Distribution of minor faults.

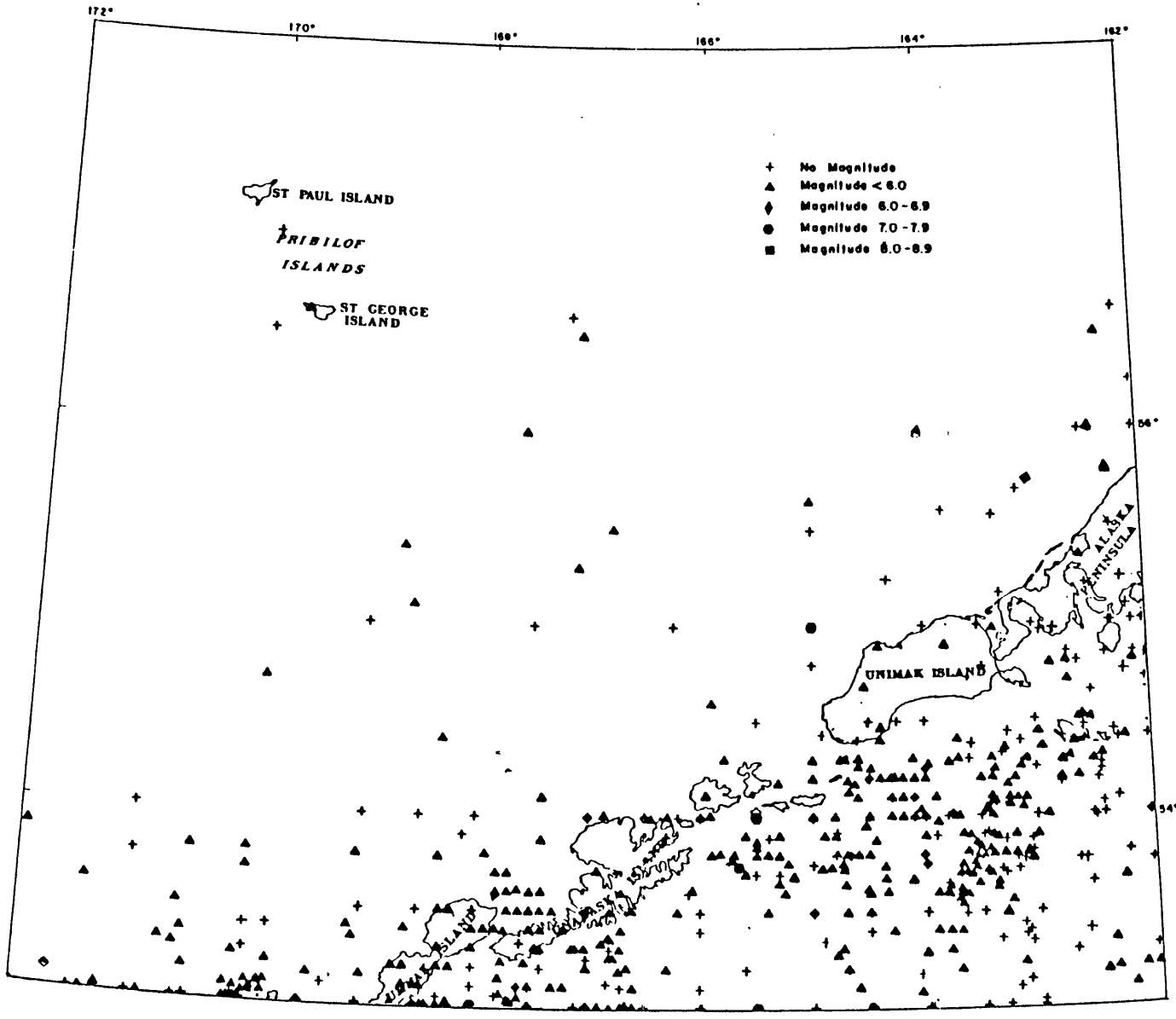

Figure 15. Epicenters up through 1964.

(Page, 1975). We believe, however, that many of the faults in the southern Bering Sea are active and that they probably respond to earthquake-induced energies and possibly to sediment loading in St. George basin.

Seafloor Instability

Areas of potentially unstable sediment masses were determined from the seismic reflection records by using one or more of the following criteria: 1) surface faults with steep scarps and rotated surfaces; 2) deformed bedding and/or discontinuous reflectors; 3) hummocky topography; 4) anomalously thick accumulation of sediment; and 5) acoustically transparent masses of sediment. Regions that show unstable sediments (e.g. gravity slides, slumps, creep, scarps, etc.) are confined to the continental slope and rise and the Pribilof and Bering Canyons. Zones of creep, as shown by irregular, hummocky topography, begin near the shelf break at depths of about 170 m and continue onto the upper continental slope. Hummocky topography occurs on the continental slope on a large scale and mass movement is a common feature. We suspect the entire continental slope and the walls of the major submarine canyons to be zones of potentially unstable sediment. Regimes of active sediment movement could respond to a variety of energy sources including earthquakes, storms, internal waves, and gravity.

Earthquake, tide, and wind induced waves affect sediment movements in the southern Bering Sea around St. George basin according to Lisitsyn (1966, p. 96-98). Earthquakes and associated tsunamis can affect shallow water sedimentary deposits. Tides also have a strong affect in shallow water, particularly in funnel-shaped estuaries such as Kuskokwim Estuary, where the tide ranges up to 8 meters and current velocities can exceed 200 cm/sec (Lisitsyn, 1966).

Wind induced waves influence sedimentation in water depths of up to 100 meters in the Bering Sea. Storms in the area are frequent, and the probability of storm waves several meters in height exceeds 20% during any given year (Lisitsyn, 1966, p. 98). The strongest and most prolonged storms occur during fall and winter seasons. In late summer and early fall waves generated by Pacific typhoons often penetrate the Aleutian Island arc and reach the southern Bering Sea.

Volcanic Activity

The Bering Sea shelf and margin near St. George basin are bounded on the south by the volcanically active Alaska Peninsula and eastern Aleutian Islands. Coats (1950) lists 25 active volcanoes in the Aleutian Islands and 11 on the Alaska Peninsula and mainland. Volcanism to the north, in the Pribilof Islands, may still be active (Hopkins, oral communication, 1976). Hazards from volcanic activity are associated with eruption of lava and ash and the attendant earthquakes. The distribution of ash is dependent on the magma composition, eruption character, wind speed and direction at the time of eruption, height of eruption, volume of material, and specific properties of the pyroclastic debris. Eruptions from the large andesitic cones on the Alaska Peninsula and Aleutian Islands are mostly the explosive-type and can spread pyroclastic materials over large areas, whereas eruption from basaltic volcanoes, such as those on the Pribilof and Nunivak Islands, are not as explosive and would have only local effects.

The largest known quantity of volcanic material erupted in historic times in the Alaska area, some 21 km^3 of ash, was erupted by Katmai volcano in 1912, when ash was carried over distances of 2000 km or more. At a distance of 180 km from the volcano, ash was deposited with a density of about 45 g/cm (Lisitsyn, 1966). According to historical data, individual ash deposits in the Bering Sea region extend 200 to 2000 km from the source, averaging about 500 km. Hazards are associated not only with the volume of ash that might be deposited but also with ground motion that often accompanies major eruptions. These forces, as well as base surges from caldera eruptions, may affect man-made structures and also shake loose pre-existing, unstable, and undercompacted sediment bodies.

Ice

Parts of the southern Bering Sea continental shelf and margin in the vicinity of St. George basin are covered with ice for several months a year (Fig. 16). Ice development reaches its maximum during March and April when unstressed floes reach 1 to 2 m in thickness (Lisitsyn, 1966). Both migratory and stationary ice form; the latter occurs along the shorelines and ranges in width from a few meters to as much as 80 km from the shore. Some ice gouging occurs around the shorelines where the ice is thickest, and man-made structures, pipelines, and ports may be affected by ice-ramming and bottom scouring.

Hydrocarbon Gases in Near Surface Sediment

Gardner and others (1979) and Kvenvolden and Redden (1979) have shown that hydrocarbon gases are present in surface and near-surface sediment of the southern Bering Sea shelf and slope. Concentrations of hydrocarbons are about the same in shelf and slope sediment in the interval from 0 to about 60 cm. On the shelf, acoustic anomalies ("bright spots" or "wipe-out zones") thought to be due to gas concentrations are common (Fig. 17), and are generally 200 to 300 m deep. However, these acoustical anomalies do not produce hydrocarbon gas anomalies in the near-surface sediment above them, except for one station (9-12, S-6-77- BS; Kvenvolden and Redden, 1979).

The concentrations and distributions of hydrocarbon gases in the sediment were examined in cores taken in the areas shown on Fig. 18. These measurements do not indicate that gas seeps are active in the areas sampled or that the gas in the sediment constitutes a geologic hazard because of high concentrations. We should emphasize that these samples are shallow cores (few meters) and may not be representative of gas-associated hazards in the sedimentary section at greater depths. Unsubstantiated rumor indicates that when the COST well was drilled south of St. George basin in 1977, engineering problems were encountered with shallow pockets of gas.

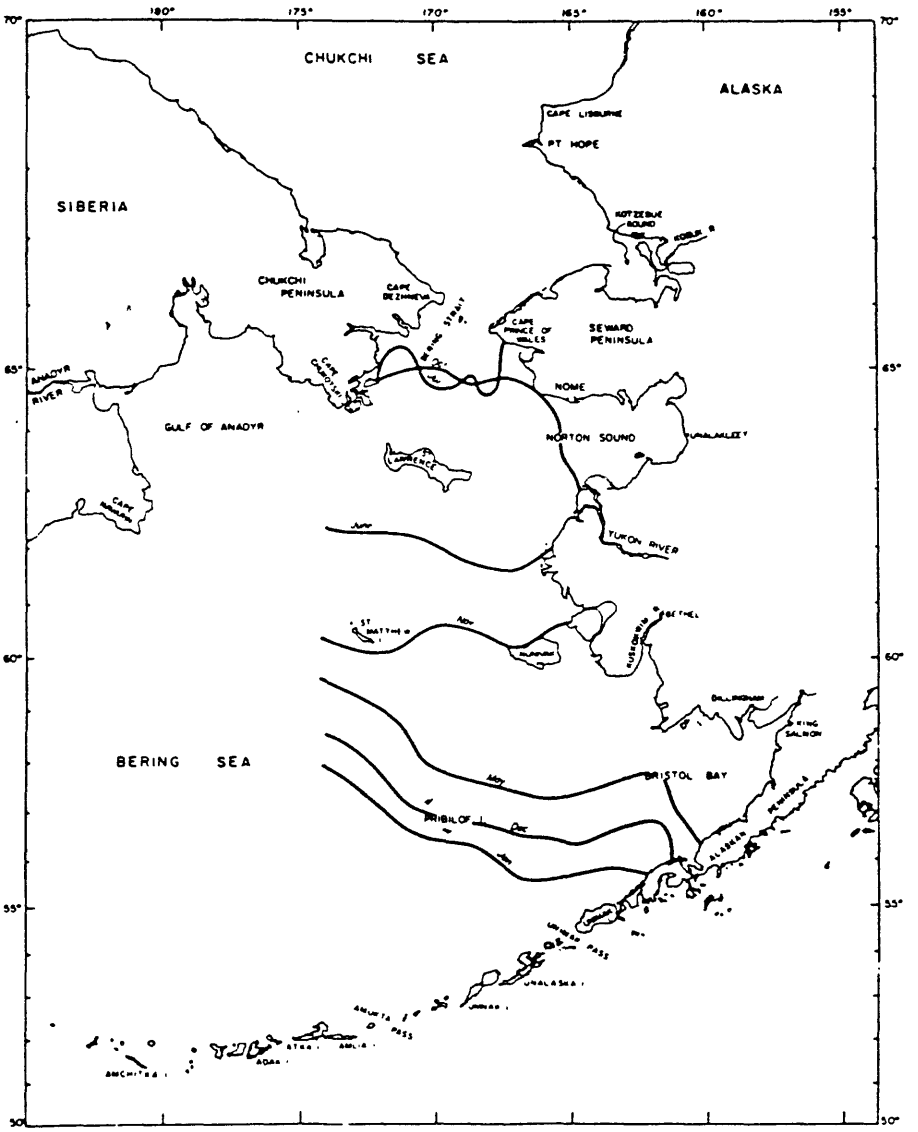

Figure 16. Ice cover of the Bering Sea. From McRoy and Goering (1974).

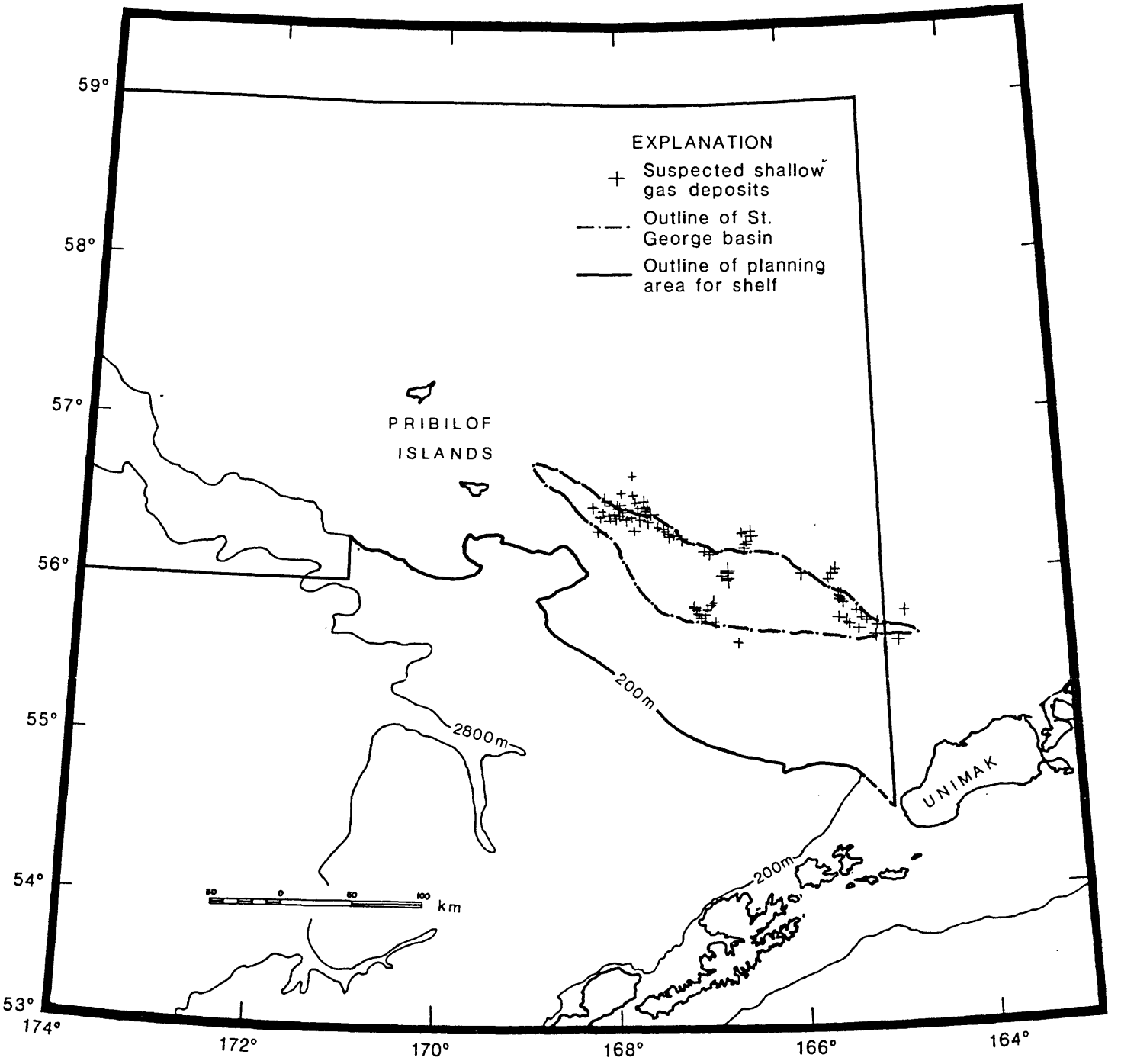

Figure 17. Distribution of acoustic anomalies ("bright spots" or "wipe-out zones") detected in seismic reflection data and thought to be due to shallow accumulations of gas.

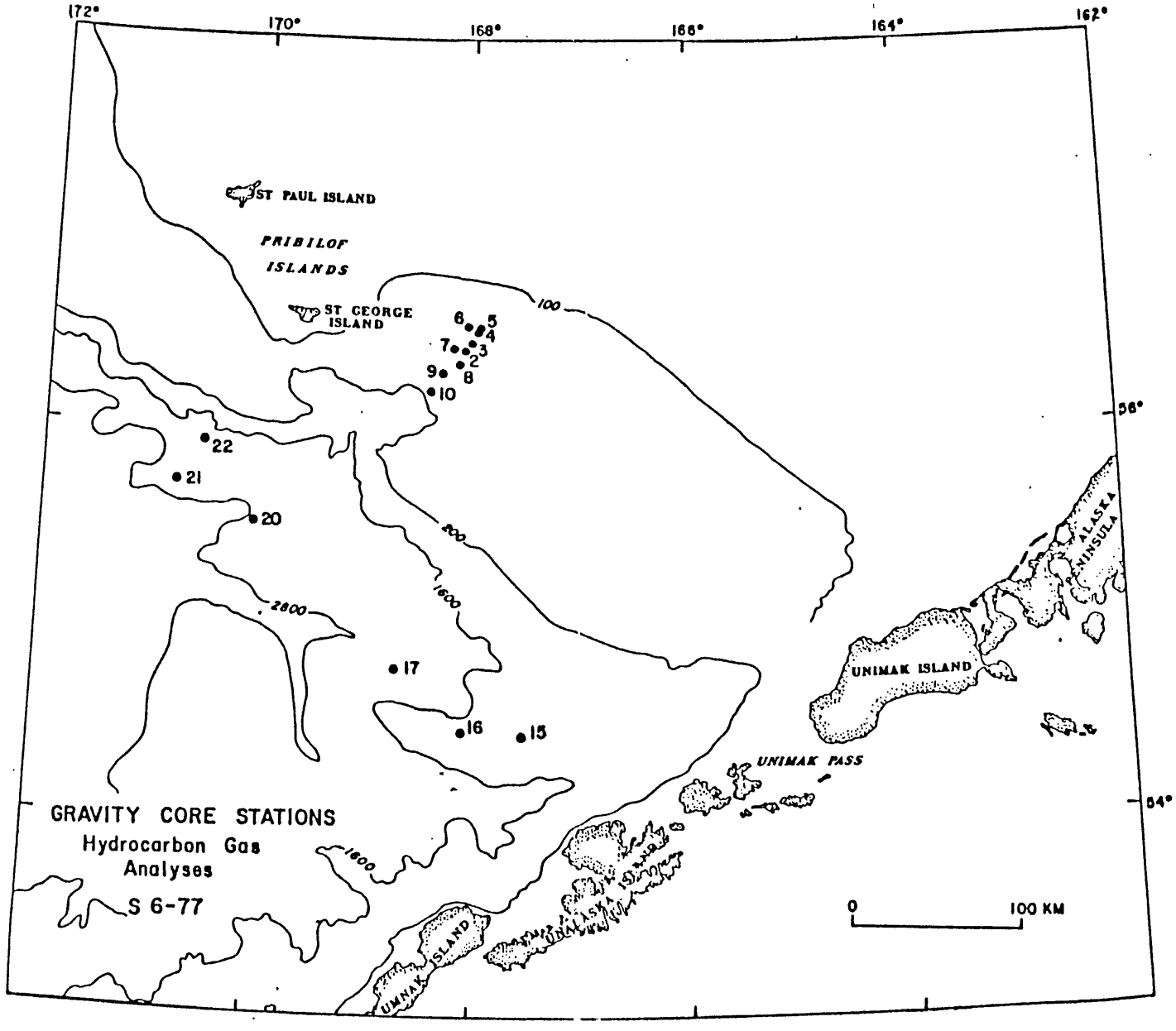

Figure 18. Locations of samples that were collected for hydrocarbon gas analysis.

CHAPTER 1-4
HARD MINERALS GEOLOGY

Hard minerals deposits are unknown in the shelf area of St. George basin. Mineralization zones are absent in the igneous rocks exposed on the Pribilof Islands.

SECTION 2: UMNAK PLATEAU REGION

This section of the report summarizes geological and geophysical data from the deep-water (greater than 200 m) region of the St. George basin planning area. This region is bounded on the northeast by the 200 m bathymetric contour, on the southeast by a line that approaches within 3 miles of the Aleutian Islands, and on the west by the 171°W longitude meridian. Hereafter, this triangular region is referred to as the Umnak Plateau region. The name is derived from a major bathymetric feature, Umnak Plateau, that covers most of the region (Fig. 19).

New data that has been collected in the Umnak Plateau region since the release of the previous summary geologic report for the area (Cooper and others, 1980) are limited to multichannel seismic reflection (MCS) and other underway geophysical data collected along tracklines in Figure 20. Nearby, to the west of the planning area, MCS data and rock-dredge samples have been acquired across the crest and flanks of the Aleutian Ridge (Fig. 21) and these data are included here. A more complete discussion of data bases, geologic observations, and previous interpretations for the Umnak Plateau region can be found in Cooper and others (1980).

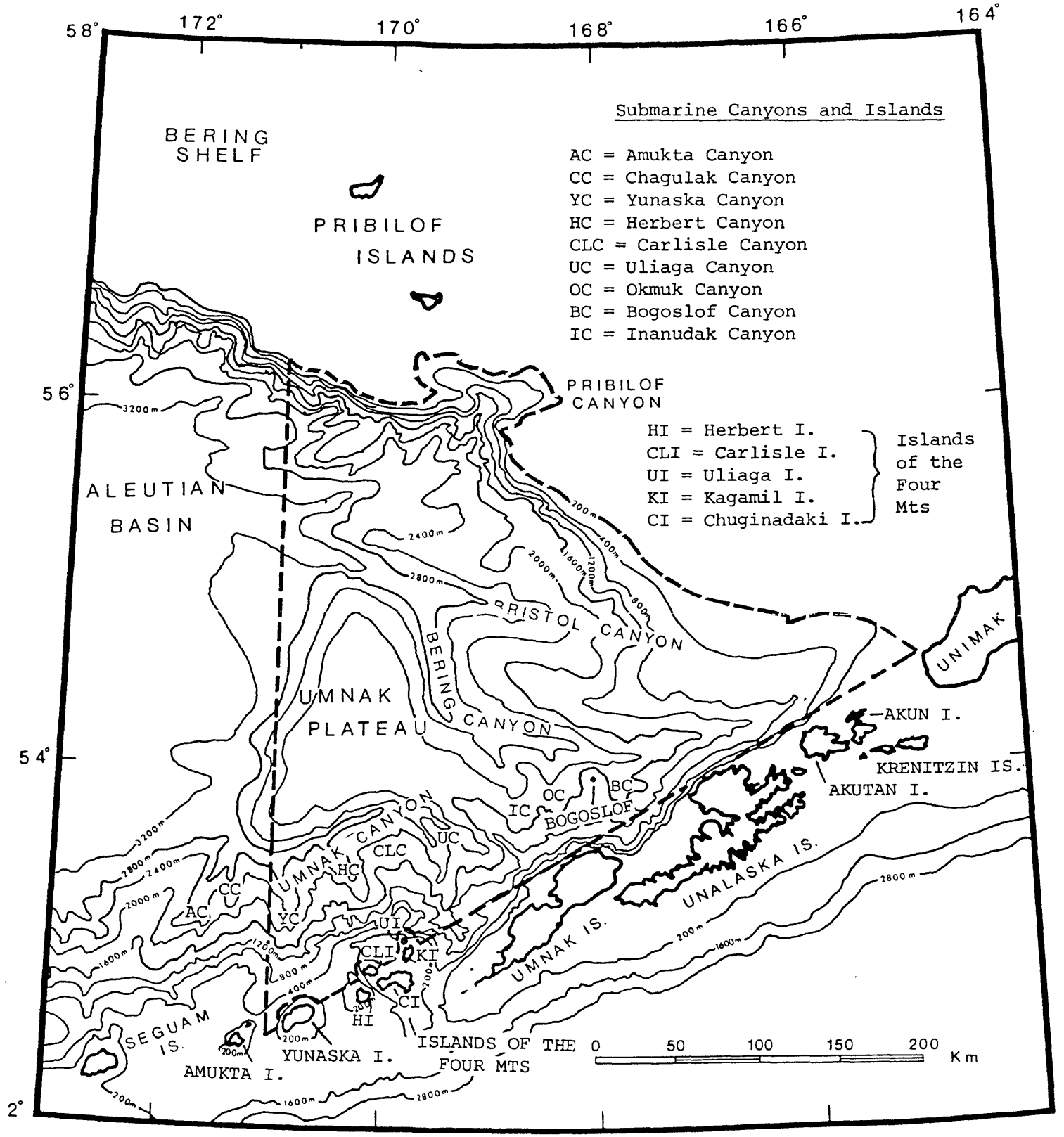

Figure 19. Index map showing physiographic features of the Umnak Plateau region.

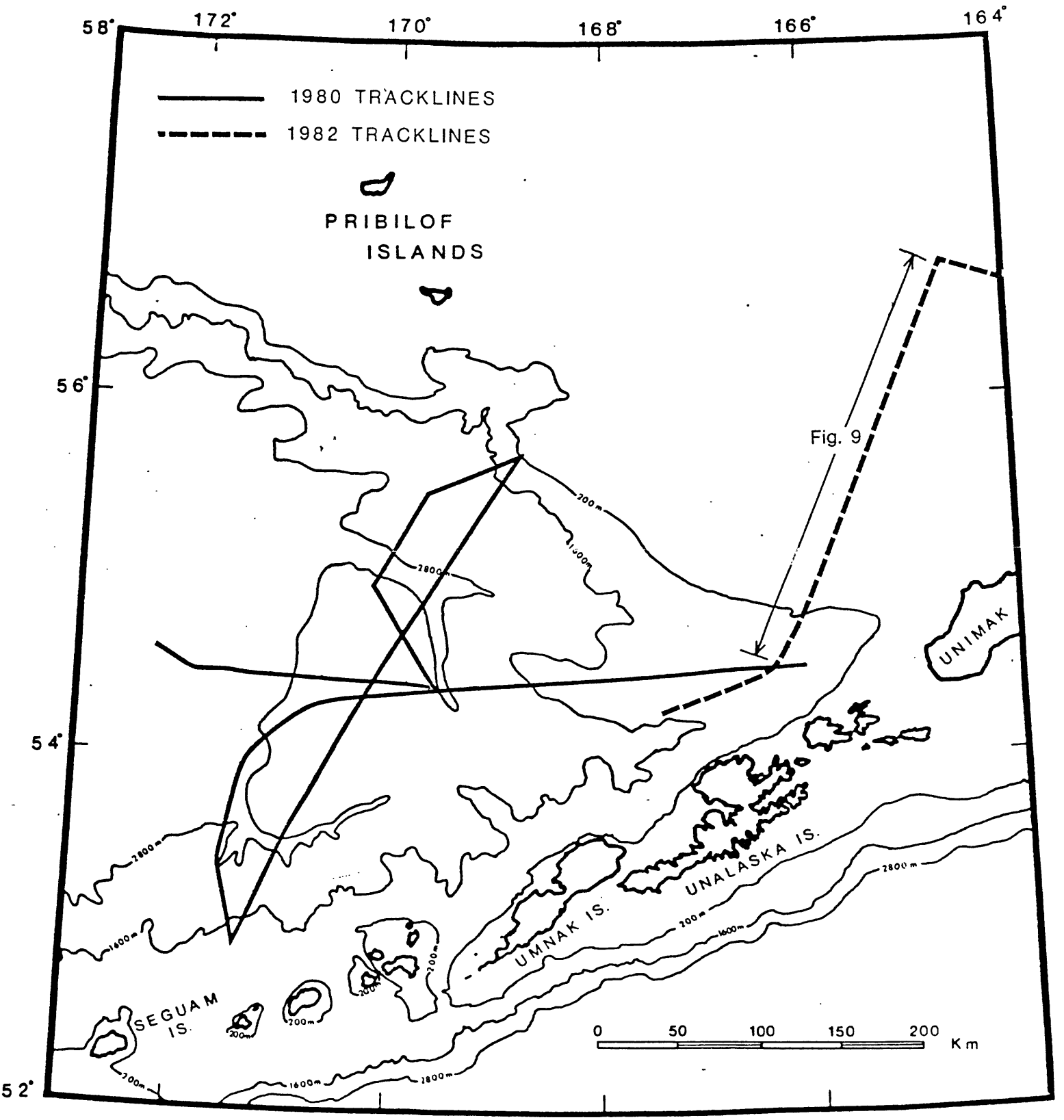

Figure 20: Trackline map of multichannel seismic-reflection data collected by the U.S. Geological Survey.

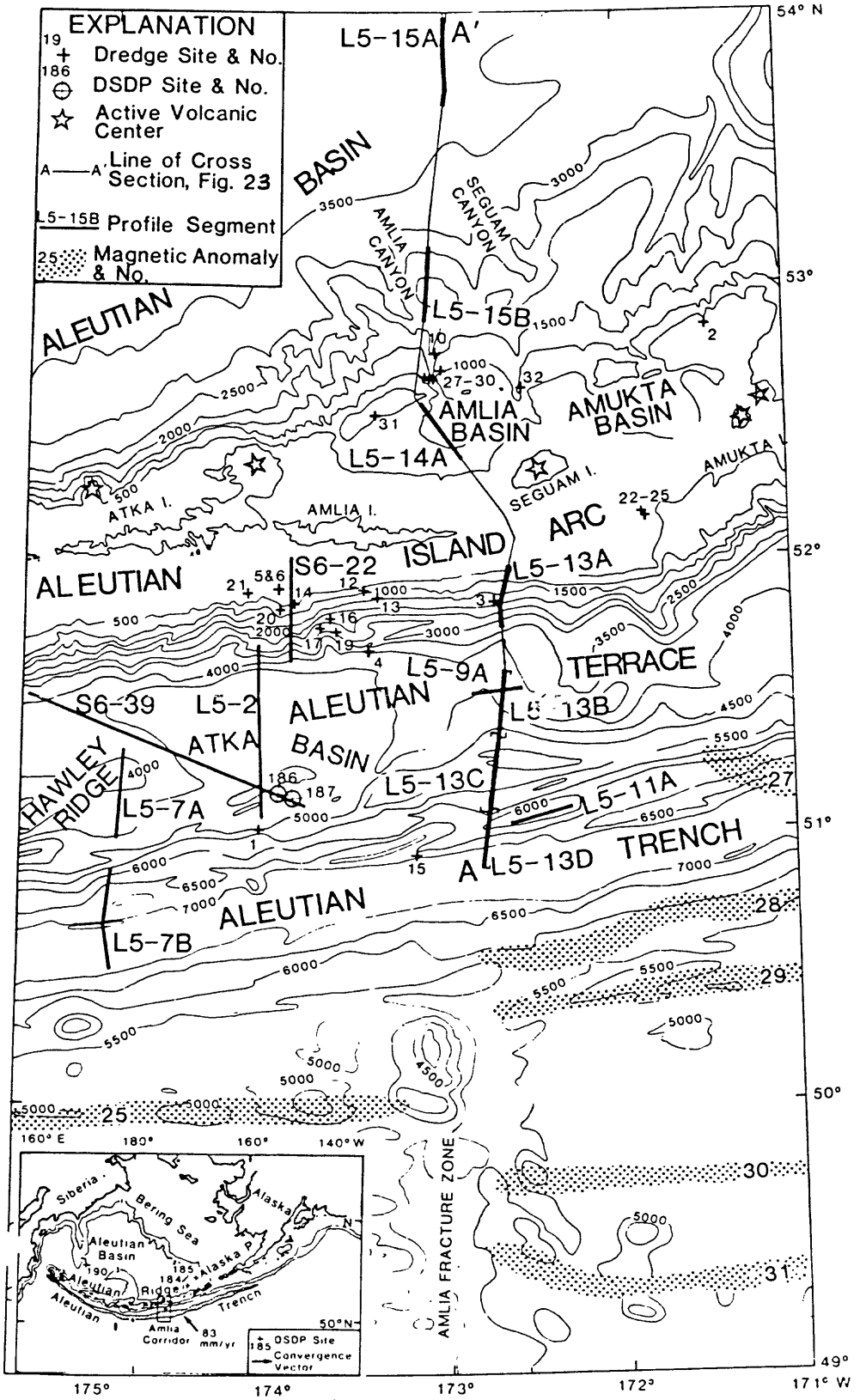

Figure 21. Location map of multichannel seismic reflection data and dredge sample stations in the Amlia corridor of the Aleutian Ridge, immediately west of the St. George basin planning area (from Scholl and others, 1983a).

CHAPTER 2-1
GEOLOGIC FRAMEWORK
Regional Tectonic Setting

The Umnak Plateau region lies at the junction of the extensive southern Bering shelf and the arcuate Aleutian Ridge. Mesozoic rocks and structures, described in the previous section, comprise the underpinnings of the shelf and form the region's northeast boundary. A younger suite of Cenozoic rocks and structures, however, are found beneath the Aleutian Ridge (Marlow and others, 1973; Scholl and others, 1975a, 1983a) along the southeastern edge of the region. On the west, the Umnak Plateau region is flanked by Mesozoic igneous crust and Cenozoic sedimentary rocks that underlie the Aleutian Basin (Cooper and others, 1976). The diverse origin of the geologic provinces is unclear.

During Mesozoic time, the Aleutian Basin may have been part of a larger oceanic plate (Kula plate) that abutted against the Bering continental margin (Scholl and others 1975a, 1983). A piece of this oceanic plate was trapped in the Aleutian Basin and subduction shifted from the Bering margin to the south side of the Aleutian Ridge. Umnak Plateau may have initially formed in early Tertiary time by:

1. uplift of the Aleutian Basin's oceanic crust during the initial construction of the Ridge (Cooper and others, 1980) or
2. collision of an existing oceanic plateau (on the Kula Plate) with the southern Bering margin prior to the development of the Aleutian Ridge (Ben-Avraham and Cooper, 1981) or
3. Subsidence of a subaerially exposed flank of the proto-Aleutian Ridge in early Tertiary time (Scholl and others, 1983).

Since early Tertiary time, the area has been covered by a 1-9 km thick sedimentary sequence derived from the nearby Aleutian Ridge and Bering shelf. The large structural relief on basement rocks at the base of the Bering margin is a result, in part, of this massive sediment loading throughout Cenozoic time (Cooper and others, 1979a). The morphology of the large submarine canyons in the region reflects primarily structurally-controlled erosional processes associated with late Cenozoic periods of glaciation and lower sea level rather than major faulting of the sedimentary section (Scholl and others, 1970).

Geology of the Umnak Plateau region

Offshore geologic data from the Umnak Plateau region are sparse (Fig. 22) and age assignments for the acoustic stratigraphy beneath the region must be projected long distances from dredged localities. Scholl and others (1983a,b), based on previous investigations (Marlow and others 1983; Scholl and others, 1975a,b) as well as on new dredge stations (Fig. 21; Table 4), describe three rock series: lower, middle, and upper, for the upper-crustal rocks of the Aleutian Ridge and part of the Umnak Plateau region. Figure 23 shows the general distribution of these three rock series across the Aleutian Ridge along a transect of the Amlia corridor, 100 km west of the Umnak region.

According to Scholl and others (1983), the Aleutian Ridge's three-tiered chronostratigraphic sequence comprises a lower series of mostly Eocene volcanic rocks; a middle series of mostly Oligocene through lower middle Miocene strata that includes large volumes of sedimentary beds; and an upper series of middle Miocene to Holocene deposits that are dominantly sedimentary beds but include the upper Cenozoic eruptive masses.

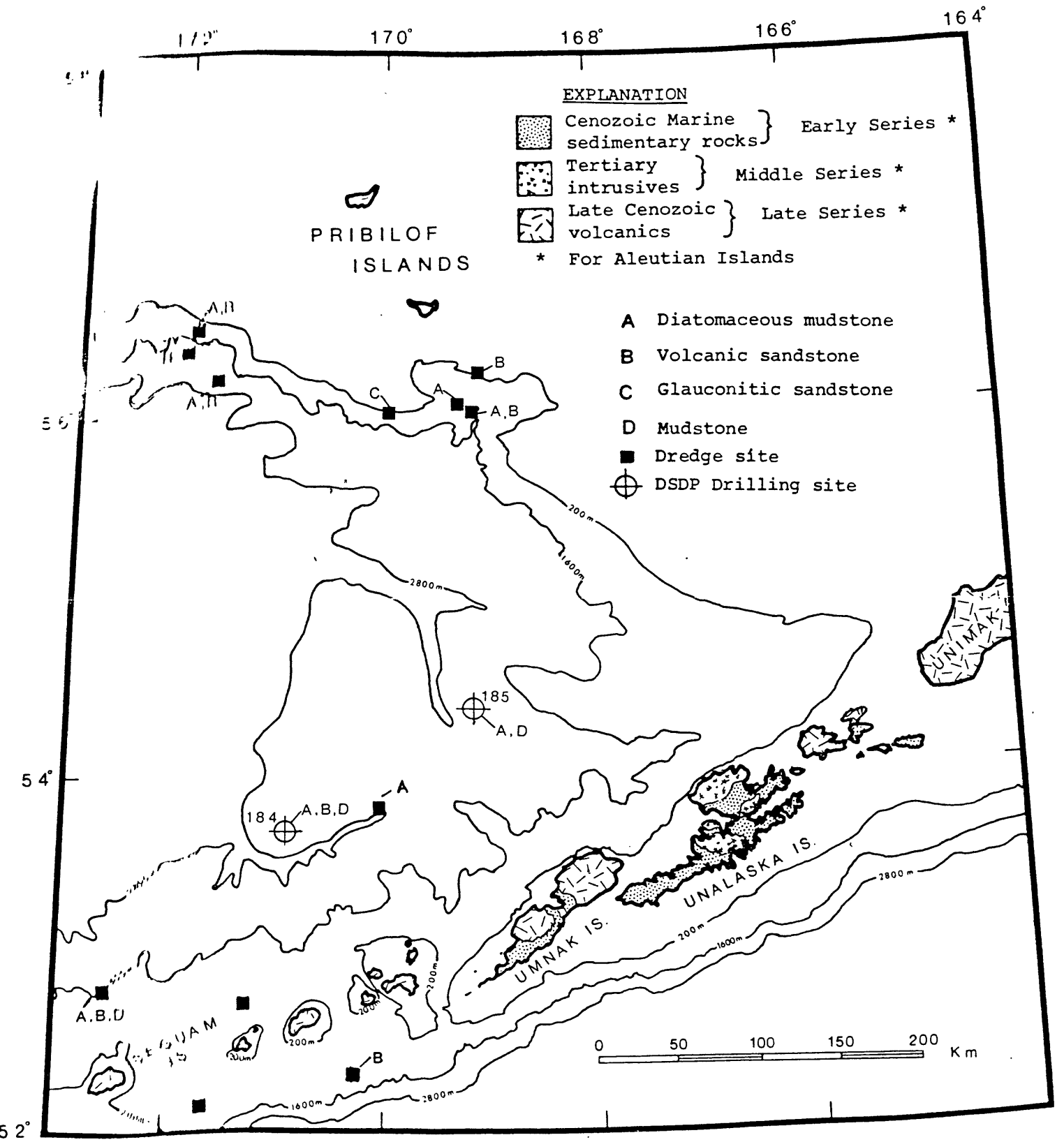

Figure 22. Geologic data for the Umnak Plateau region.

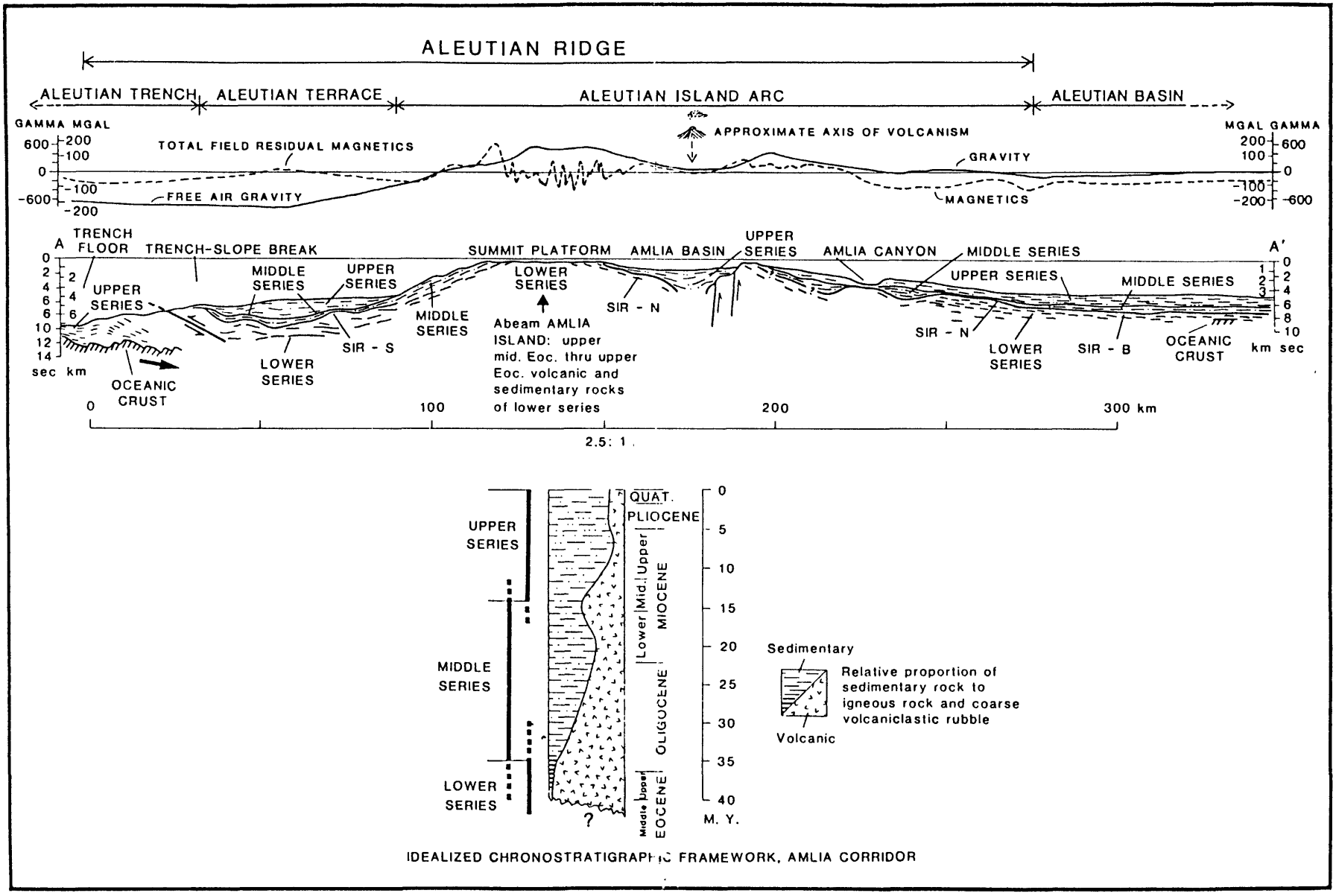

Figure 23: Generalized structural section, based on reflection events, for upper crustal rocks of the Aleutian Ridge, Amlia corridor (see figure 21 for location). SIR-B, -N, -S horizons are regionally persistent reflection events that typically separate lower from middle or upper series deposits (see figure 26). Lower figure is an idealized chronostratigraphic scheme adaptable to the onshore and offshore rock sequences of the Aleutian Ridge. Figure is from Scholl and others (1983a).

TABLE 4. Description of dredge station locations, water depths, rock ages, and major lithologies for rocks collected in 1979, 1980, and 1981 from the Aleutian Ridge. Table is from Scholl and others (1983a). See Figure 21 for location.

Dredge No.	General Location (and series)	Latitude and Longitude	Water Depth (m)	Ages	Major Lithologies
L5-80-1	Top of landward slope of Aleutian trench (late series)	50°59.8'N 174°06.3'W	5000	Late Pliocene-early Quaternary	Limestone and mudstone
L5-8-2	Northern edge of summit platform north of Amukta Island (lower or middle series)	52°52.1'N 171°28.2'W	500-400	Unknown	Volcaniclastic breccia
L9-81-3	Upper slope south of Seguam Pass (upper series with included clasts of middle series)	51°48.9'N 172°49.5'W	2250	Late Pliocene - early Quaternary with clasts of late Oligocene	Sandstone and conglomerate
L9-81-4	Lowermost slope south of Amlia Island. (middle series)	51°37.6'N 173°27.5'W	3680-3700	Late Pliocene (silt) Early middle Miocene(ss)	Soft siltstone and hard sandstone
L9-81-5 & 6	Summit platform south of Amlia Pass (lower series)	51°53.3'N 174°00.3'W	80	Unknown	Flow rocks and volcanic sandstone
L9-81-10	East wall, upper reaches of Amlia Canyon (upper series)	52°43.8'N 173°03.8'W	1500-1850	Late middle Miocene and middle Pliocene	Sandstone and mudstone
S6-79-12	Upper slope south of Amlia Island (middle series)	51°51.6'N 173°32.2'W	1000-900	Early Oligocene	Sandstone
S6-79-13	Upper slope south of Amlia Island (middle series)	51°50.0'N 173°28.1'W	1700-1650	Early Oligocene	Sandstone and tuff
S6-79-14	Uppermost slope south of Amlia Island (middle series)	51°48.9'N 173°56.3'W	500-400	Late Oligocene-early Miocene	Sandstone
S6-79-15	Inner wall of the Aleutian Trench (upper series)	50°53.1'N 173°12.9'W	7050-6600	Early Quaternary	Mud
S6-79-16	Middle slope south of Amlia Island (middle series)	51°45.8'N 173°43.4'W	2650-2450	Oligocene	Sandstone and siltstone
S6-79-17	Middle slope south of Amlia Island (middle and upper (?) series)	51°44.4'N 173°45.2'W	3100-2950	Oligocene and middle Miocene	Sandstone
S6-79-19	Middle slope south of Amlia Island (middle series)	51°43.5'N 173°41.3'W	2900-2750	Early to middle Oligocene	Sandstone
S6-79-20	Uppermost slope south of Amlia Island (upper series)	51°48.7'N 174°00.4'W	93-700	Late Miocene-early Pliocene	Sandstone
S6-79-21	Summit platform south of Atka Island (lower series)	51°52.1'N 174°12.9'W	120	Unknown	Flow rocks and volcanic sandstone
S6-79-22	Summit platform south of Amukta Pass and Seguam Island (lower series)	52°08.9'N 171°51.9'W	450-300	Middle Eocene-early Oligocene	Tuff, sandstone and siltstone
S6-79-25	Summit platform south of Amukta Pass and Seguam Island (lower series)	52°09.6'N 171°52.2'W	260	Unknown	Flow rocks and tuff
S6-79-27	West wall of Amlia Canyon, north side Aleutian Ridge (upper series)	52°39.2'N 173°07.8'W	1550-1500	Early Pliocene-Holocene	Sandstone, siltstone and tuff
S6-79-28	West wall of Amlia Canyon (upper series)	52°39.7'N 173°09.9'W	1350-1225	Middle late Miocene early Pliocene	Breccia and conglomerate
S6-79-29	West wall of Amlia Canyon (upper series)	52°39.8'N 173°09.9'W	1200-1100	Late Miocene-early Pliocene(?)	Sandstone and breccia
S6-79-30	East wall of Amlia Canyon (upper series)	52°41.1'N 173°04.3'W	1550-1400	Middle middle Miocene	Sandstone, breccia, and conglomerate
S6-79-31	Fault scarp on northwest side of Amlia Basin (lower or middle series)	52°30.8'N 173°27.4'W	580-300	Unknown	Volcaniclastic breccia and flow rocks
S6-79-32	East wall of Seguam Canyon, North side of Aleutian Ridge (upper series)	52°37.5'N 172°35.2'W	975-900	Late Miocene-early Pliocene	Sandstone and breccia

The ridge's upper crustal framework is a massive antiform consisting of a sediment-draped igneous massif of chiefly lower series rocks produced rapidly by voluminous submarine volcanism prior to about 35 million years ago. In post-Eocene time, igneous activity effectively ceased over the flanks of the ridge and, except for a pulse in early middle Miocene time, greatly diminished along the arc's summit region. In Oligocene through early Neogene time, debris eroded from the regionally elevated and volcanically dying crest of the arc accumulated on the submerged (or submerging) flanks and basal regions of the ridge as middle series deposits.

The post-middle Miocene history of the ridge crest records the dominance of extensional collapse and erosion over continuing but localized volcanic buildup of the arc's igneous massif. Wave-base erosion carved a summit platform across the top of the arc. The truncation was accompanied by the deposition of basinal sequences of upper series beds in summit grabens and perhaps by extensive subsidence of the arc's sloping flanks.

Rocks of the lower, middle, and upper series underlie Umnak Plateau but only the upper 973 meters of the 1 to 9 km thick sedimentary sequence has been drilled by DSDP. The oldest rocks recovered are from the upper series, and are early Pliocene or late Miocene in age (Fig. 24). The sediment in the upper 600 meters of the DSDP holes is primarily diatomaceous ooze with silt, clay, ash and limestone, but at greater depths is diagenetically altered to lithified clayey siltstone. Similar rocks have been dredged from outcrops along the inner wall of Pribilof Canyon. Most of these rocks are believed to be derived (from sediment sources on the Aleutian Ridge) by longshore transport and turbidity currents. Bedrock beneath Umnak Plateau has not been sampled and the type (igneous or sedimentary) and origin (oceanic, continental, or island-arc) of these rocks are unknown; however they are presumed by Scholl and others (1983a) to be equivalent to lower series rocks of the northern Aleutian Ridge flank (Fig. 23).

STRATIGRAPHY

The acoustic stratigraphy of the Umnak Plateau region is described by Scholl and others (1968, 1970, 1983a,b) and Cooper and others (1980). In this section we briefly review these papers, and show new examples from recent USGS multichannel seismic reflection data.

On the basis of pre-1968 seismic reflection records, Scholl and others (1968) define four acoustic units for the Umnak Plateau region: Acoustic Basement (AB), Main Layered Sequence (MLS), Rise Unit (RU), and Surface Mantling Unit (SMU; Fig. 25). The RU, SMU, and upper part of the MLS are equivalent with the upper series (Scholl and others 1983a, b); the lower part of the MLS, in places, lies within the middle series.

The Main Layered Sequence forms the bulk of the Neogene sedimentary section (Vp = 1.6 to 3.4 km/sec) and is often several kilometers thick. The Rise Unit is primarily Pleistocene turbidites that cover the MLS in the abyssal Aleutian Basin and that pinch out at the base of the continental slope. The flanks of the Plateau's submarine canyons are covered unconformably by late Cenozoic diatomaceous and terrigenous rocks of the Surface Mantling Unit.

The Acoustic Basement (AB) is a horizon of highly variable acoustic character, geomorphic relief, and geologic age. Near the Bering shelf, AB is Mesozoic sedimentary rock (Vp = 4.9 to 5.3 km/sec; Marlow and others 1979c). Beneath Umnak Plateau and the Aleutian Ridge flank, AB is probably Paleogene early series rocks (Vp = 3.4 to 4.8 km/sec) and underneath the Aleutian Basin

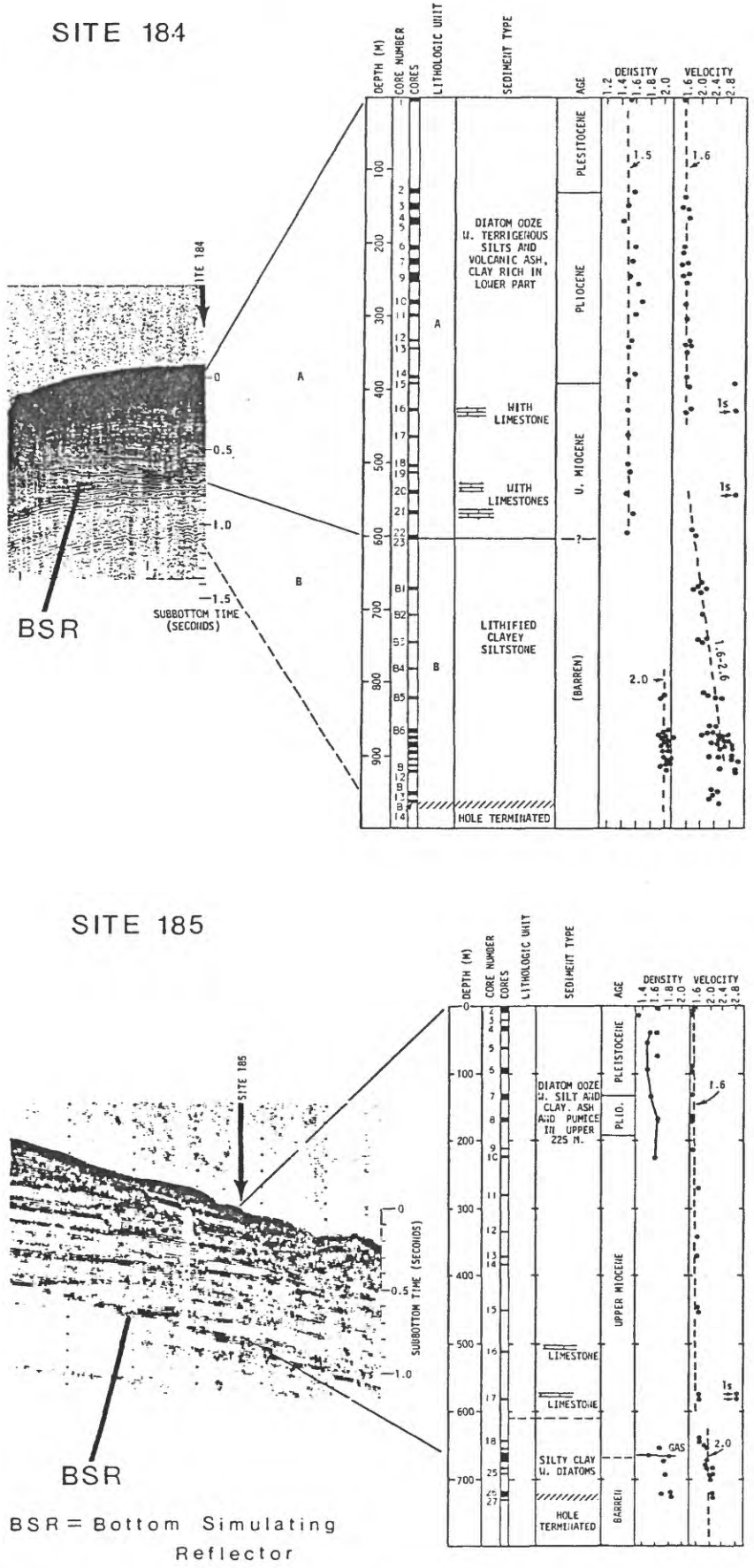

Figure 24. DSDP drilled sections at sites 184 and 185.

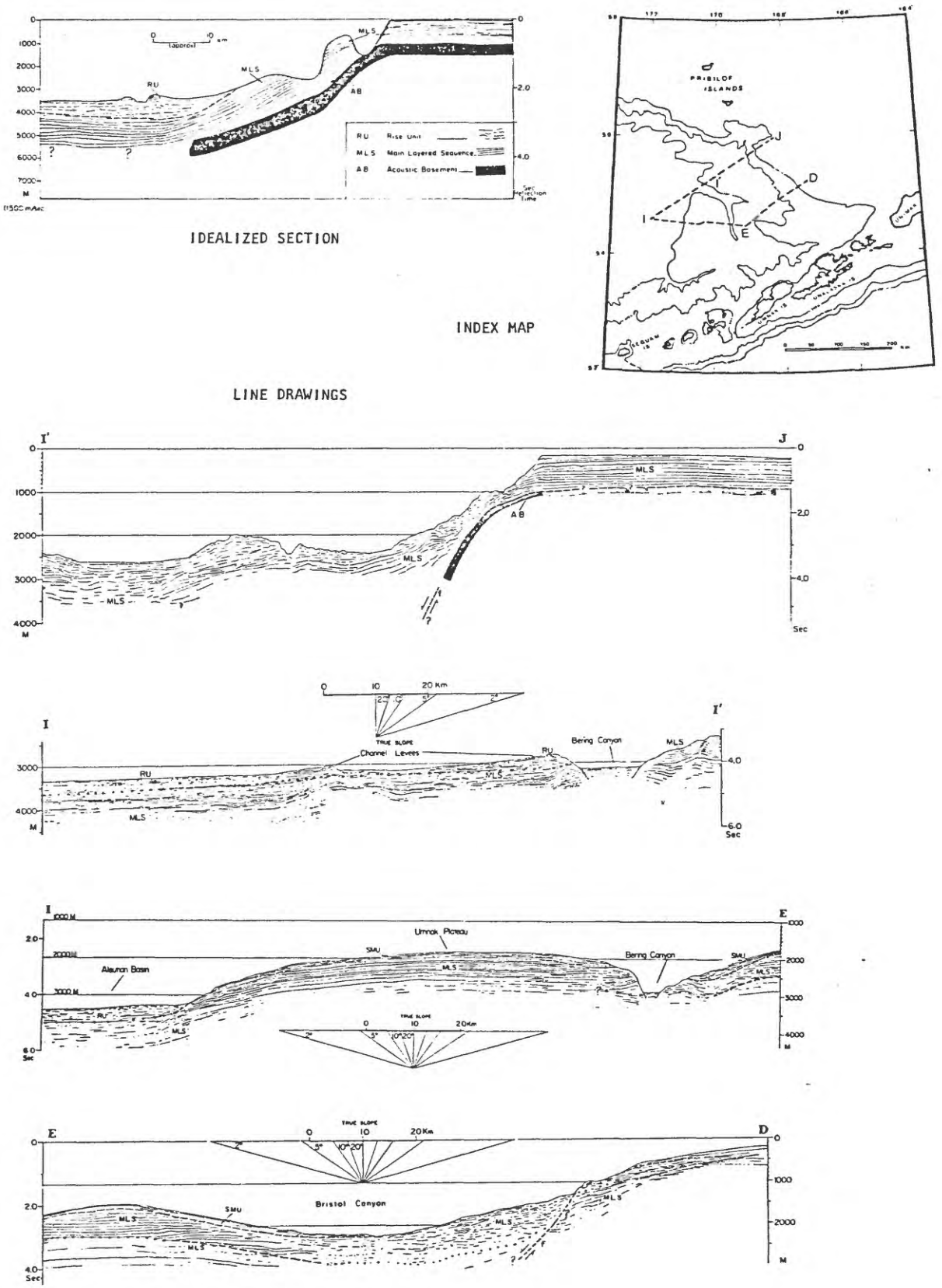

Figure 25. Seismic reflection profiles across the Umnak Plateau region (from Scholl and others, 1968).

(Cooper and others, 1981), AB is Mesozoic oceanic basalt (Vp = 5.0 to 5.8 km/sec).

Aleutian Ridge

The acoustic stratigraphy of the northern Aleutian Ridge flank has been described by Scholl and others (1983a,b; Fig. 26). Upper Cenozoic beds of the upper series are characteristically either slope-conforming or basin-filling deposits and are typically little deformed. They unconformably overlie the wave-planed summit platform that cuts across middle and lower series rocks (Fig. 26). Beds of the upper series are typified acoustically by good internal reflectivity and by laterally coherent and prominent reflection horizons.

Middle series deposits are more deformed, but beneath the sloping flanks of the ridge they are subparallel to the sea floor and overlie upper series beds (Fig. 26). Beneath these slopes middle series beds unconformably overlie rocks of the lower series. Middle series beds acoustically exhibit strong to weak internal reflectivity; and acoustic stratification can be laterally persistent or discontinuous and irregular.

In contrast, rocks of the underlying lower series are internally poorly reflective. Beneath the lower flanks of the ridge the upper surface of the lower series is typically a persistent and strong sub-bottom irregular reflection interface (designated SIR-type reflection horizon, Fig 26). In some areas, weak but laterally coherent acoustic horizons occur in the lower series.

The lower series rocks are probably massive accumulations that are slope-forming rather than basin-filling sequences; beneath the ridge's crestal area, they are dominantly submarine volcanic flows and related hypabyssal intrusive masses and coarse volcaniclastic debris. Seaward, beneath the flanks, beds of the middle series are composed dominantly of marine sedimentary deposits. Upper series beds are everywhere marine sedimentary deposits of volcaniclastic detritus and intermixed and interbedded pelagic debris.

Umnak Plateau and continental slope

Across most of the Umnak Plateau and the continental slope, seismic reflection profiles (Fig. 27) illustrate generally good continuity of the reflection horizons above acoustic basement; these horizons (upper and middle series Main Layer Sequence-MLS) reach a cumulative thickness of 1 to 9 km. Prior to the late Cenozoic excavation of the large submarine canyons, the MLS was probably continuous across the entire region. The MLS is not severely deformed except in areas of steep slopes and shallow diapiric features; in these areas, reflectors are discontinuous and arched by folding, slumping, and faulting.

Beneath Umnak Plateau, the middle series rocks show the greatest variation in thickness (Fig. 28) and in places pinch out against the acoustic basement (early series?). The unconformity(?) at the top of acoustic basement, which is internally discontinuous, can be followed from the Aleutian Ridge to most areas throughout the region (Figs. 23, 26, 28, 29). The limited quality of deep-penetration seismic reflection data for the thickest sedimentary sections (Fig. 29), prevents identification of basement structure and stratigraphy in thse areas; however, refraction data (Fig. 30) indicates large basement offsets (faults?) exist along the base of the continental slope (Fig 29).

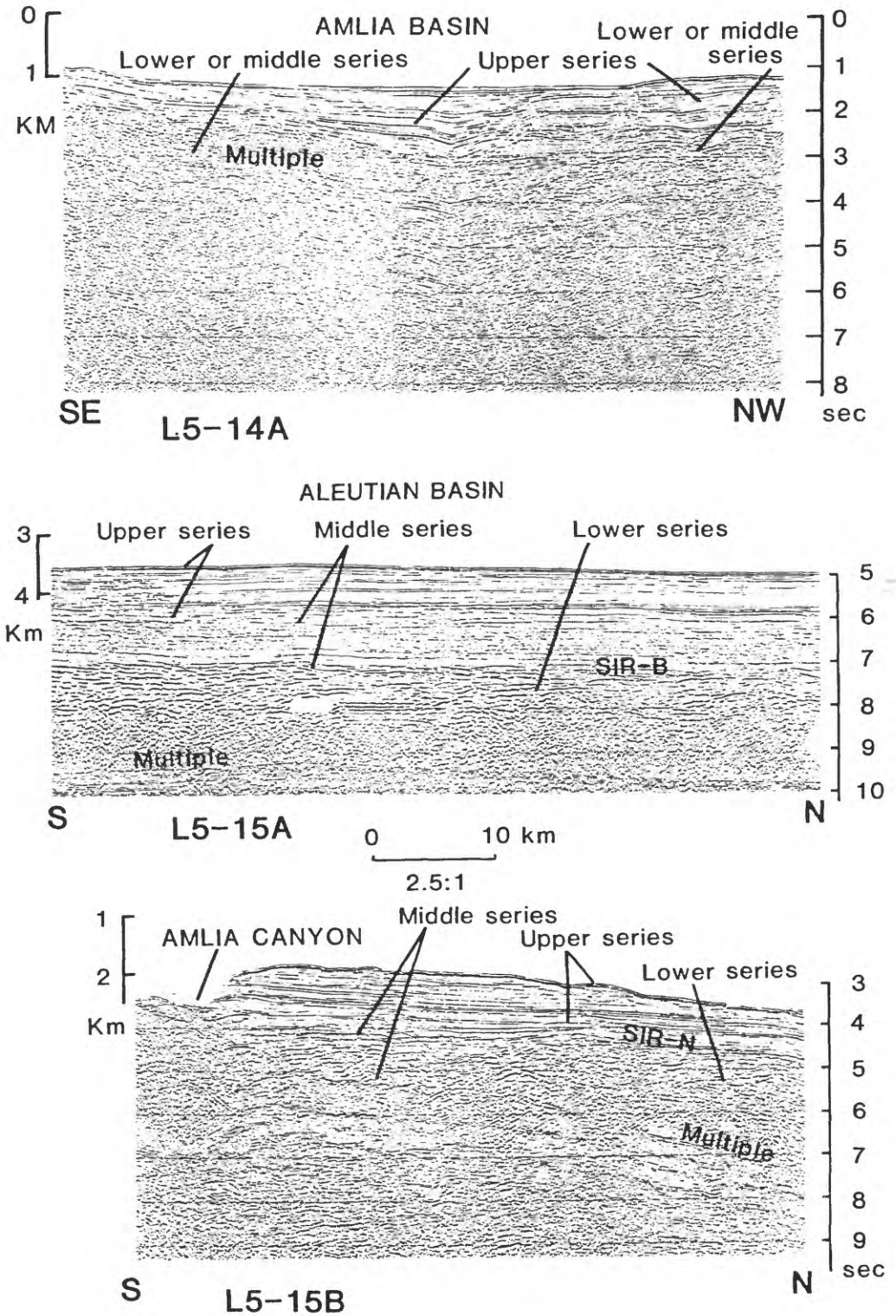

Figure 26: Examples of multichannel seismic-reflection data across the Aleutian Ridge and adjacent Aleutian Basin. See figure 21 for location. Examples are from Scholl and others (1983a).

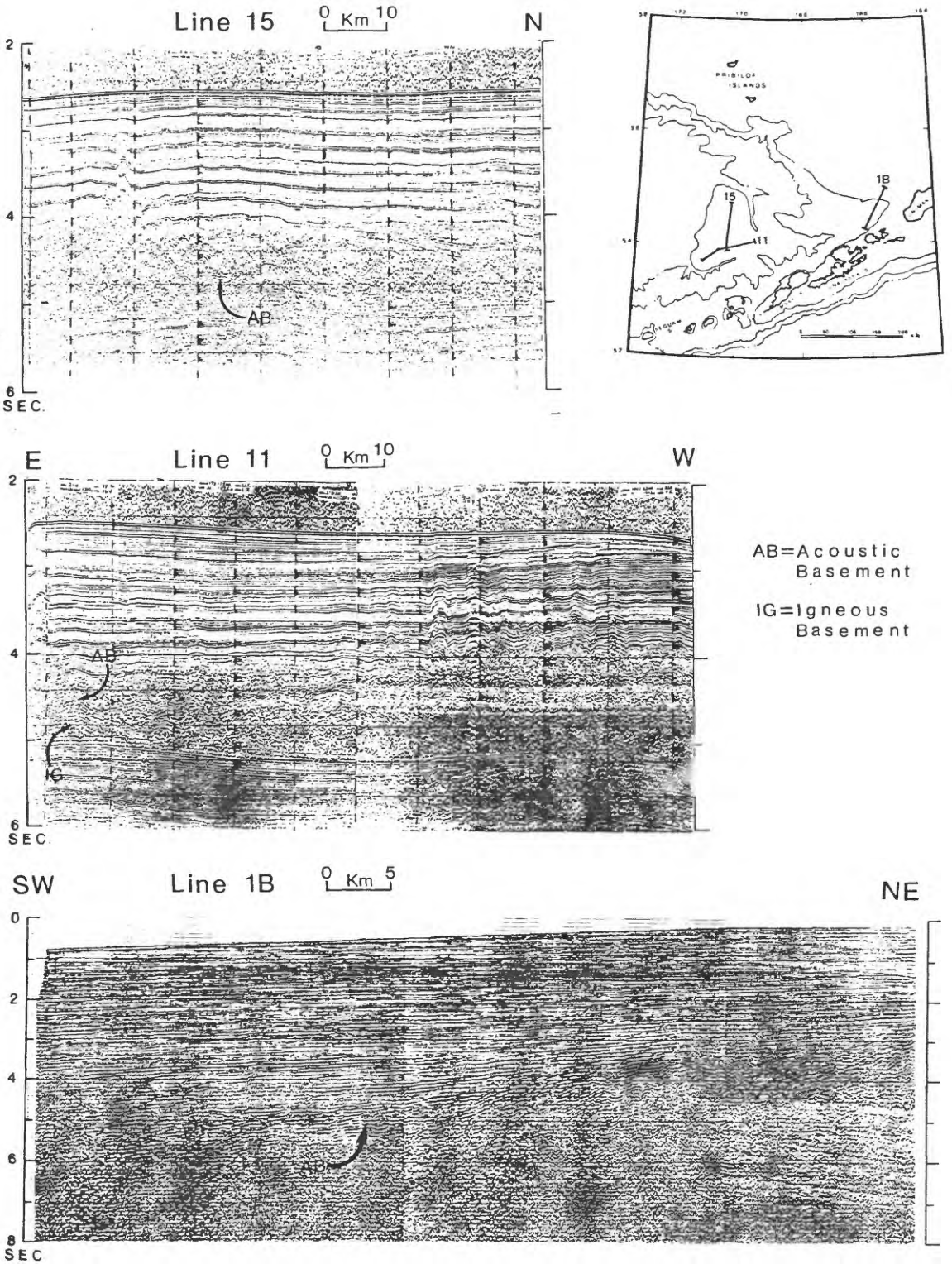

Figure 27. Seismic reflection records across the Umnak Plateau region. Profiles 11 and 15 are single channel records; line 1B is a multi-channel record.

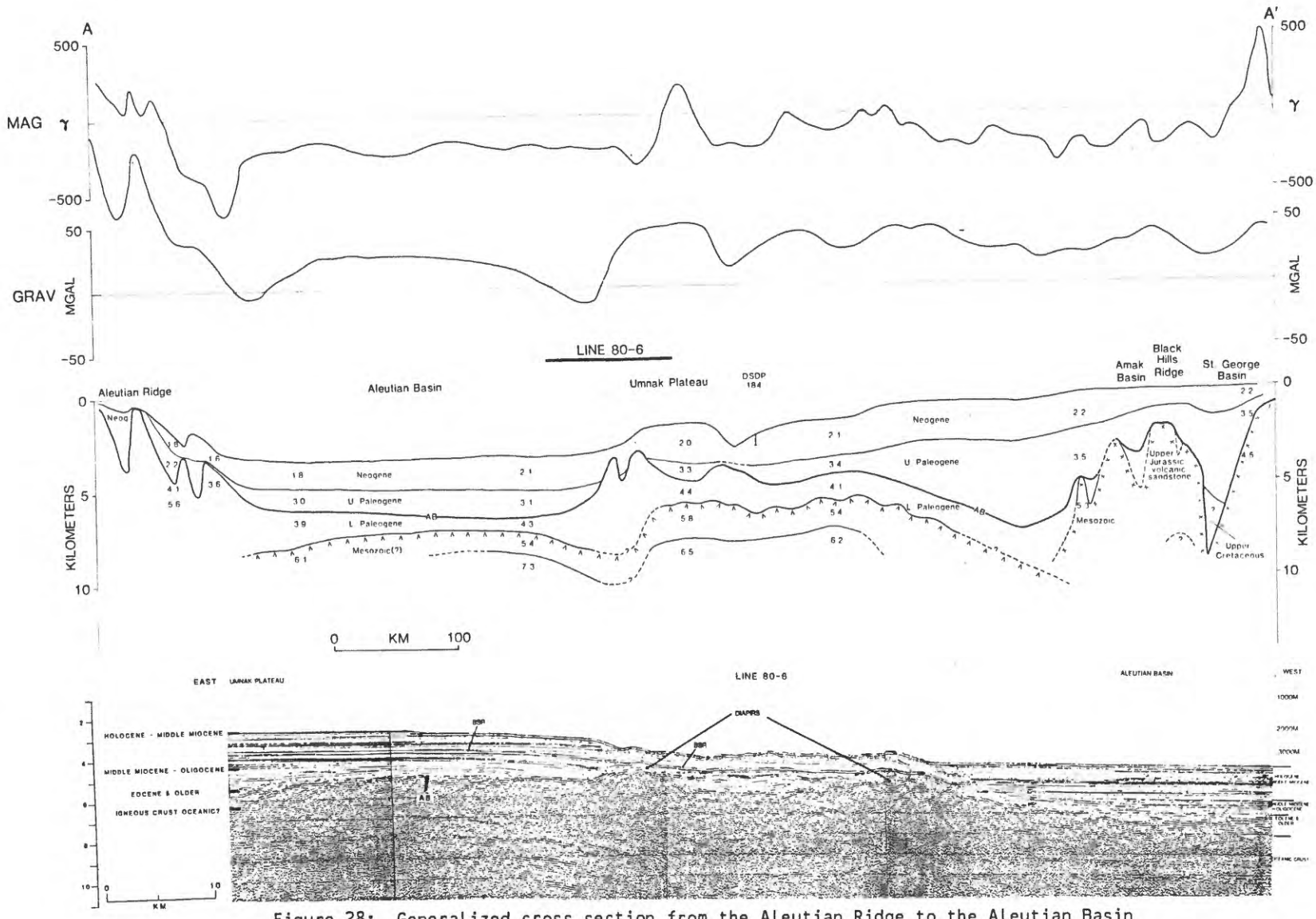

Figure 28: Generalized cross section from the Aleutian Ridge to the Aleutian Basin and to the Bering shelf (St. George basin). See figure 29 for location. The section shows the general distribution of upper series (Neogene), middle series (U. Paleogene), and lower series (L. Paleogene) rocks, as described by Scholl and others (1983a). AB is acoustic basement. Numbers are acoustic velocities in km/sec.

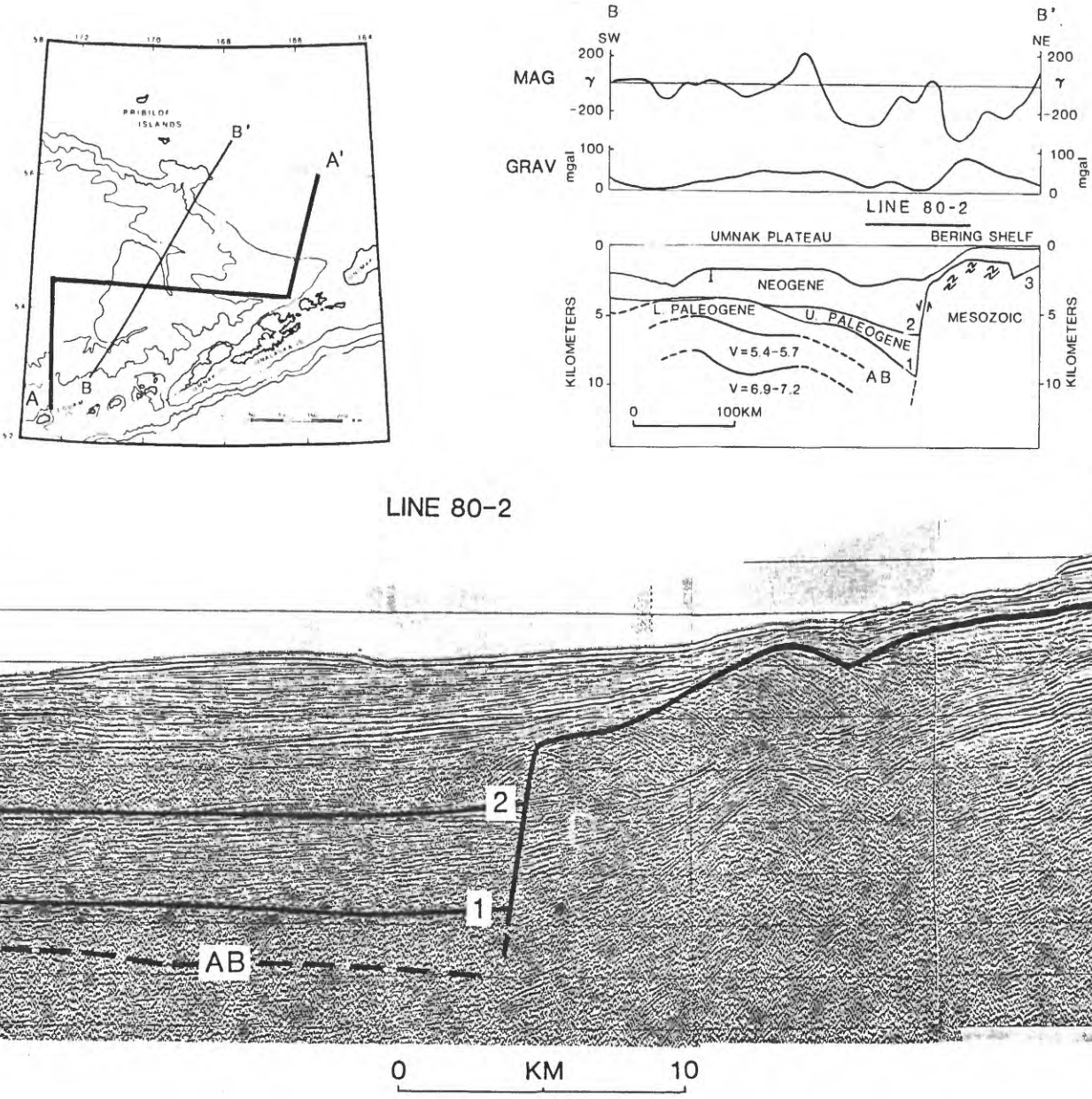

Figure 29: Example of multichannel seismic reflection data, with interpreted horizons, across the thick sedimentary deposits that lie beneath the Bering continental slope in the Umnak Plateau region. Track AA' on index map refers to Figure 28.

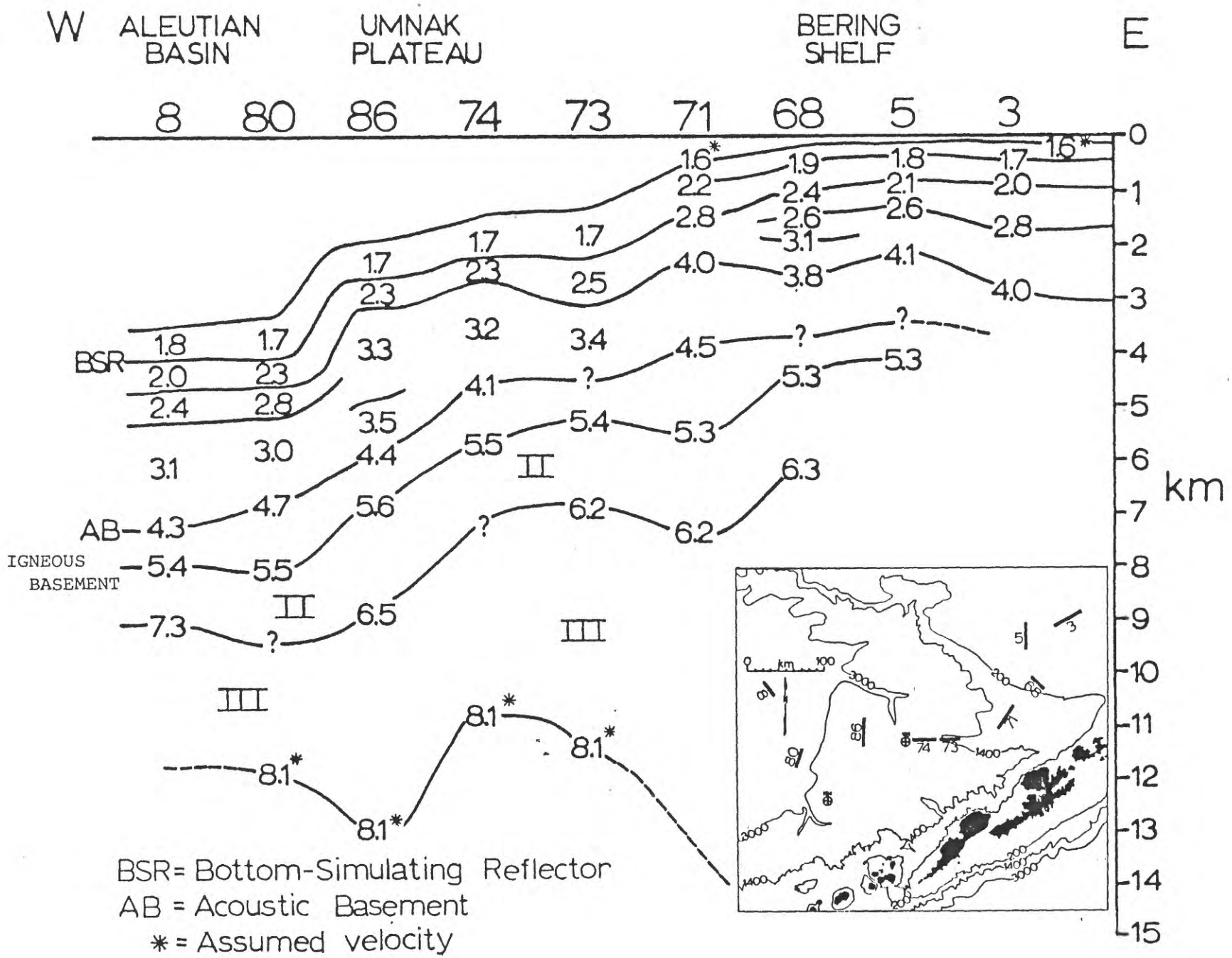

Figure 30. Crustal velocity profiles across the Umnak Plateau region derived from sonobouy data.

Structure and Isopach Maps

The depth to the top of acoustic basement, as determined from the seismic reflection data (Cooper and others, 1980), is shown in the structure-contour map on Figure 31; a companion isopach map showing the total thickness of sediment above acoustic basement is illustrated in Figure 32.

These maps indicate that the thickest parts of the sedimentary section (4 to 9 km thick) are found in deep basement depressions that lie beneath the upper continental slope along the north side of the Aleutian Ridge and the southern Bering margin. Beneath other parts of the Umnak Plateau region the acoustic basement surface forms ridges, troughs, and isolated piercement features with a relief of 1.5 to 2.5 km. The sediment thickness in these areas generally ranges from 2 to 4 km.

Sonobouy studies (Childs and others, 1979) indicate that igneous basement may lie 1.0 to 1.5 km below the acoustic basement; consequently the depths and thicknesses for the sedimentary section are likely to be 1.0 to 1.5 km deeper and thicker than shown on the structure-contour and isopach maps. On refraction data the igneous basement (Vp = 5.0 to 5.3 km/sec) is not conformable with acoustic basement thus implying local thickening and thinning of the lower series(?) basement layer.

Diapirs

Numerous diapirs have been documented beneath Umnak Plateau (Fig. 33) and are thought to be cored by shale (Scholl and Marlow, 1970), which may originate from a sedimentary unit within the lower series acoustic basement layer (Childs and others, 1979). These diapirs occur as isolated features and diapiric ridges or clusters (Figs. 28, 33, and 34), with a relief of 500 to 1500 meters. The larger diapirs are more common around the perimeter of the plateau.

Folding and Faulting

Most of the Umnak Plateau is covered by a sequence of flat-lying sediment that is relatively undeformed. There are, however, areas of the plateau and the surrounding continental slope that show local deformation caused by basement faulting, diapirism, slumping, marginal collapse, and cut and fill features. Basement faults, with veritcal offsets up to several kilometers, are the major structural features that dominate the Umnak Plateau region. One zone of faults with a cumulative offset of 2 to 3 km is buried beneath the continental slope and parallels the Bering shelf edge (Fig. 29). Subsidence across this part of the continental slope has occurred nearly continuously since early Tertiary time (Cooper and others, 1979); however, most of the faults are old features that do not reach the sea floor.

Another major basement fault zone may be present along the north side of the Aleutian Ridge, northeast of Unalaska Island (Fig. 31). Here a narrow depression, with a relief of 8 to 9 km formed during the early Tertiary to present constructional phase of the Aleutian Ridge. An underformed sedimentary section lies within the depression and abuts against the Aleutian Ridge (Line 1B, Fig. 27). Faulting of the sedimentary section occurs only at the extreme southern edge of the depression and does not break the sea floor. Other basement faults (Figs. 12, 13, and 14) under Umnak Plateau generally

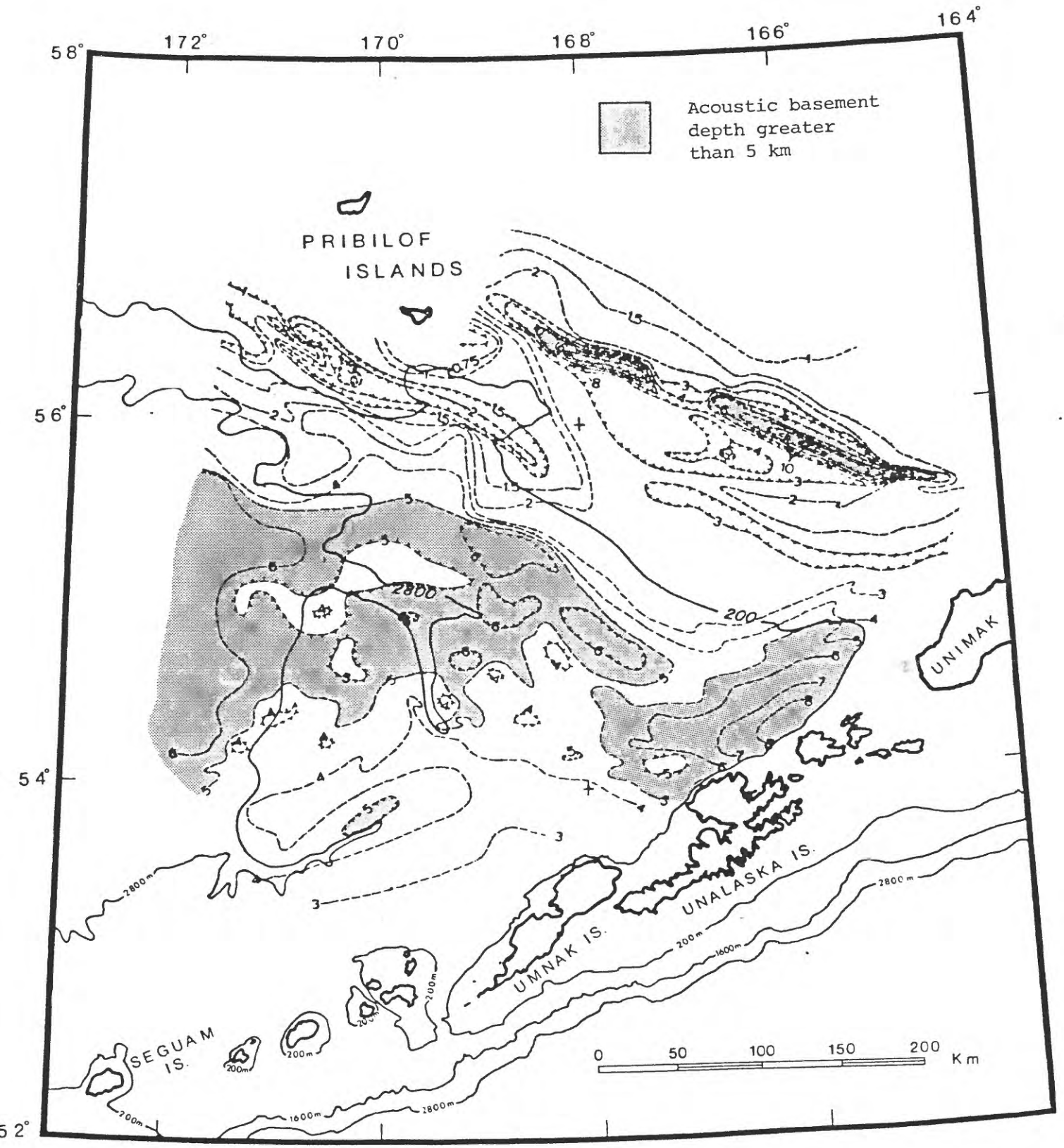

Figure 31. Structure-contour map showing the depth from sea level to acoustic basement.

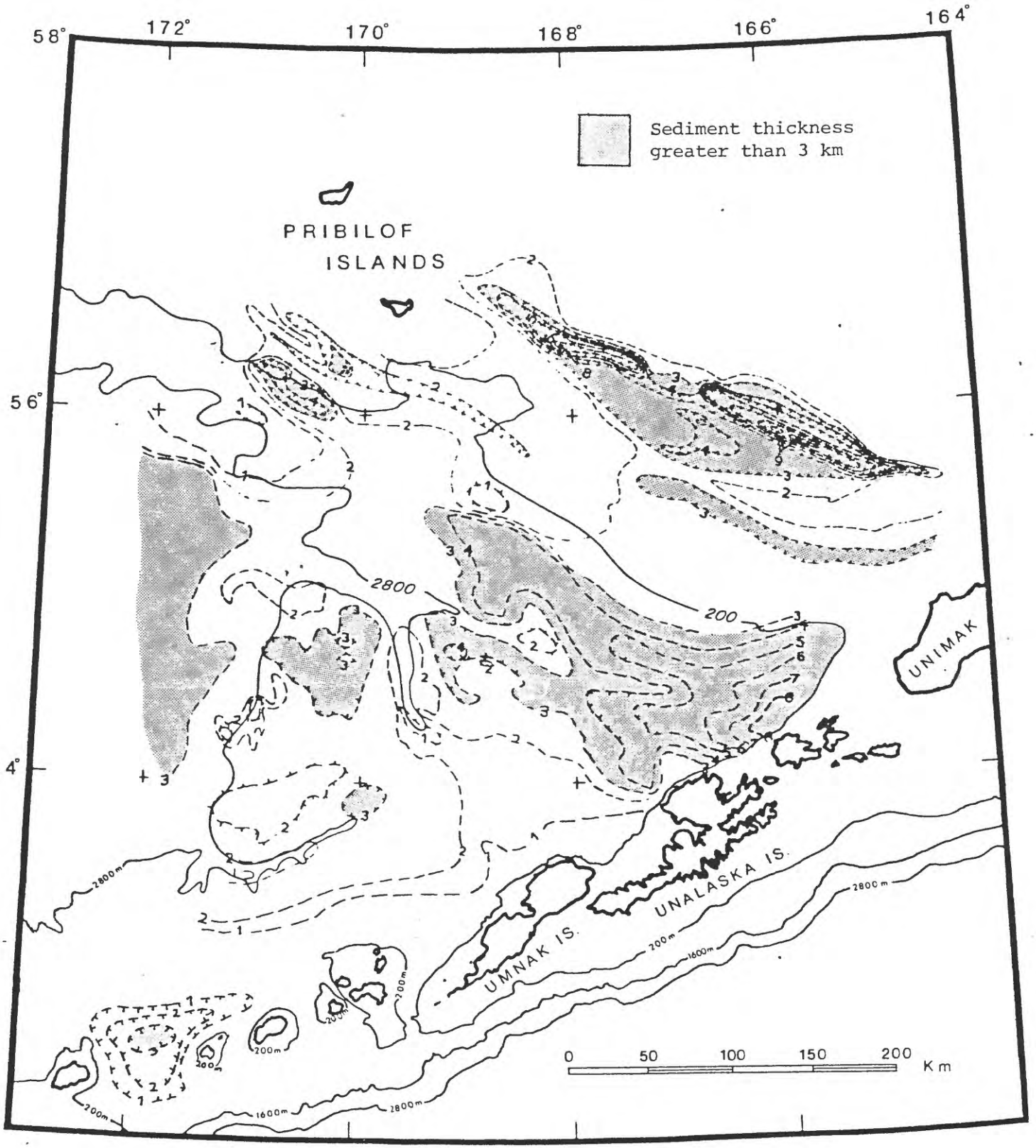

Figure 32. Isopach map showing the thickness of sediment above acoustic basement.

trend in the same direction as the fault zones along the Aleutian Ridge and the Bering slope. The displacement on these faults is 0.5 to 1.5 km, and the initiation of this faulting was probably in late Cenozoic time, as evidenced by the uplift and faulting of late Cenozoic sediments (Fig. 34).

Around most edges of Umnak Plateau, the sedimentary section is locally uplifted by underlying basement diapirs or faulted basement blocks (Fig. 34). These basement uplifts formed prior to or during the cutting of the submarine canyons. Above the uplifts, the steep sides of the canyons are scarred by cut and fill features, and by large bodies of sediment that have slumped or have collapsed from the edge of the plateau. The slumps and collapse structures are features that formed during and after the Pleistocene period of canyon cutting.

Summit basins - Aleutian Ridge

Beneath the ridge's summit platform, beds of the middle (?) and late series thicken substantially (2-4 km) in summit or perched basins (Scholl and others, 1983a). Only a small part of one of these basins, Amukta Basin, lies within the Umnak Plateau region. Amukta Basin is structurally contiguous with Amlia Basin (Figs. 21 and 26) and is bordered on the north by a fault scarp parallel to the Aleutian Ridge.

The formation of Amukta Basin records the beginning of extensional rifting of the ridge's summit platform and infilling with sedimentary deposits of the upper series. The upper series beds of Amukta and Amlia basins are locally folded and faulted along trends that mostly parallel the axis of the Aleutian Ridge.

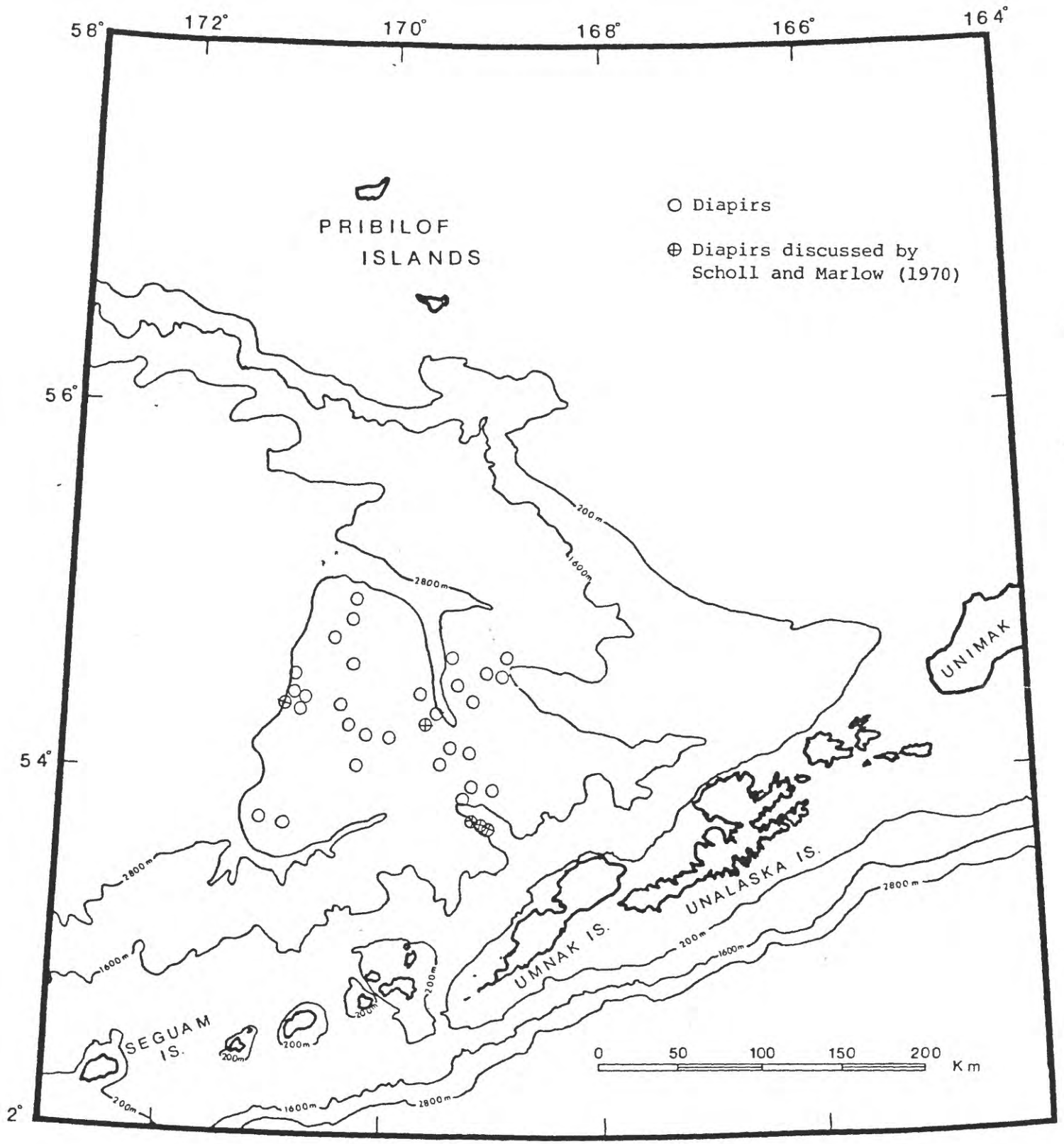

Figure 33. Map showing the location of diapirs within the Umnak Plateau region.

CHAPTER 2-2
PETROLEUM GEOLOGY

In the following discussion we incorporate new dredge sample information (Scholl and others, 1983a,b) and geophysical data (Fig. 20) into the previous studies of Cooper and others (1980) on the petroleum geology of the Umnak Plateau region.

Hydrocarbon deposits, other than methane gas at DSDP drilling Site 185, have not been sampled in the Umnak Plateau region. However, most of the factors commonly associated with hydrocarbon-producing areas exist within this region:

- Numerous structural and stratigraphic features that may be associated with hydrocarbon traps.
- A 1 to 9 km thick sedimentary sequence (early Tertiary to Holocene age) that has a temperature history favorable to the generation of hydrocarbons.
- Potential reservoir beds within the diatomaceous and clastic sedimentary sections.
- An organic carbon value range of 0.50-0.66% which incicates potential source beds could be present throughout the Cenozoic sedimentary section.

These factors, although favorable for hydrocarbon generation, are not definitive evidence that hydrocarbon accumulations are present. Acoustic evidence, such as 'bright spots' and 'VAMPs' (Velocity Amplitude features) is sparse and a mechanism for sealing the potential diatomaceous reservoir beds has not been identified.

Source Beds

A 0.50-0.66% organic carbon content of the dredge samples from the Umnak Plateau region indicates that adequate source beds could be present within the 1 to 9 km thick sedimentary section.

Organic carbon values for rocks recently dredged from the Aleutian Ridge (Table 5; Fig. 21; Scholl and others, 1983a) range from 0.42 to 1.01% with a median value of 0.66%. The age of the dredged rocks extends from Oligocene to early Pliocene; hence these organic carbon values are for rock units of the upper and middle series.

In other parts of the Umnak Plateau region, the average organic carbon value for 85 rock samples obtained from DSDP drilling (Bode, 1973; Underwood and others, 1979) and from dredging (Marlow and others, 1979b; Underwood and others, 1979) is 0.5 $\pm$0.21%. Nearly 60% of these samples are from the late Miocene to Holocene diatomaceous siltstones recovered at DSDP sites 184 and 185. Other samples are from the middle to late Miocene age diatomaceous rocks dredged in the Pribilof Canyon. Three Paleogene dredge samples have an average organic carbon content of 0.5%. Four samples of Cretaceous mudstone from Pribilof Canyon have as much as 1% organic carbon but the average for the four samples is 0.62%.

The middle Miocene and younger mudstones that have been dredged from the continental slope near Pribilof Canyon are from the upper part of the sedimentary sequence that blankets the Umnak Plateau region. The organic carbon content of these fine-grained mudstones may be representative of other more deeply buried Tertiary mudstones beneath the region, based on the uniformity of organic carbon measurements and the similarity of depositional environments for Miocene time (and presumably older) and the present.

TABLE 5. Organic carbon and physical property measurements for rocks dredged from the Aleutian Ridge. See figure 21 for location. Age information is included on table 4. Table is from Scholl and others (1983b).

Sample No. S6-79-	Sand (percent)	Silt (percent)	Clay (percent)	Sand/Mud	Median (Ø)	Organic Carbon (percent)	CaCO3 (percent)
12-2*	88.38	11.42	0.206	7.60	3.50	0.58	0.18
12-3	93.66	6.13	0.211	14.78	3.44	0.43	0.25
12-6	80.41	19.30	0.297	4.10	3.55	0.70	0.66
13-1	94.38	5.29	0.331	16.79	2.43	0.82	0.73
13-3	94.82	5.11	0.075	18.29	2.66	0.84	0.55
14-1	94.86	4.93	0.202	18.47	3.11	0.69	0.16
14-3	92.42	7.27	0.313	12.19	3.12	0.66	0.28
15-1	28.74	65.04	6.219	0.40	5.67	0.74	0.14
16-1	91.42	8.07	0.506	10.66	3.08	0.62	0.55
17-1	86.40	13.17	0.432	6.35	3.04	0.73	0.19
19.3	99.76	0.23	0.003	421.12	2.51	0.42	0.23
19-4	84.19	14.72	1.094	5.32	3.39	1.01	0.38
20-1	97.98	1.95	0.074	48.43	2.12	-	-
20-2	94.23	0.64	0.089	129.65	1.51	0.69	0.14
20-4	99.25	0.73	0.027	131.65	1.65	0.43	0.14
28-12	96.41	3.52	0.076	26.82	2.51	0.58	0.19
29-2	94.51	5.35	0.141	17.23	3.01	-	-
30-4	98.41	1.54	0.052	61.92	1.78	0.58	0.13
30-7	99.72	0.27	0.015	351.09	2.79	0.67	4.27
32-5	95.77	4.05	0.174	22.66	2.53	0.43	0.29
32-2	-	-	-	-	-	0.52	0.25
33-3	-	-	-	-	-	0.68	1.27

* Designates sample is no. 2 from dredge station S6-79-12 (i.e., station 12, sixth cruise of the R/V SEA SOUNDER, 1979).

Reservoir Beds

Combined porosity and permeability measurements have been made on only a few Tertiary rocks dredged from the Bering slope (Marlow and others, 1979a), and on Pliocene diatomaceous sediment recovered from DSDP Sites 188 and 190 in the Bowers and Aleutian Basins (Cooper and others, 1979c). Other measurements of porosity alone have been reported for the Miocene to Holocene sedimentary sections at DSDP Sites 184 and 185 on Umnak Plateau (Creager and others, 1973), and for other dredge samples along the Bering slope. Recent porosity and permeability measurement on upper and middle series rocks from the Aleutian Ridge (Scholl and others, 1983a) are given in Table 6.

The porosity of the diatomaceous oozes and siltstone in the upper 600 meters of the sedimentary section at DSDP Sites 184 and 185 ranges from 60 to 80%. A sharp decrease in porosity from 75 to 40% occurs at a depth of 600 to 650 meters across a silica diagenetic boundary between overlying diatomaceous oozes and underlying silicified mudstone (Lee, 1973). Porosities of mid-Oligocene to late Miocene rocks dredged from the Bering slope fall into two porosity ranges; mudstone, siltstone, and tuffs range from 45% to 68% and calcareous argillite and lithic wackes range from 14 to 29%. The data demonstrate that highly porous horizons may be found throughout the sedimentary section.

Only four permeability values have been reported for the dredge samples from along the Bering slope and these values (5, 1, 19, 2 mdarcy) are for late Oligocene to middle Miocene mudstone, siltstone, and tuffs. Cooper and others (1979c) discuss the permeability of diatomaceous sediment with porosities and diatom contents that are similar to those found under Umnak Plateau (Fig. 35). They note that the permeabilities of diatoms are large (6 to 49 mdarcy), permeability increases with depth from about 10 mdarcy at 150 meters depth to about 30 mdarcy at 600 meters depth and permeabilities decrease from 35 to .01 mdarcy across the silica diagenetic boundary between oozes and mudstone. The sedimentary sections on Umnak Plateau contain a larger volcanogenic and terrigenous component than the two sites studied by Cooper and others (1979) hence the permeability values may differ in the two areas.

The degree of diagenesis and lithification within the sedimentary section, especially at the diagenetic boundary between the diatomaceous oozes and indurated mudstone, has had a significant effect on the permeability and the porosity of potential reservoir beds. The areal distribution of the diagenetic boundary is an important factor that may limit the regional extent of reservoir beds that may exist in the thick Tertiary sedimentary section. High porosities (45 to 80%) and potentially good permeabilities (Cooper and others, 1979c), however, are favorable indicators that potential reservoir units for the accumulation of hydrocarbons may exist in the upper 600 meters of the sedimentary section. These favorable indicators also exist in adjacent areas of the Aleutian Basin (Cooper and others, 1979c).

Porosity values for upper and middle series rocks (Table 6) are, with one exception, large (36-59%); however, the permeability values are quite variable (0.2 to 45 mdarcy). The large permeability and porosity values in some sandstone samples indicates that adequate reservoirs could be present in both the upper and middle series rocks.

Seals

A mechanism for the trapping and accumulation of hydrocarbons within the

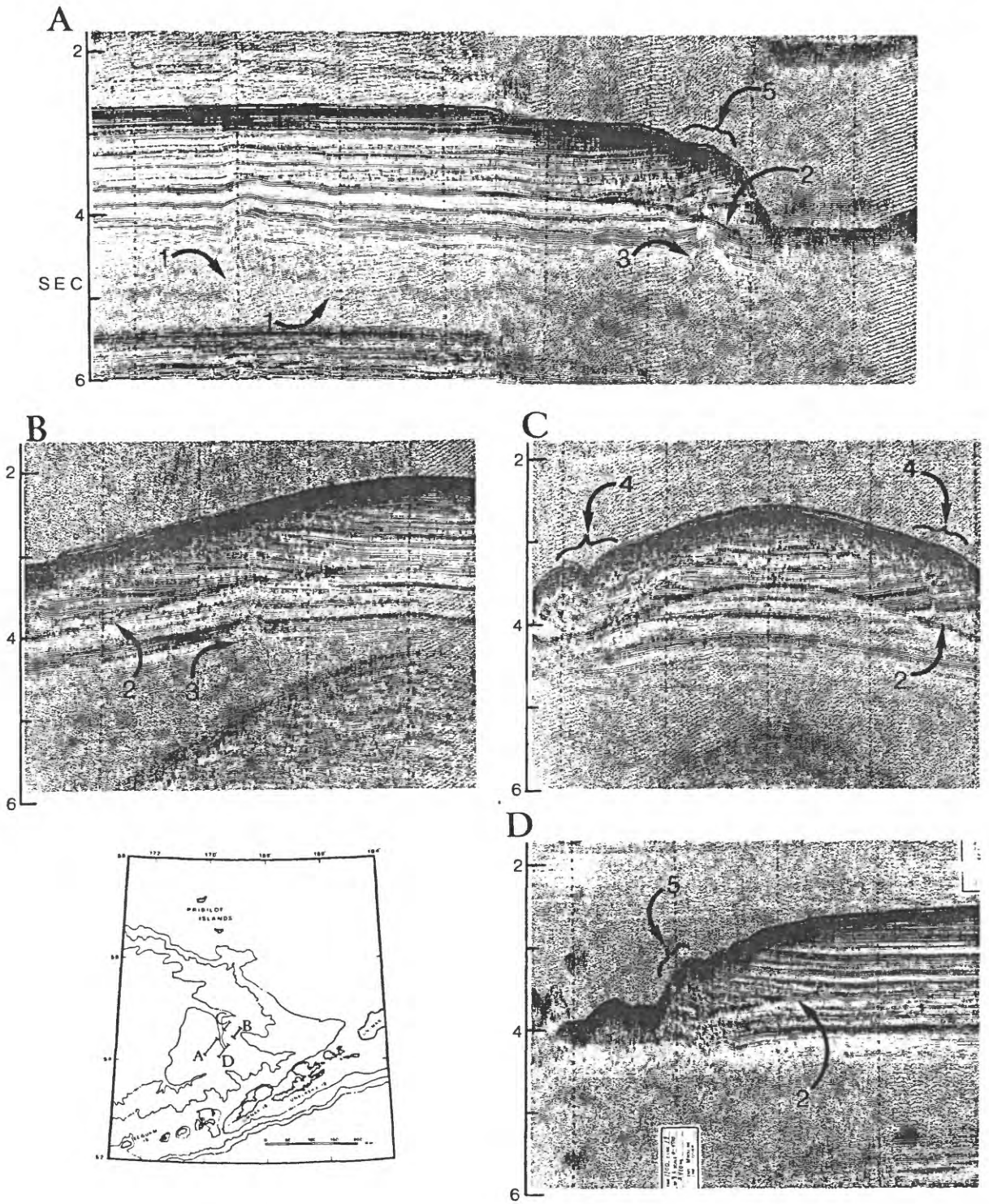

Figure 34. Seismic reflection profiles across the Umnak Plateau region. (1) Basement fault, (2) Bottom simulating reflector, (3) Diapir, (4) Slumps and cut and fill features, (5) Uplifted sedimentary bodies.

TABLE 6. Porosity and permeability values for rocks dredged from the Aleutian Ridge. See figure 21 for location. Table is from Scholl and others (1983b).

Sample number	Ages	Lithology	Permeability* (millidarcys)	Porosity (percent helium)
S6-79-12-6**	Early Oligocene	Silty sandstone	0.09	36.3
S6-79-13-3	Early Oligocene	Sandstone	11.5	52.5
S6-79-16-1	Oligocene	Sandstone	0.23	56.9
S6-79-17-1	Oligocene	Silty sandstone	0.30	52.9
S6-79-19-3	Early - middle Oligocene	Sandstone	38.0	42.3
S6-79-20-4	Late Miocene - early Pliocene	Sandstone	45.0	43.7
S6-79-28-12	Late Miocene- early Pliocene	Sandstone	4.73	55.3
S6-79-29-2	Late Miocene	Sandstone	1.23	58.7
S6-79-30-4	Middle middle Miocene	Sandstone	22.0	43.8
S6-79-32-2	Late Miocene - early Pliocene	Siltstone	2.81	13.9

* Results reported by Core Laboratories, Inc. Dallas, Texas
** Designated sample is no. 6 from dredge station S6-79-12 (table 1).

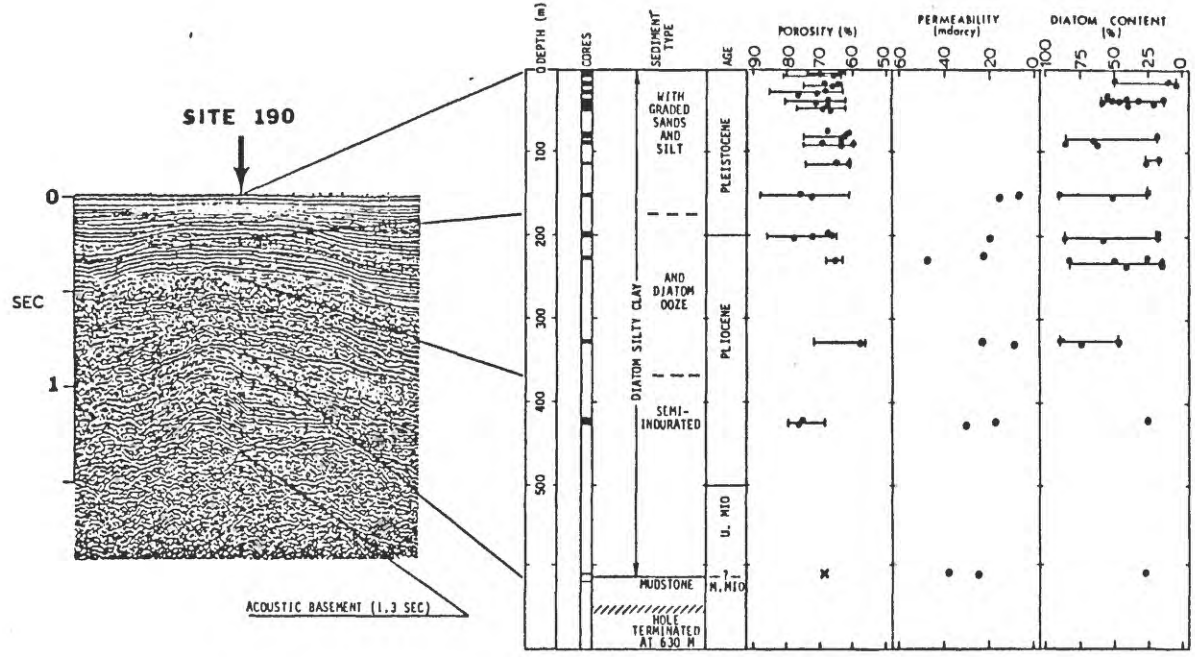

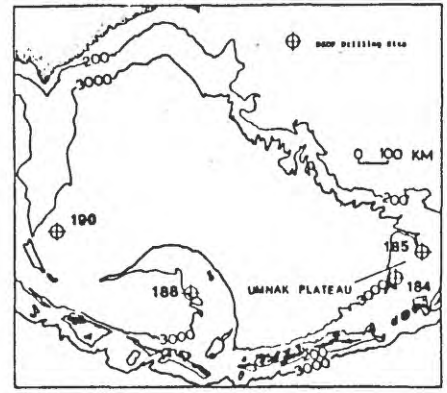

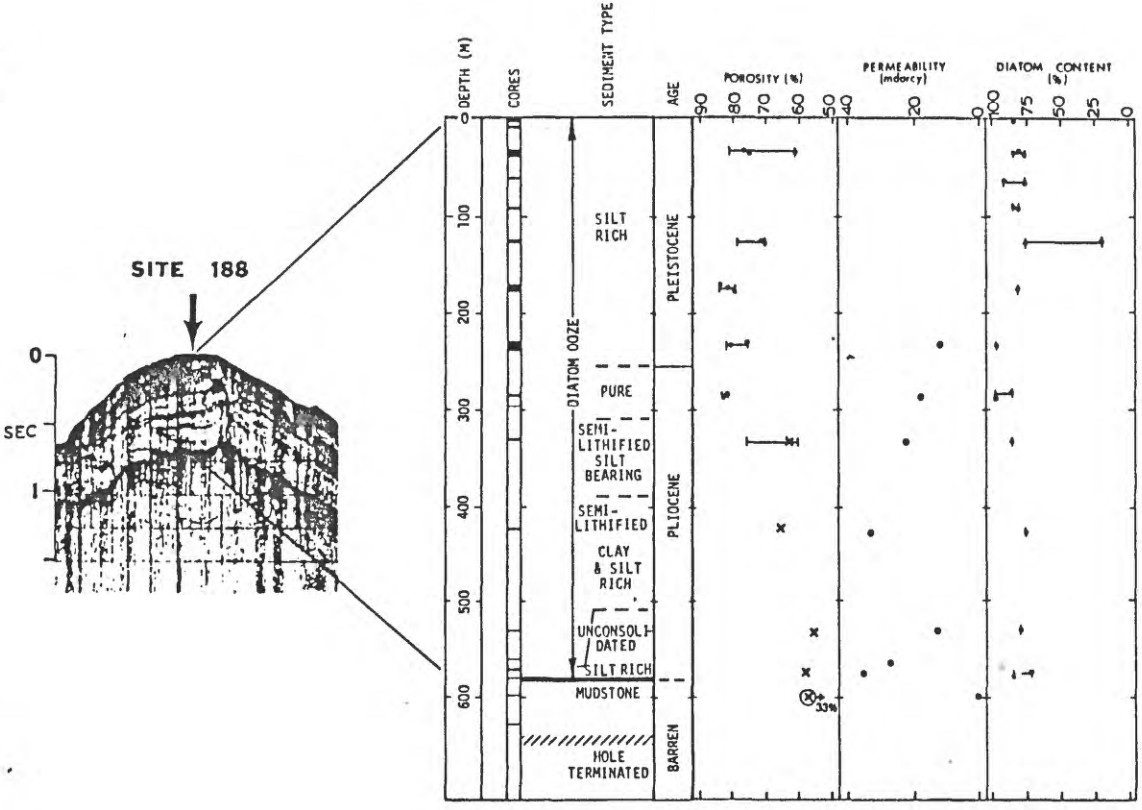

Figure 35. DSDP drilling sections at sites 188 and 190 in the Bering Sea (from Cooper and others, 1979).

porous diatomaceous sediment sections of abyssal basins has been proposed for the Aleutian Basin (Cooper and others, 1979c) and the Sea of Japan (Schlanger and Combs, 1975). These models allow hydrocarbons to be stored within a porous diatomaceous sedimentary section that is sandwiched between underlying mudstone and overlying turbidites. The turbidite unit is the stratigraphic seal that caps the diatomaceous reservoir unit. In the Aleutian Basin, velocity-amplitude features (VAMPs; Cooper and others, 1979c), which are acoustic features indicative of gas-charged sediment (Fig. 36), are found at the base of the turbidite unit.

A similar mechanism for the accumulation of hydrocarbons may be possible for parts, but not all, of the Umnak Plateau region. Preliminary inspection of the seismic reflection records indicates that the turbidite seals that probably exist in the Aleutian Basin may not be present in the Umnak Plateau region. Only one VAMP has been found in the region and this VAMP was observed beneath the flat-lying sediment section of the upper continental slope. Although the underlying mudstone and the diatomaceous sediment are present, the capping turbidite layer may only be present at the base of Umnak Plateau and in the floors and overbank deposits of the submarine canyons. If hydrocarbons are being generated within deeply buried mudstone beds, then other seals, such as an impermeable layer of altered volcanic sediment or an overlying clathrate layer must be present to trap the generated hydrocarbons.

Traps

Structural and stratigraphic traps similar to those in nearby areas of the Aleutian Basin and continental slope (Cooper and others, 1979c) may be present throughout the Umnak Plateau region. Structures such as diapirs, uplifted sedimentary bodies, and buried faults (Fig. 34) are common and may be associated with hydrocarbon traps. The deep sediment-filled depressions beneath the upper continental slope (Fig. 29) and the north side of the Aleutian Ridge (Fig. 27) are presumed to be bounded by deeply buried faults. Also, some basement uplifts beneath Umnak Plateau are fault bounded. These basement faults also fracture deep sediment layers and deform the overlying sediment horizons (Fig. 34). Although these deep faults do not break the sea floor, they may provide sub-surface routes along which fluids/gases can migrate upward from deeply buried sources and be trapped within the uplifted and folded sedimentary section.

Stratigraphic features such as pinchouts, filled channels, lateral diagenetic variations, and buried slumps are common and may also trap hydrocarbons. These features are all found beneath the continental slope, although they are more common in the canyon-scarred areas of the slope. The lateral diagenetic variations beneath Umnak Plateau, may, however, be the most important stratigraphic trapping mechanism. Pinchouts are common in all areas of the Umnak Plateau region where the sedimentary section has undergone rapid vertical displacement. Pinchouts are observed above structural depressions beneath the continental slope (Figs. 27, 29), over basement warps beneath Umnak Plateau (Figs. 28, 34), and near diapiric intrusions at the edge of Umnak Plateau (Fig. 34). Old filled channels found near the edge of the present submarine canyons are depositional features that formed during the late Cenozoic period of canyon cutting. These features may be of limited importance in the accumulation of hydrocarbons because they are relatively young.

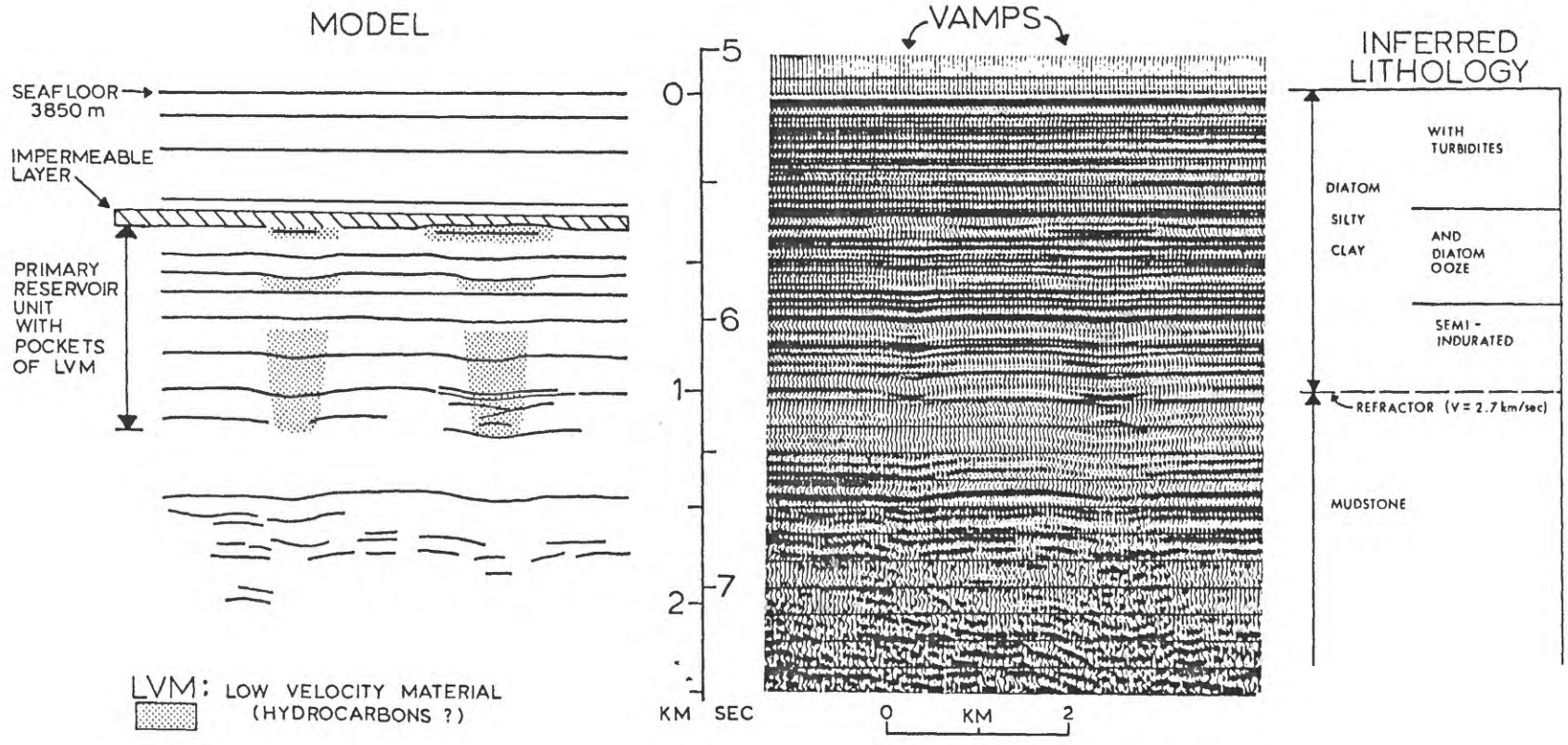

Figure 36. Model explaining the occurrence of VAMPs (from Cooper and others, 1979).

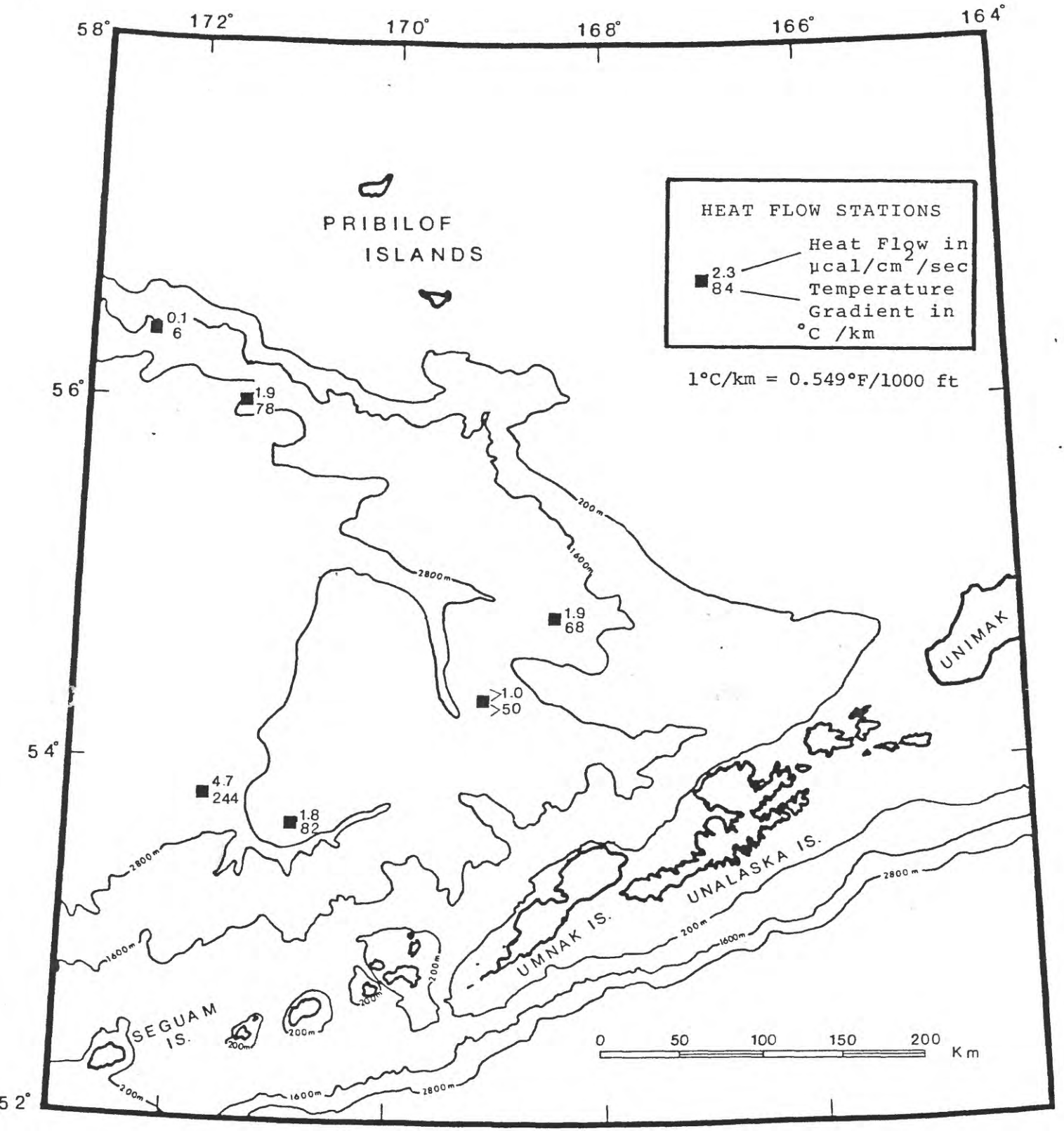

Figure 37. Heat flow stations in the Umnak Plateau region.

Thermal History

The hydrocarbon potential of a sedimentary sequence is largely dependent upon the burial time at temperatures necessary for the kerogen-hydrocarbon transformation (Schlanger and Combs, 1975). Observed temperature gradients in the Umnak Plateau region are large (50 to 82°C/km or 27 to 45°F/1000 ft; Fig. 37; Cooper and others, 1980) possibly because of the proximity to the Aleutian Ridge. Similar temperature gradients have probably existed throughout Cenozoic time as a consequence of episodic magmatic activity along the Aleutian Ridge.

If the observed gradients are projected downward into the 2 to 8 km thick section, then the onset temperatures for hydrocarbon generation (50 to 100°C) will be reached at relatively shallow sub-bottom depths (0.6 to 2.0 km). The age of the sediment at these sub-bottom depths is upper Miocene and older. The age of sediment below 0.9 km is unknown from drilling but deep sediment layers may be as old as Eocene age since Eocene rocks were dredged near Pribilof Canyon. If the temperature versus age curves for known oil and gas producing basins (Schlanger and Combs, 1975; Figs. 4, 5) are applied to the Umnak Plateau region and an average sedimentation rate of 100 mm/m.y. is assumed (Creager, 1973), then the generation of hydrocarbons could occur in horizons as young as early to middle Miocene age (16 to 24 m.y.) throughout the region. Locally higher temperature gradients, as might be expected adjacent to a volcanically active island arc, or higher sedimentation rates would allow hydrocarbons to be generated in horizons younger than middle to early Miocene age.

Diagenetic Boundary - Bottom Simulating Reflector (BSR)

The diagenetic boundary that occurs at a sub-bottom depth of 600 meters, and that causes a prominent reflection horizon (BSR) beneath most of the Umnak Plateau region may play an important role in the distribution of any hydrocarbons that may exist in the region:

- The boundary is believed to represent an isothermal surface (Hein and others, 1978) that cuts across stratigraphic time horizons and affects all Tertiary diatomaceous rocks.
- A major change in the lithology and physical properties (porosity, permeability, density, acoustic velocity) of the sediment occurs across the boundary.
- The boundary is associated with higher than normal concentrations of methane gas at Site 185 but is not associated with gas at Site 184. This gas may be a byproduct of the diagenetic process (Hein and others, 1978) or may be biogenic/thermogenic gas trapped within the thin diagenetic zone.
- The boundary may be a nearly impermeable barrier that controls the trapping or channeling of migrating hydrocarbons in areas where sediment is faulted or folded, such as along the sides of the submarine canyons, along the continental slope, and above diapiric intrusions on Umnak Plateau.

Aleutian Ridge

Over the crest of the Aleutian Ridge, adequate sediment thickness for

hydrocarbon generation is found only in Amukta Basin, a small portion of which lies within the Umnak Plateau region (Fig. 21). This basin is filled with diatomaceous and tuffaceous siltstone and mudstone, and sandy and silty turbidites which may be 1-4 km thick (Scholl and others, 1983a).

Upper and middle series beds underlying Amukta Basin are gently folded and disrupted by high-angle faults along the basin's northern and southern limits. Growth structures are also common.

Summit basins of Cenozoic island arcs are not generally viewed as likely habitats of petroleum resources, especially because their sedimentary sequences are presumably dominated by diagenetically unstable volcanic debris. However, the late Cenozoic summit basins of the Aleutian Ridge have a history of sedimentation and deformation that recommends a more optimistic appraisal about their potential for hydrocarbon resources. For example, the bulk of the terrigenous beds filling them is thought to be constructed of second-cycle clastic detritus derived chiefly from deformed, intruded (granodioritic stocks and batholiths) and altered volcanic and sedimentary rocks of Eocene through early Miocene age. Some large porosity and permeability values have been measured in sandstone horizons from the arc (Table 6). Fine-grained deposits, likely source beds for hydrocarbons, could be included in the older units of the basin fill; dredged rocks from the arc contain about 0.7% organic carbon (Table 5).

Associated andesitic volcanism undoubtedly contributed unstable minerals and glassy debris to these basins, but significantly altered and tightly cemented volcaniclastic deposits are not found at nearby DSDP sites (Creager, Scholl and others, 1973). In fact, volcanism may have increased the thermal gradient within the basin, a possibility that would aid in the generation of petroleum products. Seismic reflection profiles clearly reveal that folding and faulting of the late series beds took place in conjunction with sedimentation. Growth structures are abundant and could have trapped hydrocarbons as they were generated and migrated. And, finally, during the Neogene, the far north Pacific-Aleutian-Bering Sea region has been an area of high organic productivity (Scholl and Creager, 1973). If recoverable energy resources are present anywhere along the Aleutian Ridge, then they presumably could be contained within its large summit basins and along its sometimes thick flank deposits.

CHAPTER 2-3
REGIONAL HAZARDS

The major potential geologic hazards are 1) volcanic activity, 2) seismicity, 3) active faulting, 4) submarine slumping, 5) current- and wave-induced sediment transport, and 6) diapirism. Minor hazards such as shoreline effects by storm waves and landsliding can be locally important.

Volcanic Activity

Studies of the Aleutian Islands volcanoes (Coats, 1950) indicates a total of at least 76 major volcanic centers of which 36 have been active since 1760. Although all of the islands within the Umnak Plateau region are of volcanic origin only 14 of the region's 23 volcanoes are active (Fig. 38). Most active volcanoes lie along the axis of the Aleutian Ridge, but Bogoslof lies about 40 km north of Umnak Island.

Aleutian volcanoes are the type that can give highly explosive eruptions. Several Aleutian volcanoes outside of the Umnak Plateau region have erupted explosively and catastrophically during the past 10,000 years (Miller and Smith, 1977).

Since historic records of cataclysmic eruptions in the Umnak Plateau region are limited, we cannot effectively evaluate the potential hazards of these great volcanoes. Some of the violent eruptions were probably similar to the eruption at Krakatau in 1883. If facilities are sited near one of these volcanoes, the potential risks are large. In 1944, for example, a spectacular eruption of Okmok volcano on Umnak Island nearly caused the evacuation of a military airbase (Robinson, 1947).

Seismicity

The southern boundary of the Umnak Plateau region falls within the 300 km wide Aleutian seismic zone (Figs. 15 and 38), one of the most active zones in the world. Investigations of this zone are summarized by Davies and House (1979).

Earthquakes in the Umnak Plateau region occur at increasingly greater depth with distance north of the Aleutian Ridge. The northward-dipping (45-50 degrees) seismic zone lies at a subsurface depth of approximately 40 km beneath the southern edge of the summit platform and 200 km beneath the north ridge flank.

Earthquakes pose three distinct geohazards in the Umnak Plateau region: (1) severe ground shaking caused by a great earthquake (magnitude greater than 7; Sykes, 1971), (2) frequent earthquakes of low to moderate magnitude that may be associated with progressive rupturing of the sea floor, and (3) tsunamis or seismic sea waves. Great earthquakes, and their destructive potential in terms of violent ground motion and associated tsunamis, occur commonly in the vicinity of the Umnak Plateau region. At least 16 great earthquakes have occurred along the Aleutian seismic zone since 1929 (Sykes, 1971). Six of these quakes, with magnitudes varying from 7.0 to 8.6, occurred along or adjacent to the southern part of the Umnak Plateau region (Fig. 38). One of these quakes, the 1946 shock seaward of Unimak Island, generated one of the most destructive tsunamis recorded in the Pacific (Sykes, 1971). Davies and House (1979) emphasize that the Shumagin Island region immediately

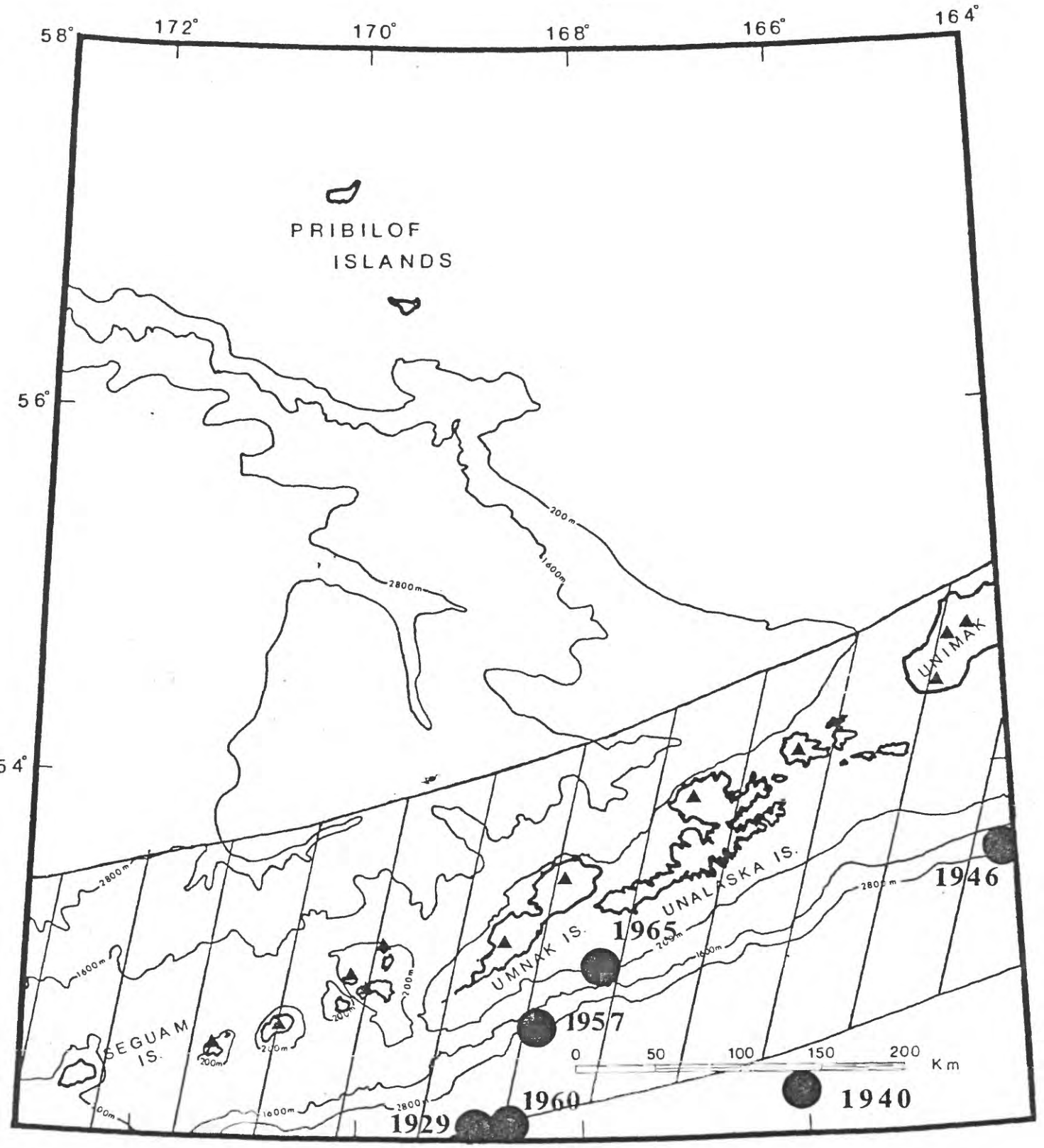

Figure 38. Seismicity of the Aleutian Ridge. Ruled areas show approximate limits of the Aleutian seismic zone. Large dots are approximate locations of great earthquakes (magnitude larger than 7.0) listed by Sykes (1971). Solid triangles are active volcanoes.

east of the southeast corner of the lease area has been identified as a seismic gap, which is a section of the Aleutian seismic zone that has not been ruptured by a great earthquake within the past 20 to 30 years. This circumstance predicts the likelihood that a potentially destructive and possibly tsunami-generating earthquake will occur close to the Umnak Plateau region within the next few decades.

Seismic reflection profiles commonly reveal fault scarps cutting the Aleutian Ridge summit platform and sloping flanks. Epicenteral information is presently too meager to determine if low and moderate magnitude earthquakes are associated with these scarps, but the inference is that a relationship seems likely.

Active Faulting

Numerous scarps, some as high as 150 m, rupture the Aleutian Ridge summit platform (Fig. 23). These scarps apparently are fault-controlled because they border summit basins, disrupt the basin's sedimentary fill, and determine the locations of inter-island passes and straits. The length of these fault scarps is not known but is important because active-fault length can be related to the magnitude of earthquakes associated with the faults. Faults on the ridge summit are likely to be active because their scarps are well expressed geomorphically.

Active volcanism and regional seismicity beneath the northern flank of the ridge imply that the shallow-water part of the ridge flank is probably affected by surface rupturing. Surface faults have been observed in seismic reflection profiles from parts of Umnak Plateau and the continental slope along the eastern part of the area, but detailed mapping has not been attempted. The lengths, offsets, and types of slope faults are unknown. Many of the faults are commonly associated with large slumps.

Submarine Slumps

Many portions of the slopes surrounding the Umnak Plateau region are marked by scars and hummocky topography that most likely are related to submarine slumping. Detached sediment bodies are common in the steep areas, especially along submarine canyon walls; shallow deformed sediment is observed along the more gentle slopes between the Pribilof and Bering submarine canyons. Slump bodies are common on seismic reflection profiles across margins of Umnak Plateau. The areas of greatest slump potential are those that have thick sequences of semi-consolidated middle and upper series beds (MLS sequence) and steep slopes.

Sediment Transport

Tide-generated currents as swift as 9 to 10 knots sweep through narrow passes between islands along the Aleutian Ridge. These currents are swift enough to move coarse grained sediments and to generate moving bedforms.

Seismic reflection profiles taken across Amukta basin reveal bedforms that imply swift currents also exist in deeper water areas. The bedforms appear to be large (10 x 200 m to 10 x 1000 m) sediment waves. These bedforms may be presently active or moving. An alternative explanation is that they

are relict features, possibly formed in lower sea level regimes during the last glaciation.

Sediment, therefore, is moved rapidly in tide-dominated shallow-water passes, and probably in deep water areas of the summit platform as well. The rate and the net direction of transport, and the volume of debris being transported are virtually unknown factors for most areas of the summit platform and its flanking slopes.

Part of the sediment that sweeps through the passes may be deposited in the submarine canyons that cut the north flank of the Aleutian Ridge. Turbidity currents and debris flows associated with the mass movement of this sediment would be transported down the submarine canyons and out onto the floor of the Aleutian Basin.

The effects of wave erosion, wave transport, and longshore currents have not been evaluated. We suspect that the irregularities of the shoreline plus the frequency and strengths of the storms in the area produce significant erosion and transport of sediment.

Diapirism

Numerous diapirs of probable sedimentary origin are found on Umnak Plateau and along the north flank of the Aleutian Ridge. The origin of the diapirs on Umnak Plateau may be the injection of a mobile shale unit into the sedimentary section. Hence, overpressured shale units may be present in the area of diapirs, a potential hazard to drilling operations.

CHAPTER 2-4
HARD MINERALS GEOLOGY

Potential hard mineral resources in the Aleutian Island Arc are Manganese-Cobalt (Mn-Co) crusts and massive (Kuroko-type) sulfide deposits. Neither of these has been investigated to determine their resource potential.

Mn-Co crusts have been dredged from along the Aleutian ridge, but no source data are available. Preliminary investigations in other island arcs have identified hydrothermal sources for some of the crusts, which means that they definitely should be evaluated in the Aleutian offshore.

Kuroko-type base/precious metal deposits are related to island arc volcanism. The processes (e.g. source of metals, structural and geochemical controls for sulfide deposition, origin and composition of ore fluids, and evolution of the source and depositional systems in time and space), however, are problematic and poorly understood.

We do know that hydrothermal activity created metal deposits along the arc in the past as shown by sulfide deposits on Unalaska Island and on the Soviet-held Komandorsky islands. This implies that they should occur elsewhere in the older rocks of the islands; preliminary investigations on Attu and Atka islands show that hydrothermal activity has occurred and that at least those islands need to be mapped in more detail in order to determine whether potential ore bodies occur.

Active hydrothermal activity is occurring along the island arc and there is some potential that metal-depositing submarine vents occur, similar to those found on the East Pacific Rise and the Juan de Fuca Ridge. At least 30 volcanoes have been active since 1700. The segmented line of volcanoes runs from Unimak Island at the tip of the Alaska Peninsula to Buldir Island, a distance of 1300 km. West of Buldir Island, along and within a ridge-top graben, the presence of several seamounts suggests that active submarine volcanism is taking place. That area should be evaluated.

REFERENCES

Askren, D. R., 1972, Holocene stratigraphic 7ramework southern Bering Sea continental shelf: MS Thesis, Univ. of Washington, 104 p.

Bailey, K. A., Cooper, A. K., Marlow, M. S., and Scholl, D. W., 1976, Preliminary residual magnetic map of the eastern Bering shelf and parts of western Alaska: U.S. Geol. Survey Misc. Geol. Inv. Map 1-71.

Ben-Avraham, Z., and Cooper, A. K., 1981, The early evolution of the Bering Sea by collision of oceanic rises and North Pacific subduction zones: Bull. Geol. Soc. Amer., v. 92, p. 485-495.

Berggren, W. A., 1969, Cenozoic chronostratigraphy, planktonic foraminiferal zonations and the radiometric time scale: Nature, v. 224, no. 5224, p. 1072-1075.

Bode, G. W., 1973, Carbon-Carbonate, in Creager, J. S., ed., and others, Initial reports of the Deep Sea Drilling Project, v. 19: Washington, D.C., U.S. Government Printing Office, p. 663-666.

Brockway, R., Alexander, B., Day, P., Lyle, W., Hiles, R., Decker, W., Polski, W., and Reed, B., 1975, Bristol Bay region, "Stratigraphic correlation section," southwest Alaska: The Alaska Geological Society, P. O. Box 1288, Anchorage, AK 99510.

Burk, C. A., 1965, Geology of the Alaska Peninsula Island arc and continental margin: Geol. Soc. America Mem. 99, 250 p.

Childs, J. R., Cooper, A. K., and Parker, A. W., 1979a, Sonobuoy studies of Umnak Plateau, Bering Sea (abs.): EOS (Am. Geophys. Union Trans.) Vol. 60, No. 18, p. 390.

Coats, R. R., 1950, Volcanic activity in the Aleutian arc: U.S. Geol. Survey Bull. 974-B, p. 35-47.

Cooper, A. K., Marlow, M. S., and Scholl, D. W., 1976a, Mesozoic magnetic lineations in the Bering Sea marginal basin: Jour. Geophys. Res., v. 81, p. 1916-1934.

Cooper, A. K., Scholl, D. W., and Marlow, M. S., 1976b, Plate tectonic model for the evolution of the eastern Bering Sea Basin: Geol. Soc. America Bull., v. 87, p. 1119-1126.

Cooper, A. K., Marlow, M. S., and Scholl, D. W., 1979a, Thick sediment accumulations beneath continental margin of outer Bering Sea (abs): AAPG-SEPM program, Annual Convention, April 1979, p. 72.

Cooper, A. K., Marlow, M. S., Parker, A. W., and Childs, J. R., 1979b, Structure-contour map on acoustic basement in the Bering Sea: U.S. Geological Survey map, MF 1165, 1 p.

Cooper, A. K., Scholl, D. W., Marlow, M. S., Childs, J. R., Redden, G. R., Kvenvolden, K. A., and Stevenson, A. J., 1979c, Hydrocarbon exploration in the Aleutian Basin, Bering Sea: Bull. AAPG, v. 63, p. 2070-2087.

Cooper, A. K., Scholl, D. W., Vallier, T. L., and Scott, E. W., 1980, Resource report for the deep-water areas of proposed OCS Lease Sale No. 70, St. George basin, Alaska: U.S. Geological Survey Open-File Report OF 80-246, 90 p.

Cooper, A. K., Marlow, M. S., and Ben-Avraham, Zvi, 1981, Multichannel seismic evidence bearing on the origin of Bowers Ridge, Bering Sea: Bull. Geol. Soc. Amer., v. 92, p. 474-484.

Creager, J. S., Scholl, D. W., and others, 1973, Initial reports of the Deep Sea Drilling Project, v. 19: Washington, D.C., U.S. Govt. Printing Office, p. 193.

Davis, J. N., and House, L., 1979, Aleutian subduction zone seismicity, volcano-trench separation and their relation to great thrust-type earthquakes: Jour. Geophy. Research, v. 84, p. 4583-4591.

Gardner, J. V., Vallier, T. L., Dean, W. E., Kvenvolden, K. A., and Redden, G. D., 1979, Sedimentology and Geochemistry of surface sediments and the distribution of faults and potentially unstable sediments, St. George basin region of the outer continental shelf, southern Bering Sea: U.S. Geol. Survey Open-File Rept. 79-1562, 89 p.

Hatten, C. W., 1971, Petroleum potential of Bristol Bay Basin, Alaska: Am. Assoc. Pet. Geol. Mem., 15, v. 1, p. 105-108.

Hein, J. R., Scholl, D. W., Barron, J. A., Jones, M. G., and Miller, J., 1978, Diagenesis of late Cenozoic diatomaceous deposits and formation of the bottom simulating reflector in the southern Bering Sea: Sedimentology, v. 25, p. 155-181.

Hoare, J. M., 1961, Geology and tectonic setting of lower Kuskokwim-Bristol Bay region, Alaska: Am. Assoc. Pet. Geol. Bull., v. 45, no. 5, p. 594-611.

Hopkins, D. M., 1967, The Cenozoic history of Beringia -- a synthesis, in Hopkins, D. M., ed., The Bering Land Bridge: Stanford Univ. Press, Stanford, CA., p. 451-484.

Hopkins, D. M., Scholl, D. W., Adicott, W. O., Pierce, R. L., Smith, P. B., Wolfe, J. A., Gershanovich, D., Kotenev, B., Lohman, K. E., Lipps, J. H., and Obradovich, J., 1969, Cretaceous, Tertiary, and early Pleistocene rocks from the continental margin in the Bering Sea: Geol. Soc. America Bull., v. 80, p. 1471-1480.

Hopkins, D. M., and Scholl, D. W., 1970, Tectonic development of Beringia, late Mesozoic to Holocene (abs.): Am. Assoc. Pet. Geol., v. 54, no. 12.

Jones, D. M., Kingston, M. J., Marlow, M. S., Cooper, A. K., Barron, J. A., Wingate, F. H., and Arnol, R. E., 1981, Age, mineralogy, physical properties, and geochemistry of dredge samples from the Bering Sea continental margin: U.S. Geological Survey Open-File Report OF 81-1297, 68 p.

Kvenvolden, K. A. and Redden, G. D., 1979, Hydrocarbon gas in sediment from the shelf, slope, and basin of the Bering Sea.

Lee, H. J., 1973, Measurements and estimates of engineering and other physical properties, Leg 19, in Creager, J. S., Scholl, D. W., and others, Initial reports of the Deep Sea Drilling Project, v. 19: Washington, D.C., U.S. Govt. Printing Office, p. 701-719.

Lisitsyn, A. P., 1966, Recent sedimentation in the Bering Sea (in Russian): Inst. Okeanol. Akac. Nauk USSR, (translated by Israel Program for Scientific Translation), available from U.S. Dept. Commerce, Clearinghouse for Fed. Sci. and Tech. Info., 1969, 614 pp.

Lyle, W. M., Morehouse, J. A., Palmer, I. F., Jr., and Bolm, J. G., 1979, Tertiary formation and associated Mesozoic rocks in the Alaska Peninsula area, Alaska, and their petroleum-reservoir and source-rock potential: State of Alaska, Division of Geological and Geophysical Surveys, Geologic Report 62, 65 p. .

Marlow, M. S., Scholl, D. W., Buffington, E. C., and Alpha, T. R., 1973, Tectonic history of the western Aleutian arc: Geol. Soc. America Bull., v. 84, p. 1555-1574.

Marlow, M., McLean, H., Vallier, T., Scholl, D., Gardner, J., and Powers, R., 1976a, Preliminary report on the regional, oil and gas potential, and environmental hazards of the Bering Sea Shelf south of St. Lawrence Island, Alaska: U.S. Geol. Survey Open-File Report OF 76-785, 60 p.

Marlow, M. S., Scholl, D. W., Cooper, A. K., Buffington, E. C., 1976b, Structure and evolution of Bering Sea shelf south of St. Lawrence Island: Am. Assoc. of Pet. Geol. Bull., v. 60, no. 2, p. 161-183.

Marlow, M. S., Scholl, D. W., Cooper, A. K., and Jones, D. L., 1979a, Mesozoic rocks from the Bering Sea: The Alaska-Siberia Connection: (abs.) Cordilleran Section Geol. Soc. Amer. Ann. Mtg. 1979, v. 11, no. 3, p. 90.

Marlow, M. S., Cooper, A. K., Scholl, D. W., Vallier, T. L., and McLean, H., 1979b, Description of dredge samples from the Bering Sea Continental Margin: U.S. Geological Survey Open-File Report OF 79-1139, 5 p.

Marlow, M. S., Gardner, J. V., Vallier, T. L., McLean, H., Scott, E. W., and Lynch, M. B., 1979c, Resource report for proposed OCS Lease Sale No. 70 St. George basin, shelf area, Alaska: U.S. Geological Survey Open-File Report OF 79-1650, 79 p.

Marlow, M. S., and Cooper, A. K., 1984, Regional geology of the Beringian continental margin: Proceedings of the OJI International Seminar of the Formation of Ocean Margins, Univ. Tokyo, Tokyo, Japan, (in press).

McLean, Hugh, 1977, Organic geochemistry, lithology, and paleontology of Tertiary and Mesozoic rocks from wells on the Alaska Peninsula: U.S. Geol. Survey Open-File Report OF 77-813, 63 p.

Meyers, H., Brazee, R. J., Coffman, L. L., and Lessig, S. R., 1976, An analysis of earthquake intensities and recurrence rates in and near Alaska: N.O.A.A. Tech. Memorandum, EDS NGSDC-3, 101 p.

Miller, T. P., and Smith, R. L., 1977, Spectacular mobility of ash flows around Aniakchak and Fisher Calderas, Alaska: Geology, v. 5, p. 173-176.

Moore, D. G., 1969, Reflection profiling studies of the California continental borderland: structure and Quaternary turbidite basins: Geol. Soc. Amer. Spec. Paper 197, 142 p.

Nelson, Hans, Hopkins, D. M., and Scholl, D. W., 1974, Cenozoic sedimentary and tectonic history of the Bering Sea, in Hood, D. W., and Kelley, E. J., eds., Oceanography of the Bering Sea: University of Alaska Institute of Marine Sciences, Occasional Publication No. 2, p. 485-516.

Page, R. A., 1975, Evaluation of seismicity and earthquake shaking at offshore sites: Offshore Technology Conference Proceedings, p. 179-190.

Patton, W. W., Jr., Lanphere, M. A., Miller, T. P., and Scott, R. A., 1974, Age and tectonic significance of volcanic rocks on St. Matthew Island, Bering Sea, Alaska (abs): Geol. Soc. America Abs. with Programs, v. 6, p. 9905-9906.

Patton, W. W., Jr., Lanphere, M. A., Miller, T. P., and Scott, R. A. 1976, Age and tectonic significance of volcanic rocks on St. Matthew Island, Bering Sea, Alaska: U.S. Geol. Survey Jour. Research, v. 4, no. 1, p. 67-73.

Pratt, R. M., Rutstein, M. S., Walton, F. W., and Buschur, J. A., 1972, Extension of Alaska structural trends beneath Bristol Bay, Bering shelf, Alaska: Jour. Geophys. Research, v. 77, no. 26, p. 4994-4999.

Reed, B. L., and Lanphere, M. A., 1973, Alaska-Aleutian range batholith: Geochronology, chemistry, and relation to circum-Pacific plutonism: Geol. Soc. America Bull., v. 84, p. 2583-2610.

Robinson, G. D., 1947, Objectives, methods, and progress of Alaskan volcano investigations of the United States Geological Survey: U.S. Geological Survey Alaskan Volcano Investigations, Rept. no. 2, Progress of Investigations in 1946, p. 3-5.

Schlanger, S. O., and Combs, J., 1975, Hydrocarbon potential of marginal basins bounded by an island arc: Geology, July, p. 397-400.

Scholl, D. W., Buffington, E. C., and Hopkins, D. M., 1968, Geologic history of the continental margin of North America in Bering Sea: Marine Geology, v. 6, p. 297-330.

Scholl, D. W., Buffington, E. C., Hopkins, D. M., and Alpha, T. R., 1970a, The Structure and Origin of the large Submarine Canyons of the Bering Sea: Marine Geol. 8, p. 187-210.

Scholl, D. W., Greene, H. G., and Marlow, M. S., 1970, Eocene age of Adak "Paleozoic(?)" rocks, Aleutian Islands, Alaska: Geol. Soc. America Bull., v. 81, p. 3582-3592.

Scholl, D. W., and Marlow, M. S., 1970, Diapirlike structures in the Southeastern Bering Sea: Am. Assoc. Pet. Geol. Bull., v. 54, no. 9, p. 1644-1650.

Scholl, D. W., and Creager, J. S., 1973, Geologic synthesis of Leg 19 (DSDP) results; far north Pacific, and Aleutian Ridge, and Bering Sea, in Creager, J. S., Scholl, D. W., and others, Initial Reports of the Deep Sea Drilling Project, v. 19: Washington, D.C., U.S. Government Printing Office, p. 897-913.

Scholl, D. W., Buffington, E. C., and Marlow, M. S., 1975, Plate tectonics and the structural evolution of the Aleutian-Bering Sea region, in Forbes, R. B., (ed.), Contributions to the geology of the Bering Sea basin and adjacent regions: Geol. Soc. America Spec. Paper 151, p. 1-32.

Scholl, D. W., Vallier, T. L., and Stevenson, A. J., 1983a, Arc, forearc, and trench sedimentation and tectonics; Amlia Corridor of the Aleutian Ridge, in Watkins, J. S., and Drake, C. L., eds., Studies in continental margin geology: AAPG Memoir 34, p. 413-439.

Scholl, D. W., Vallier T. L., and Stevenson, A. J., 1983b, Geologic evolution of the Aleutian Ridge--Implications for petroleum resources: J. Alaska Geol. Soc., p. 33-85.

Sharma, G. D., 1974, Contemporary depositional environment of the eastern Bering Sea, in Hood, D. W., and Kelley, E. J., eds., Oceanography of the Bering Sea: Inst. of Marine Science, Univ. of Alaska, Occasional Publ. 2, p. 517-540.

Sykes, L. R., 1971, Aftershock zones of great earthquakes, seismicity gaps, and earthquake prediction for Alaska and the Aleutians: Jour. Geophys. Research, v. 76, p. 8021-8041.

Underwood, M. B., Vallier, T. L., Gardner, J. V., and Barron, J. A., 1979, Age, grain size, mineralogy, and carbon/carbonate content of Miocene and Pliocene samples from dredge hauls, DSDP holes 184b and 185, and the Sandy River Well, southern Bering Sea continental margin and Alaska Peninsula: U.S. Geol. Survey Open File Rept. OF79-450.

Watts, A. B., 1975, Gravity field of the northwest Pacific ocean basin and its margin - Aleutian Island Arc - Trench system: Geological Society of America Map-Chart Series MC-10.